A TREATMENT OF ATOMIC MEAN SQUARE DISPLACEMENT IN HIGHER ORDER PERTURBATION THEORY

by

Jeffrey Howard Martin, B.Sc.

A Thesis
Submitted to
the Department of Physics
Brock University

In partial fulfillment
of the requirements for the degree
Master of Science

Brock University
St. Catharines, Ontario
April 1990

To my parents,
without whose love, support and guidance
none of this would have been possible.
I love you both.

ABSTRACT

A general derivation of the anharmonic coefficients for a periodic lattice invoking the special case of the central force interaction is presented. All of the contributions to mean square displacement (MSD) to order λ^4 perturbation theory are enumerated. A direct correspondance is found between the high temperature limit MSD and high temperature limit free energy contributions up to and including $O(\lambda^4)$. This correspondance follows from the detailed derivation of some of the contributions to MSD. Numerical results are obtained for all the MSD contributions to $O(\lambda^4)$ using the Lennard-Jones potential for the lattice constants and temperatures for which the Monte Carlo results were calculated by Heiser, Shukla and Cowley. The Peierls approximation is also employed in order to simplify the numerical evaluation of the MSD contributions. The numerical results indicate the convergence of the perturbation expansion up to 75% of the melting temperature of the solid (T_M) for the exact calculation; however, a better agreement with the Monte Carlo results is not obtained when the total of all λ^4 contributions is added to the λ^2 perturbation theory results. Using Peierls approximation the expansion converges up to 45% of T_M. The MSD contributions arising in the Green's function method of Shukla and Hübschle are derived and enumerated up to and including $O(\lambda^8)$. The total MSD from these selected contributions is in excellent

agreement with their results at all temperatures. Theoretical values of the recoilless fraction for krypton are calculated from the MSD contributions for both the Lennard-Jones and Aziz potentials. The agreement with experimental values is quite good.

AKNOWLEDGEMENTS

I would like to thank Dr. R. C. Shukla for suggesting this research project. His enthusiasm and suggestions throughout this work were invaluable.

The financial assistance I received from the Ontario Graduate Scholarship program was greatly appreciated. This work was also supported by the Natural Sciences and Engineering Research Council of Canada.

There are a number of individuals and groups who must be recognized for their assistance throughout the course of this research. The Brock University Physics Department and Mrs. Joyce Cowan for making my stay here memorable. The Brock University Computer Services Department for all their help during the computational part of this work. Dr. D. C. Moule and The Brock University Chemistry Department for the use of their facilites.

Finally, I wish to thank a few people who helped in putting this thesis in its finished form: Frank Benko, Caroline Starrs, my parents Howard and Shirley Martin and a special thanks to Francesca Ioannoni.

TABLE OF CONTENTS

LIST OF TABLES

LIST OF FIGURES

I INTRODUCTION

In the study of crystal lattice vibrations the harmonic approximation has been introduced since the early work of Born, von Karman and Debye. This approximation enters in lattice vibrations when the Taylor's expansion of the crystal potential energy in the Hamiltonian (H) is truncated at the quadratic term. The quantization of this Hamiltonian yields quanta of energy which are known as phonons. They are characterized by the frequency $\omega(\vec{q}j)$ and eigenvector $\vec{e}(\vec{q}j)$ where $\vec{q}$ is the wave vector and j is the branch index. The dispersion curves (ω versus $\vec{q}$ relationship) have been observed experimentally by inelastic neutron scattering techniques in a wide variety of monatomic, diatomic and mixed crystals.

Nevertheless, there are other crystals such as solid helium, metallic hydrogen and to some extent solid neon where the harmonic approximation breaks down (in other words $\omega(\vec{q}j)$ are imaginary). In such situations it becomes necessary to consider terms in the Hamiltonian beyond the harmonic approximation. Collectively, the left-out terms in the potential energy are known as the anharmonic terms. The harmonic approximation in normal circumstances is also inadequate in explaining the behaviour of specific heat at high temperatures (its departure from the Dulong-Petit law 3R), thermal conductivity (which is infinite in the harmonic approximation) and thermal expansion (which is zero in this

approximation) to name a few. All of these properties can be explained by the introduction of anharmonic terms.

Sometimes, partial anharmonicity can be introduced in the harmonic approximation by changing $\omega(\vec{q}j)$ with volume. This is known as the quasiharmonic approximation (QH). It is obvious that unless the collectively left-out terms in the potential energy can <u>all</u> be included, a full anharmonic theory cannot be constructed. One method is to not expand the potential energy and evaluate the contribution to a physical property, α, from a given potential function. This can be done only by simulation techniques such as the Molecular Dynamics (MD) and the Monte Carlo (MC) methods; each of which involves a different averaging process for the calculation of α (a time average for MD and an ensemble average for MC). These methods give, in principle, all anharmonic contributions to α, but they are valid only in the high temperature limit (when the temperature T is greater than the Debye temperature Θ_D).

The analytical method of incorporating anharmonicity in the calculation of the Helmholtz free energy (F) or atomic mean square displacement (MSD) usually requires a treatment of double infinite series. This is necessary because the anharmonic contributions to F or MSD arise from the consideration of the infinite series due to the expansion of the operator $e^{-\beta H}$ where H is in itself an infinite series. Sometimes, it is possible to sum a selected class of

contributions in closed form for α. When this approach is followed, the first-order self-consistent phonon theory (SC1) is obtained. In this theory, the contributions to α are evaluated from only the even terms of the infinite series (quadratic, quartic etc). However, the most elementary treatment of a one-dimensional harmonic oscillator which can be found in standard quantum mechanics text (Landau and Lifshitz (1965)) shows that the contribution to α from the quartic term is as important as the contribution from the cubic term. For example, the contribution to energy from both these terms is proportional to the same power of $\hbar$ and the same power of the quantum number n. Thus, because of the limitations of the theory the cubic term cannot be included and hence the SC1 theory is limited in scope.

Clearly then, the calculation of α by a perturbation method will require some kind of ordering parameter, λ, (Van Hove (1961)). Terms of given order in λ have to be collected for the calculation of α. In the high temperature limit all the contributions of a given order in λ have the same temperature dependence (for example there are 8 contributions of order λ^4 in F and each of them has a T^3 dependence (Shukla and Cowley (1971)). Similar kinds of temperature dependences are expected to arise in the calculations of other physical properties.

The difficulty of the perturbation method lies in the convergence of the series generated for α. Some evidence of

the convergence of the Helmholtz function and of the various thermodynamic quantities calculated from F exists in the literature. From the work of Klein et al. (1969) it is seen that the perturbation theory to $O(\lambda^2)$ converges up to 1/3 of the melting temperature, T_M, of the solid and the theory to $O(\lambda^4)$ converges well up to 40% of T_M [Shukla and Cowley (1971), Shukla and Wilk (1974) and Shukla and Cowley (1985)]. This conclusion is based on the detailed calculations performed for the equation of state of a nearest-neighbour central-force (NNCF) model of a face centered cubic (fcc) lattice using the 6-12 Lennard-Jones (L-J) potential. If a different choice of potential is made for the same model of the solid, for example Morse, the degree of convergence is much better for both the λ^2 and the λ^4 theories (Shukla and Shanes (1985)).

Until very recently, not much work was done for MSD other than its evaluation in the harmonic approximation. For a list of these calculations see the references cited in Gupta (1983). The MSD is of fundamental importance in determining the Debye-Waller factor (DWF) which enters in the calculation of the intensity of x-rays and neutron scattering and the Mössbauer fraction. The MSD also arises in the theory of melting through the Lindemann approach and in the determination of the ordering parameter λ (defined as the square root of MSD divided by the nearest neighbour distance at a temperature T). The first anharmonic calculation (cubic and quartic anharmonic contributions) of DWF (which is related

to MSD) was carried out by Maradudin and Flinn (1963) for the NNCF model of the fcc lattice. These authors performed the calculations in the leading term approximation (which requires approximating the Cartesian tensor derivatives by their product of Cartesian coordinates and the highest ordered radial derivative) and did not evaluate the $\vec{q}\to 0$ limit of the cubic and quartic contributions to $\langle u^2 \rangle$. As will be seen later, the long wavelength limit ($\vec{q}\to 0$) contributions are weighted heavily in the calculation of $\langle u^2 \rangle$. In the calculation of MSD by Goldman (1968) a volume-dependent average anharmonic frequency shift was used.

The MD and λ^2 anharmonic contributions to MSD have been evaluated for the long range potentials by Shukla and Mountain (1982) and Shukla and Heiser (1986) for body centered cubic alkali metals without making the leading term approximation, but the $\vec{q}\to 0$ limit was taken only in the latter. A comparison of the MD and λ^2 results for the MSD, for these potentials, shows the adequacy of the λ^2 theory in accounting for the anharmonic effects.

The first rigorous calculation of MSD for the NNCF model of an L-J solid has been carried out by Heiser, Shukla and Cowley (1986), HSC, for the lowest order anharmonic contributions. These authors did not make the leading term approximation and extracted the $\vec{q}\to 0$ limit of the quasiharmonic and $O(\lambda^2)$ contributions to MSD. To assess the convergence of the perturbation theory in the context of MSD they compared

the numerical results of the λ^2 theory with those of the MD and MC methods. In the latter two methods HSC used the same model potential as the λ^2 theory calculations. The agreement between the λ^2 and MC method results was quite good up to 3/4 of T_M. Because the MC results contain all anharmonic contributions the discrepancy between the λ^2 theory and the MC results from 3/4 T_M to T_M has to be accounted for in any analytical theory like the λ^2 and λ^4 theories. Shukla and Hübschle (1989) proposed a Green's function method to remove this discrepancy. In this analytical method the only two contributions of $O(\lambda^2)$ in MSD are selected and then summed to all orders of anharmonicity. Unfortunately, the discrepancy still exists for $T \approx T_M$ between the Green's function method and the MC results. These authors also calculated the λ^2 contributions to MSD and extracted the $\vec{q} \to 0$ limit of the cubic term. Thus, the total MSD contribution to $O(\lambda^2)$ is more accurately given in their work than in HSC. This affects the MSD results only at higher temperatures. Two other methods have been used in MSD calculations: the cell-cluster method and the correlated particles expansion method. The former method has been employed by Cowley and Nur (1975) and the latter method by Hardy and Day (1988). The drawback of these methods is that the long wavelength limit contributions to MSD are not adequately accounted for.

This research was proposed in order to examine the convergence of the perturbation expansion for the case of MSD.

This is accomplished by evaluating the ratio of the total of all $O(\lambda^4)$ contributions to the total of the two $O(\lambda^2)$ contributions. This has already been done for the free energy by Shukla and Wilk (1974). In this work for the case of MSD, it was necessary to first generate all of the $O(\lambda^4)$ anharmonic contributions. By evaluating the $O(\lambda^2)$ and $O(\lambda^4)$ contributions to MSD for the reduced temperatures of HSC, the convergence of the perturbation expansion is examined up to the melting temperature of the solid. In order to see if a better agreement with the MC results can be achieved the total of <u>all</u> $O(\lambda^4)$ and $O(\lambda^2)$ contributions is examined.

The basic principles of lattice dynamics are reviewed in the first part of Section II with the remainder of that section being devoted to the derivation of the general anharmonic coefficient necessary for the implementation of the perturbation theory (PT) in practice. This was prompted by the lack of availability of such a derivation in the existing literature. Though the numerical calculations in this work will be carried out strictly for a monatomic fcc lattice it is important to see what changes occur when a more general lattice is considered. Section III outlines the derivation of the anharmonic contributions to MSD to $O(\lambda^4)$ PT. Diagrams will be associated with each of the MSD contributions in order to facilitate discussions of individual contributions (these diagrams are shown to be derivable from the free energy diagrams of Shukla and Cowley (1971)). After a few of the

$O(\lambda^4)$ MSD contributions were derived (and the high temperature limit was taken) it was noticed that there was a direct correlation with the corresponding high temperature free energy contributions of Shukla and Cowley (1971). As a result, the remaining high temperature MSD contributions were derived from these free energy contributions. Consequently, the high temperature free energy expressions of Shukla and Cowley (1971) are presented in Section III.

In any lattice dynamics calculation one must contend with wave vector sums over the first Brillouin zone. Depending on the size of the mesh used in the evaluation of the sums and the number of wave vector sums present in any given contribution, the evaluation of some contributions become very computer-time intensive. For more complicated crystal structures (diatomics for example), the evaluation of some anharmonic contributions would become extremely complicated and time consuming. What is needed is an approximation (Peierls (1955)) that allows for the zone sums to be evaluated analytically. As outlined in Section IV, this approximation treats the anharmonic coefficient as a slowly varying function of its arguments, meaning that it can be taken to be constant. What remains is to conserve the momentum and take proper precautions concerning the number of unit cells.

In Section V the numerical techniques employed in the calculations of the $O(\lambda^2)$ and $O(\lambda^4)$ MSD and F contributions are reviewed and the results of these computations are tabulated

for the six reduced temperatures of HSC. As a check to the methods involved in these calculations all of the MSD and F contributions are calculated for the equilibrium case and the F results are compared with the results of Shukla and Wilk (1974). All of the anharmonic contributions to MSD and F are also evaluated using the Peierls approximation, for equilibrium and the six reduced temperatures, in order to test its validity as a computer-time saving tool.

In Section VI, the anharmonic contributions arising in the Green's function method of Shukla and Hübschle (1989), up to and including $O(\lambda^8)$ contributions, are evaluated as well as identifying the $O(\lambda^4)$ contributions with those arising in the $O(\lambda^4)$ set. The diagrams and expressions for the contributions from $O(\lambda^6)$ and $O(\lambda^8)$ are presented. The numerical results, for each contribution, are tabulated (for the reduced temperatures of HSC), and the importance of these contributions as a function of temperature are examined.

Gilbert and Violet (1968) have experimentally measured the recoilless fraction of solid krypton, for 9.3 keV gamma rays, at a range of temperatures, and Gupta (1983) has related these results to the Debye-Waller factor. The theoretical calculation performed by Gupta (1983) shows a close agreement with the experimental points. However, the anharmonicity was included in that calculation by introducing the cubic and quartic anharmonic contributions to the zero point energy only in fitting the potential parameters. What is required is to

see how the perturbation theory results, properly calculated, agree with the experimental results. Consequently, in Section VII, the MSD contributions to order λ^4 PT are evaluated for the Lennard-Jones potential (with appropriate parameters for Kr) for the reduced temperatures of HSC. Aziz (1979) proposed a potential function for krypton. The parameters of this potential are <u>not</u> determined from the solid state data. In a nearest neighbour calculation of phonon dispersion curves this potential yields results in good agreement with experiments. As a result, the high temperature QH as well as all the $O(\lambda^2)$ and $O(\lambda^4)$ anharmonic contributions to MSD were calculated for this potential. The results for both potentials are converted to recoilless fractions and compared to the experimental results of Gilbert and Violet (1968) as corrected by Kolk (1971). Sections VIII and IX contain discussions and conclusions.

II DERIVATION OF ANHARMONIC COEFFICIENTS

The formal expression for the Fourier transform of the n^{-th} order anharmonic coefficient can be found in Born and Huang (1954). However, for calculational purposes it is worthwhile to present here a brief outline of its derivation, specialized for the central force potential.

When discussing an infinite crystal, one is really discussing a crystal lattice composed of an infinite number of identical constructs called unit cells. Each unit cell is a parallepiped bounded by three noncoplanar vectors $\vec{a}_1$, $\vec{a}_2$, $\vec{a}_3$ (known as the primitive translation vectors of the direct lattice). The equilibrium position of the atoms in the l^{-th} unit cell, relative to a specified origin, is

$$\vec{x}(l) = l_1\vec{a_1} + l_2\vec{a_2} + l_3\vec{a_3} \tag{2.1}$$

where l_1, l_2, l_3 are integers, positive, negative or zero (to be referred to collectively as l for brevity). If there is more than one atom per unit cell and the locations of these r atoms in the unit cell are defined by the position vectors $\vec{x}(k)$ $(k=1,\ldots,r)$, then the position of the k^{-th} atom in the l^{-th} unit cell is given as

$$\vec{x}(lk) = \vec{x}(l) + \vec{x}(k) \tag{2.2}$$

In the case of a monatomic lattice, $\vec{x}(l)$ defines the positions of the atoms.

When each atom is displaced from its equilibrium position by an amount $\vec{u}(lk)$, the total kinetic energy of the lattice is

$$T = \frac{1}{2}\sum_{l,k,\alpha} M_k \dot{u}_\alpha^2(lk) \tag{2.3}$$

where M_k is the mass of the atom of type k and $u_\alpha(lk)$ is the α-Cartesian component of $\vec{u}(lk)$ (α=x,y,z).

The total potential energy of the crystal, which is a function of the instantaneous atomic positions (equilibrium + displacement), is expanded in a Taylor's series in powers of $\vec{u}(lk)$ up to the quadratic terms. This gives

$$\Phi = \Phi_0 + \sum_{l_1 k_1 \alpha} \Phi_\alpha(l_1 k_1) u_\alpha(l_1 k_1) +$$

$$+ \frac{1}{2!}\sum_{l_1 k_1 \alpha}\sum_{l_2 k_2 \beta} \Phi_{\alpha\beta}(l_1 k_1; l_2 k_2) u_\alpha(l_1 k_1) u_\beta(l_2 k_2) \tag{2.4}$$

The above is known as the harmonic approximation. In Eq.(2.4) Φ_0 is the static or equilibrium potential energy of the crystal, and, the coefficients are defined by

$$\Phi_\alpha(l_1 k_1) = \left(\frac{\partial \Phi}{\partial u_\alpha(l_1 k_1)}\right)_{\text{equil.}} \tag{2.5}$$

$$\Phi_{\alpha\beta}(l_1 k_1; l_2 k_2) = \left(\frac{\partial^2 \Phi}{\partial u_\alpha(l_1 k_1)\partial u_\beta(l_2 k_2)}\right)_{\text{equil.}} \tag{2.6}$$

where the derivatives are evaluated at the equilibrium configuration of the crystal. From Eq.(2.5) it is seen that $\Phi_\alpha(l_1k_1)$ is actually the negative of the force acting in the α-direction on the atom at $\vec{x}(l_1k_1)$ in equilibrium. However, since the force on any atom in the equilibrium configuration is zero, then $\Phi_\alpha(l_1k_1) = 0$. From Eq.(2.6) the coefficient $\Phi_{\alpha\beta}(l_1k_1;l_2k_2)$ (known as the atomic force constant of second order) is the negative of the force exerted in the α-direction on the atom at $\vec{x}(l_1k_1)$ due to a unit displacement, in the β-direction, of the atom at $\vec{x}(l_2k_2)$ while all other atoms remain at their equilibrium positions.

If each atom of the crystal is displaced through a common vector $\vec{v}$, the result is that the crystal as a whole will be displaced through the vector $\vec{v}$. Such a rigid body translation of the crystal will leave the potential energy unchanged since the instantaneous positions of the atoms relative to each other remain unchanged. The invariant behaviour of the first and second order atomic force constants are related through the following conditions (as per Maradudin et al. (1971))

$$\sum_{l_1k_1} \Phi_\alpha(l_1\,k_1) = 0 \tag{2.7}$$

$$\sum_{l_2k_2} \Phi_{\alpha\beta}(l_1\,k_1;l_2\,k_2) = 0 \tag{2.8}$$

Similarly, if the crystal as a whole is transformed under an infinitesimal rigid body rotation, the potential energy will remain invariant. Each displacement is described by

$$u_\alpha(l_1 k_1) = \sum_\beta \omega_{\alpha\beta} x_\beta(l_1 k_1) \tag{2.9}$$

where the parameters $\omega_{\alpha\beta}$ are the elements of an infinitesimal antisymmetric matrix ($\omega_{\alpha\beta} = -\omega_{\beta\alpha}$). The conditions on the atomic force constants become

$$\sum_{l_1 k_1} \Phi_\alpha(l_1 k_1) x_\beta(l_1 k_1) = \sum_{l_1 k_1} \Phi_\beta(l_1 k_1) x_\alpha(l_1 k_1) \tag{2.10}$$

$$\sum_{l_2 k_2} \left\{ \Phi_{\alpha\beta}(l_1 k_1; l_2 k_2) x_\gamma(l_2 k_2) - \Phi_{\alpha\gamma}(l_1 k_1; l_2 k_2) x_\beta(l_2 k_2) \right\} =$$

$$= \delta_{\alpha\beta} \Phi_\gamma(l_1 k_1) - \delta_{\alpha\gamma} \Phi_\beta(l_1 k_1) \tag{2.11}$$

Within the harmonic approximation, the harmonic (or zeroth order) Hamiltonian of the crystal is

$$H_0 = \Phi_0 + \frac{1}{2} \sum_{l_1 k_1 \alpha} M_{k_1} \dot{u}^2_\alpha(l_1 k_1) +$$

$$+ \frac{1}{2} \sum_{l_1 k_1 \alpha} \sum_{l_2 k_2 \beta} \Phi_{\alpha\beta}(l_1 k_1; l_2 k_2) u_\alpha(l_1 k_1) u_\beta(l_2 k_2) \tag{2.12}$$

This Hamiltonian is used to find the equations of motion of the crystal lattice, which when solved yield

$$\omega^2(\vec{q} j) e_\alpha(k_1 | \vec{q} j) = \sum_{k_2 \beta} D_{\alpha\beta}(k_1 k_2 | \vec{q}) e_\beta(k_2 | \vec{q} j) \tag{2.13}$$

where

$$D_{\alpha\beta}(k_1 k_2|\vec{q}) = \left(M_{k_1} M_{k_2}\right)^{-1/2} \sum_{l_2} \Phi_{\alpha\beta}(l_1 k_1; l_2 k_2) e^{-i\vec{q}\bullet[\vec{x}(l_1) - \vec{x}(l_2)]} \tag{2.14}$$

are the elements of the dynamical matrix. In the above, $\vec{q}$ is known as the wave vector, j is the branch index (j=1,...,3r), $\omega(\vec{q}j)$ is the eigenvalue (or phonon frequency) and $e_\alpha(k|\vec{q}j)$ is the α-component of the eigenvector corresponding to given values of $\vec{q}j$. The eigenvectors $\vec{e}(k|\vec{q}j)$ satisfy the following orthonormality and closure conditions

$$\sum_{k\,\alpha} e^{*}_{\alpha}(k|\vec{q}\,j_1) e_{\alpha}(k|\vec{q}\,j_2) = \delta_{j_1 j_2} \tag{2.15}$$

$$\sum_{j} e^{*}_{\beta}(k_1|\vec{q}\,j) e_{\alpha}(k_2|\vec{q}\,j) = \delta_{\alpha\beta}\,\delta_{k_1 k_2} \tag{2.16}$$

where

$$e^{*}_{\alpha}(k|\vec{q}\,j) = e_{\alpha}(k|-\vec{q}\,j) \tag{2.17}$$

Also, the frequencies $\omega(\vec{q}j)$ obey the following

$$\omega^{2}(-\vec{q}\,j) = \omega^{2}(\vec{q}\,j) \tag{2.18}$$

To introduce the anharmonic contributions as a perturbation, it is necessary to include the higher order terms previously neglected in the expansion of the potential

energy (Eq.(2.4)). With the inclusion of these terms the Hamiltonian becomes

$$H = H_0 + \frac{1}{3!}\sum_{l_1 l_2 l_3}\sum_{k_1 k_2 k_3}\sum_{\alpha\,\beta\,\gamma}\Phi_{\alpha\beta\gamma}(l_1 k_1; l_2 k_2; l_3 k_3)u_\alpha(l_1 k_1)u_\beta(l_2 k_2)u_\gamma(l_3 k_3) +$$

$$+\frac{1}{4!}\sum_{l_1 l_2 l_3 l_4}\sum_{k_1 k_2 k_3 k_4}\sum_{\alpha\,\beta\,\gamma\,\delta}\Phi_{\alpha\beta\gamma\delta}(l_1 k_1; l_2 k_2; l_3 k_3; l_4 k_4)u_\alpha(l_1 k_1)u_\beta(l_2 k_2)u_\gamma(l_3 k_3)u_\delta(l_4 k_4) \tag{2.19}$$

where H_0 is defined by Eq.(2.12) and the next two terms are the cubic and quartic contributions. The expansion coefficients $\Phi_{\alpha\beta\gamma}(l_1k_1;l_2k_2;l_3k_3)$ and $\Phi_{\alpha\beta\gamma\delta}(l_1k_1;l_2k_2;l_3k_3;l_4k_4)$ are known as the tensor atomic force constants of third and fourth order, respectively. These are higher order derivatives of the type shown in Eqs.(2.5) and (2.6). These force constants are also invariant to rigid body translations and rotations.

The Fourier representation of the α-component of the atomic displacement $u_\alpha(lk)$, needed in the diagonalization of the dynamical matrix $D_{\alpha\beta}(\vec{q})$, is

$$u_\alpha(l\,k) = \left(\frac{\hbar}{2NM_k}\right)^{1/2}\sum_{\vec{q}j}\frac{e_\alpha(k|\vec{q}\,j)}{[\omega(\vec{q}\,j)]^{1/2}}e^{i\vec{q}\cdot\vec{x}(l\,k)}A(\vec{q}\,j) \tag{2.20}$$

where $\hbar$ is Planck's constant divided by 2π and N is the number of unit cells. The operator $A(\vec{q}j)$ is defined by

$$A(\vec{q}\,j) = a(\vec{q}\,j) + a^{+}(\vec{q}\,j) \tag{2.21}$$

where $a(\vec{q}j)$ and $a^{\dagger}(\vec{q}j)$ are the phonon annihilation and creation operators, respectively. At this point for the sake

of convenience the following shorthand notation is introduced.

$$\lambda_i = \vec{q}_i j_i \tag{2.22}$$

and

$$-\lambda_i = -\vec{q}_i j_i \tag{2.23}$$

Substituting Eq.(2.20) into Eq.(2.19) the total Hamiltonian becomes

$$H = H_0 + \mathcal{H} \tag{2.24}$$

where

$$H_0 = \sum_{\lambda_1} \hbar\omega(\lambda_1)\left[a^+(-\lambda_1)a(\lambda_1) + 1/2\right] \tag{2.25}$$

is the harmonic Hamiltonian in the second quantized form and

$$\mathcal{H} = \sum_{\lambda_1\lambda_2\lambda_3} V(\lambda_1;\lambda_2;\lambda_3)A(\lambda_1)A(\lambda_2)A(\lambda_3) +$$

$$+ \sum_{\lambda_1\lambda_2\lambda_3\lambda_4} V(\lambda_1;\lambda_2;\lambda_3;\lambda_4)A(\lambda_1)A(\lambda_2)A(\lambda_3)A(\lambda_4) \tag{2.26}$$

represents the cubic and quartic anharmonic contributions to the Hamiltonian in operator notation. From Eq.(2.26) the general form of the anharmonic contribution to the Hamiltonian can be written with the inclusion of the ordering parameter λ

as

$$H_A = \sum_{n=3}^{6} \sum_{\lambda_1 \ldots \lambda_n} \lambda^{n-2} V(\lambda_1;\ldots;\lambda_n) A(\lambda_1)\ldots A(\lambda_n) \qquad (2.27)$$

where $V(\lambda_1;\lambda_2;\ldots;\lambda_n)$ is given by

$$V(\lambda_1;\ldots;\lambda_n) = \frac{1}{n!} \sum_{l_1\ldots l_n} \sum_{k_1\ldots k_n} \sum_{\alpha_1\ldots\alpha_n} \left(\frac{\hbar^n}{2^n N^n M_{k_1}\ldots M_{k_n}} \right)^{1/2} \Phi_{\alpha_1\ldots\alpha_n}(l_1 k_1;\ldots;l_n k_n) \times$$

$$\times \frac{e_{\alpha_1}(k_1|\lambda_1)\ldots e_{\alpha_n}(k_n|\lambda_n)}{\left[\omega(\lambda_1)\ldots\omega(\lambda_n)\right]^{1/2}} e^{i[\vec{q}_1\cdot\vec{x}(l_1 k_1) + \ldots + \vec{q}_n\cdot\vec{x}(l_n k_n)]} \qquad (2.28)$$

and $\alpha_1,\ldots,\alpha_n$ each take the values of x, y and z, respectively. The above general form requires the knowledge of elements of tensors of various ranks. For example, in the third-order, 27 elements of the tensor arising in $\Phi_{\alpha\beta\gamma}(l_1k_1;l_2k_2;l_3k_3)$ are needed. There is not enough experimental data available to find these elements even for the third rank tensor. The situation is obviously more complex for higher-order tensors. Therefore, it is necessary to introduce first the simplest approximation (namely the two-body interaction) and then specialize it for the case of central forces in setting up these anharmonic coefficients. Once a central force potential is known, all elements of $\Phi_{\alpha\beta\gamma}(l_1k_1;l_2k_2;l_3k_3)$, $\Phi_{\alpha\beta\gamma\delta}(l_1k_1;l_2k_2;l_3k_3;l_4k_4)$ and higher-order tensors can be obtained. In the following, this procedure is laid out for the derivation of $V(\lambda_1;\lambda_2;\lambda_3)$.

The coefficient of the cubic anharmonic contribution to the total Hamiltonian, $V(\lambda_1;\lambda_2;\lambda_3)$, is given by

$$V(\lambda_1;\lambda_2;\lambda_3) = \frac{1}{3!}\sum_{l_1 l_2 l_3}\sum_{k_1 k_2 k_3}\sum_{\alpha\,\beta\,\gamma}\left(\frac{\hbar^3}{8N^3 M_{k_1}M_{k_2}M_{k_3}}\right)^{1/2}\Phi_{\alpha\beta\gamma}(l_1 k_1;l_2 k_2;l_3 k_3)\times$$

$$\times\frac{e_\alpha(k_1|\lambda_1)e_\beta(k_2|\lambda_2)e_\gamma(k_3|\lambda_3)}{\left[\omega(\lambda_1)\omega(\lambda_2)\omega(\lambda_3)\right]^{1/2}}e^{i[\vec{q}_1\cdot\vec{x}(l_1 k_1)+\vec{q}_2\cdot\vec{x}(l_2 k_2)+\vec{q}_3\cdot\vec{x}(l_3 k_3)]} \qquad (2.29)$$

For two-body interactions the sums over l_1, l_2, l_3 and k_1, k_2, k_3 in Eq.(2.29) are performed under the following conditions:

a) $l_1=l_2=l_3$, $k_1=k_2=k_3$

b) $l_1=l_2$, $k_1=k_2$

c) $l_1=l_3$, $k_1=k_3$

d) $l_2=l_3$, $k_2=k_3$.

As a result, $V(\lambda_1;\lambda_2;\lambda_3)$ becomes

$$V(\lambda_1;\lambda_2;\lambda_3) = \frac{1}{3!}\left(\frac{\hbar}{2N}\right)^{3/2}\frac{1}{\left[M_{k_1}M_{k_2}M_{k_3}\omega(\lambda_1)\omega(\lambda_2)\omega(\lambda_3)\right]^{1/2}}\sum_{\alpha\,\beta\,\gamma}e_\alpha(k_1|\lambda_1)e_\beta(k_2|\lambda_2)e_\gamma(k_3|\lambda_3)\times$$

$$\times\Bigg\{\sum_{l_1 k_1}\Phi_{\alpha\beta\gamma}(l_1 k_1;l_1 k_1;l_1 k_1)e^{i[(\vec{q}_1+\vec{q}_2+\vec{q}_3)\cdot\vec{x}(l_1 k_1)]} +$$

$$+\sum_{l_1 k_1}\sum_{l_2 k_2}{}'\Phi_{\alpha\beta\gamma}(l_1 k_1;l_1 k_1;l_2 k_2)e^{i[(\vec{q}_1+\vec{q}_2)\cdot\vec{x}(l_1 k_1)+\vec{q}_3\cdot\vec{x}(l_2 k_2)]} +$$

$$+\sum_{l_1 k_1}\sum_{l_2 k_2}{}'\Phi_{\alpha\beta\gamma}(l_1 k_1;l_2 k_2;l_1 k_1)e^{i[(\vec{q}_1+\vec{q}_3)\cdot\vec{x}(l_1 k_1)+\vec{q}_2\cdot\vec{x}(l_2 k_2)]} +$$

$$+\sum_{l_1 k_1}\sum_{l_2 k_2}{}'\Phi_{\alpha\beta\gamma}(l_1 k_1;l_2 k_2;l_2 k_2)e^{i[\vec{q}_1\cdot\vec{x}(l_1 k_1)+(\vec{q}_2+\vec{q}_3)\cdot\vec{x}(l_2 k_2)]}\Bigg\} \qquad (2.30)$$

where the primes on the summation indicate the omission of the

case $(l_2k_2)=(l_1k_1)$.

At this point the central force potential is introduced into the calculation. Inherent here is the assumption that the atoms will interact in pairs as a function only of the magnitude of their separation. In this scheme the potential energy of the crystal is expressed as

$$\Phi = \frac{1}{2}\sum_{l_1k_1}\sum_{l_2k_2}{}' \phi_{k_1k_2}\left(r(l_1k_1;l_2k_2)\right) \qquad (2.31)$$

where $\phi_{k_1k_2}(r(l_1k_1;l_2k_2))$ is the potential function describing the interaction of an atom (l_1k_1) with an atom (l_2k_2), separated by the distance $r(l_1k_1;l_2k_2)$ (referred to as the instantaneous distance between the atoms (l_1k_1) and (l_2k_2)). The prime on the summation indicates that the terms where $(l_1k_1)=(l_2k_2)$ are to be omitted and the factor of $1/2$ eliminates the double counting of the pairs. The displacement of each atom, from equilibrium, by the vector $\vec{u}(lk)$ results in the following definition of $r(l_1k_1;l_2k_2)$:

$$r(l_1k_1;l_2k_2) = \left[x^2(l_1k_1;l_2k_2) + 2\vec{x}(l_1k_1;l_2k_2)\cdot\vec{u}(l_1k_1;l_2k_2) + u^2(l_1k_1;l_2k_2)\right]^{1/2} \qquad (2.32)$$

where

$$\vec{x}(l_1k_1;l_2k_2) = \vec{x}(l_1k_1) - \vec{x}(l_2k_2) \qquad (2.33)$$

and

$$\vec{u}(l_1k_1;l_2k_2) = \vec{u}(l_1k_1) - \vec{u}(l_2k_2) \qquad (2.34)$$

Eq.(2.31) can now be expanded in powers of the components

$u_\alpha(l_1k_1;l_2k_2)$ as follows

$$\Phi = \frac{1}{2}\sum_{l_1k_1l_2k_2}{}' \phi_{k_1k_1}\left(x(l_1k_1;l_2k_2)\right) +$$

$$+ \frac{1}{2}\sum_{l_1k_1l_2k_2}\sum_{n=1}^{6}\left\{\frac{1}{n!}\sum_{\alpha_1\ldots\alpha_n}\phi_{\alpha_1\ldots\alpha_n}(l_1k_1;l_2k_2)u_{\alpha_1}(l_1k_1;l_2k_2)\ldots u_{\alpha_n}(l_1k_1;l_2k_2)\right\} \quad (2.35)$$

To employ the central force potential in the calculation of $V(\lambda_1;\lambda_2;\lambda_3)$, the definition of $\vec{u}(l_1k_1;l_2k_2)$ (Eq.(2.34)) is substituted into Eq.(2.35), as per Maradudin et al. (1971), and the cubic term is expanded. In order to regroup this term, the dummy indices (l_1k_1) and (l_2k_2) are interchanged and use is made of the fact that $\phi_{\alpha\beta\gamma}(l_1k_1;l_2k_2) = -\phi_{\alpha\beta\gamma}(l_2k_2;l_1k_1)$. Comparing this term with the corresponding cubic contribution to the Hamiltonian in general tensor form (Eq.(2.19)), the following conditions arise between $\Phi_{\alpha\beta\gamma}(l_1k_1;l_2k_2;l_3k_3)$ and $\phi_{\alpha\beta\gamma}(l_1k_1;l_2k_2)$

$$\Phi_{\alpha\beta\gamma}(l_1k_1;l_1k_1;l_1k_1) = \sum_{l_2k_2}{}' \phi_{\alpha\beta\gamma}(l_1k_1;l_2k_2) \quad (2.36)$$

$$\Phi_{\alpha\beta\gamma}(l_1k_1;l_2k_2;l_1k_1) = -\phi_{\alpha\beta\gamma}(l_1k_1;l_2k_2) \qquad (l_1k_1)\neq(l_2k_2) \quad (2.37)$$

$$\Phi_{\alpha\beta\gamma}(l_2k_2;l_1k_1;l_1k_1) = -\phi_{\alpha\beta\gamma}(l_1k_1;l_2k_2) \qquad (l_1k_1)\neq(l_2k_2) \quad (2.38)$$

$$\Phi_{\alpha\beta\gamma}(l_2k_2;l_2k_2;l_1k_1) = \phi_{\alpha\beta\gamma}(l_1k_1;l_2k_2) \qquad (l_1k_1)\neq(l_2k_2) \quad (2.39)$$

The conditions outlined in Eqs.(2.36) through (2.39) can now be employed to simplify Eq.(2.30), yielding

$$V(\lambda_1;\lambda_2;\lambda_3) = \frac{1}{3!}\left(\frac{\hbar}{2N}\right)^{3/2} \frac{1}{\left[\omega(\lambda_1)\omega(\lambda_2)\omega(\lambda_3)\right]^{1/2}} \sum_{l_1 k_1 l_2 k_2} {\sum_{\alpha\beta\gamma}}' \phi_{\alpha\beta\gamma}(l_1 k_1; l_2 k_2) \times$$
$$\times \Big[W_\alpha(l_1 k_1;\lambda_1) W_\beta(l_1 k_1;\lambda_2) W_\gamma(l_1 k_1;\lambda_3) -$$
$$- W_\alpha(l_1 k_1;\lambda_1) W_\beta(l_1 k_1;\lambda_2) W_\gamma(l_2 k_2;\lambda_3) -$$
$$- W_\alpha(l_1 k_1;\lambda_1) W_\beta(l_2 k_2;\lambda_2) W_\gamma(l_1 k_1;\lambda_3) +$$
$$+ W_\alpha(l_1 k_1;\lambda_1) W_\beta(l_2 k_2;\lambda_2) W_\gamma(l_2 k_2;\lambda_3) \Big] \tag{2.40}$$

where

$$W_\alpha(l\,k;\lambda_i) = \frac{e_\alpha(k|\lambda_i)}{M_k^{1/2}} e^{i\vec{q}_i \cdot \vec{x}(l\,k)} \tag{2.41}$$

The dummy indices l_1k_1 and l_2k_2 are interchanged in Eq.(2.40) and the resulting equation (having once again utilized the condition $\phi_{\alpha\beta\gamma}(l_1k_1;l_2k_2) = -\phi_{\alpha\beta\gamma}(l_2k_2;l_1k_1)$) is added to Eq.(2.40). After some regrouping $V(\lambda_1;\lambda_2;\lambda_3)$ becomes

$$V(\lambda_1;\lambda_2;\lambda_3) = \frac{1}{2}\frac{1}{3!}\left(\frac{\hbar}{2N}\right)^{3/2} \frac{1}{\left[\omega(\lambda_1)\omega(\lambda_2)\omega(\lambda_3)\right]^{1/2}} \sum_{l_1 k_1 l_2 k_2} {\sum_{\alpha\beta\gamma}}' \phi_{\alpha\beta\gamma}(l_1 k_1; l_2 k_2) \times$$
$$\times \Big[W_\alpha(l_1 k_1;\lambda_1) - W_\alpha(l_2 k_2;\lambda_1) \Big] \Big[W_\beta(l_1 k_1;\lambda_2) - W_\beta(l_2 k_2;\lambda_2) \Big] \times$$
$$\times \Big[W_\gamma(l_1 k_1;\lambda_3) - W_\gamma(l_2 k_2;\lambda_3) \Big] \tag{2.42}$$

where the factor of 1/2 once again removes the double counting. Finally, the translational invariance of the lattice is used. Briefly, this means that the crystal is

taken into itself through a displacement by the lattice translation vector $\vec{x}(m)$. Its effect on $\vec{x}(lk)$ is

$$\vec{x}(l\,k) + \vec{x}(m) = \vec{x}(l+m\,k) \tag{2.43}$$

Applying this translation to the potential derivative $\phi_{\alpha\beta\gamma}(l_1k_1;l_2k_2)$ gives

$$\phi_{\alpha\beta\gamma}(l_1\,k_1;l_2\,k_2) = \phi_{\alpha\beta\gamma}(l_1+m\,k_1;l_2+m\,k_2) \tag{2.44}$$

and by setting $m=-l_1$ the following is obtained

$$\phi_{\alpha\beta\gamma}(l_1\,k_1;l_2\,k_2) = \phi_{\alpha\beta\gamma}(0\,k_1;l_2-l_1\,k_2) = \phi_{\alpha\beta\gamma}(0\,k_1;\bar{l}\,k_2) \tag{2.45}$$

where in the last step the dummy index l_2-l_1 has been relabelled as $\bar{l}$. Hence, carrying out the above relabelling in Eq.(2.42) and then summing over the index l_1, $V(\lambda_1;\lambda_2;\lambda_3)$ becomes

$$V(\lambda_1;\lambda_2;\lambda_3) = \frac{1}{2}\frac{1}{3!}\left(\frac{\hbar}{2N}\right)^{3/2}\frac{N\,\Delta(\vec{q_1}+\vec{q_2}+\ldots+\vec{q_n})}{\left[\omega(\lambda_1)\omega(\lambda_2)\omega(\lambda_3)\right]^{1/2}}\sum_{l_1k_1}\sum_{l_2k_2}{}'\sum_{\alpha\,\beta\,\gamma}\phi_{\alpha\beta\gamma}(0\,k_1;\bar{l}\,k_2)\times$$

$$\times\left[W_\alpha(0\,k_1;\lambda_1) - W_\alpha(\bar{l}\,k_2;\lambda_1)\right]\left[W_\beta(0\,k_1;\lambda_2) - W_\beta(\bar{l}\,k_2;\lambda_2)\right]\times$$
$$\times\left[W_\gamma(0\,k_1;\lambda_3) - W_\gamma(\bar{l}\,k_2;\lambda_3)\right] \tag{2.46}$$

where

$$\sum_{l_1} e^{i(\vec{q_1}+\vec{q_2}+\vec{q_3})\bullet\vec{x}(l)} = N\Delta(\vec{q_1}+\vec{q_2}+\vec{q_3}) \tag{2.47}$$

and the Δ function vanishes unless $\vec{q}_1+\vec{q}_2+\vec{q}_3$ equals zero or a vector of the reciprocal lattice, in which case it equals unity.

In general, for an anharmonic coefficient of order n ($n \geq 3$):

$$V(\lambda_1;\lambda_2;\ldots;\lambda_n) = \frac{1}{2}\frac{1}{n!}\left(\frac{\hbar}{2}\right)^{n/2} \frac{N^{1-n/2}\Delta(\vec{q_1}+\vec{q_2}+\ldots+\vec{q_n})}{\left[\omega(\lambda_1)\omega(\lambda_2)\ldots\omega(\lambda_n)\right]^{1/2}} \sum_{\alpha_1\ldots\alpha_n} \sum_{k_1} \sum_{l\,k_2}{}' \phi_{\alpha_1\ldots\alpha_n}(0k_1;lk_2) \times$$
$$\times \prod_{m=1}^{n} \left[\frac{e_{\alpha_m}(k_1|\lambda_m)}{M_{k_1}^{1/2}} e^{i\vec{q}_m\cdot\vec{x}(k_1)} - \frac{e_{\alpha_m}(k_2|\lambda_m)}{M_{k_2}^{1/2}} e^{i\vec{q}_m\cdot\vec{x}(lk_2)} \right] \qquad (2.48)$$

However, in all that follows only a monatomic lattice will be used. Because of this simplification the general anharmonic coefficient becomes

$$V(\lambda_1;\lambda_2;\ldots;\lambda_n) = \frac{1}{2}\frac{1}{n!}\left(\frac{\hbar}{2M}\right)^{n/2} \frac{N^{1-n/2}\Delta(\vec{q_1}+\vec{q_2}+\ldots+\vec{q_n})}{\left[\omega(\lambda_1)\omega(\lambda_2)\ldots\omega(\lambda_n)\right]^{1/2}} \sum_{\alpha_1\ldots\alpha_n} \sum_{l}{}' \phi_{\alpha_1\ldots\alpha_n}(l) \times$$
$$\times \prod_{m=1}^{n} \left[e_{\alpha_m}(\lambda_m)(1 - e^{i\vec{q}_m\cdot\vec{x}(l)}) \right] \qquad (2.49)$$

For computational purposes the expansion coefficients (or potential derivatives) for the central force potential are defined as

$$\phi_\alpha(l_1 k_1;l_2 k_2) = \left\{ \frac{\partial}{\partial x_\alpha} \phi_{k_1k_2}(r) \right\} \Bigg|_{r=x(l_1 k_1;l_2 k_2)} =$$
$$= \left\{ \frac{x_\alpha}{r} \phi'_{k_1k_2}(r) \right\} \Bigg|_{r=x(l_1 k_1;l_2 k_2)} \qquad (2.50)$$

$$\phi_{\alpha\beta}(l_1 k_1;l_2 k_2) = \left\{ \frac{x_\alpha x_\beta}{r^2} B(r) + \frac{\delta_{\alpha\beta}}{r} \phi'_{k_1k_2}(r) \right\} \Bigg|_{r=x(l_1 k_1;l_2 k_2)} \qquad (2.51)$$

$$\phi_{\alpha\beta\gamma}(l_1 k_1;l_2 k_2) = \left\{ \frac{x_\alpha x_\beta x_\gamma}{r^3} C(r) + \right.$$

$$\left. + \frac{1}{r^2}\left(x_\gamma\delta_{\alpha\beta} + x_\alpha\delta_{\beta\gamma} + x_\beta\delta_{\alpha\gamma}\right) B(r) \right\} \Bigg|_{r=x(l_1 k_1;l_2 k_2)} \qquad (2.52)$$

$$\phi_{\alpha\beta\gamma\mu}(l_1 k_1;l_2 k_2) = \left\{ \frac{x_\alpha x_\beta x_\gamma x_\mu}{r^4} D(r) + \right.$$

$$+ \frac{1}{r^3}\left(x_\alpha x_\beta\delta_{\gamma\mu} + x_\beta x_\gamma\delta_{\alpha\mu} + x_\alpha x_\gamma\delta_{\beta\mu} + x_\alpha x_\mu\delta_{\beta\gamma} + x_\beta x_\mu\delta_{\alpha\gamma} + x_\gamma x_\mu\delta_{\alpha\beta}\right) C(r) +$$

$$\left. + \frac{1}{r^2}\left(\delta_{\alpha\beta}\delta_{\gamma\mu} + \delta_{\beta\gamma}\delta_{\alpha\mu} + \delta_{\alpha\gamma}\delta_{\beta\mu}\right) B(r) \right\} \Bigg|_{r=x(l_1 k_1;l_2 k_2)} \qquad (2.53)$$

$$\phi_{\alpha\beta\gamma\mu\nu}(l_1 k_1;l_2 k_2) = \left\{ \frac{x_\alpha x_\beta x_\gamma x_\mu x_\nu}{r^5} E(r) + \right.$$

$$+ \frac{1}{r^4}\left(x_\alpha x_\beta x_\nu\delta_{\gamma\mu} + x_\beta x_\gamma x_\nu\delta_{\alpha\mu} + x_\alpha x_\gamma x_\nu\delta_{\beta\mu} + x_\alpha x_\mu x_\nu\delta_{\beta\gamma} + x_\beta x_\mu x_\nu\delta_{\alpha\gamma} + \right.$$

$$\left. + x_\gamma x_\mu x_\nu\delta_{\alpha\beta} + x_\beta x_\gamma x_\mu\delta_{\nu\alpha} + x_\alpha x_\gamma x_\mu\delta_{\nu\beta} + x_\alpha x_\beta x_\mu\delta_{\nu\gamma} + x_\alpha x_\beta x_\gamma\delta_{\mu\nu}\right) D(r) +$$

$$+ \frac{1}{r^3}\left[\delta_{\gamma\mu}\left(x_\beta\delta_{\alpha\nu} + x_\alpha\delta_{\beta\nu}\right) + \delta_{\alpha\mu}\left(x_\gamma\delta_{\beta\nu} + x_\beta\delta_{\gamma\nu}\right) + \delta_{\beta\mu}\left(x_\alpha\delta_{\gamma\nu} + x_\gamma\delta_{\alpha\nu}\right) + \right.$$

$$+ \delta_{\beta\gamma}\left(x_\mu\delta_{\alpha\nu} + x_\alpha\delta_{\mu\nu}\right) + \delta_{\alpha\gamma}\left(x_\mu\delta_{\beta\nu} + x_\beta\delta_{\mu\nu}\right) + \delta_{\alpha\beta}\left(x_\mu\delta_{\gamma\nu} + x_\gamma\delta_{\mu\nu}\right) +$$

$$\left. \left. + x_\nu\left(\delta_{\alpha\beta}\delta_{\gamma\mu} + \delta_{\beta\gamma}\delta_{\mu\alpha} + \delta_{\alpha\gamma}\delta_{\beta\mu}\right)\right] C(r) \right\} \Bigg|_{r=x(l_1 k_1;l_2 k_2)} \qquad (2.54)$$

$$\phi_{\alpha\beta\gamma\mu\nu\eta}(l_1 k_1; l_2 k_2) = \left\{ \frac{x_\alpha x_\beta x_\gamma x_\mu x_\nu x_\eta}{r^6} F(r) + \right.$$

$$+ \frac{1}{r^5}\Big(x_\alpha x_\beta x_\nu x_\eta \delta_{\gamma\mu} + x_\beta x_\gamma x_\nu x_\eta \delta_{\alpha\mu} + x_\alpha x_\gamma x_\nu x_\eta \delta_{\beta\mu} + x_\alpha x_\mu x_\nu x_\eta \delta_{\beta\gamma} + x_\beta x_\mu x_\nu x_\eta \delta_{\alpha\gamma} +$$

$$+ x_\alpha x_\beta x_\gamma x_\nu \delta_{\eta\mu} + x_\alpha x_\beta x_\gamma x_\eta \delta_{\mu\nu} + x_\mu x_\beta x_\gamma x_\eta \delta_{\nu\alpha} + x_\mu x_\alpha x_\gamma x_\eta \delta_{\nu\beta} + x_\mu x_\alpha x_\beta x_\eta \delta_{\nu\gamma} +$$

$$+ x_\mu x_\alpha x_\beta x_\gamma \delta_{\nu\eta} + x_\mu x_\alpha x_\beta x_\nu \delta_{\gamma\eta} + x_\mu x_\beta x_\gamma x_\nu \delta_{\alpha\eta} + x_\mu x_\gamma x_\alpha x_\nu \delta_{\beta\eta} + x_\mu x_\gamma x_\eta x_\nu \delta_{\alpha\beta} \Big) E(r) +$$

$$+ \frac{1}{r^4}\Big[\delta_{\nu\alpha}\big(x_\gamma x_\eta \delta_{\beta\mu} + x_\beta x_\eta \delta_{\gamma\mu} + x_\beta x_\gamma \delta_{\eta\mu} \big) + \delta_{\nu\beta}\big(x_\gamma x_\eta \delta_{\alpha\mu} + x_\alpha x_\eta \delta_{\gamma\mu} + x_\alpha x_\gamma \delta_{\eta\mu} \big) +$$

$$+ \delta_{\nu\gamma}\big(x_\beta x_\eta \delta_{\alpha\mu} + x_\alpha x_\eta \delta_{\beta\mu} + x_\alpha x_\beta \delta_{\eta\mu} \big) + \delta_{\nu\eta}\big(x_\beta x_\gamma \delta_{\alpha\mu} + x_\alpha x_\gamma \delta_{\beta\mu} + x_\alpha x_\beta \delta_{\gamma\mu} \big) +$$

$$+ \delta_{\gamma\eta}\big(x_\beta x_\nu \delta_{\alpha\mu} + x_\alpha x_\nu \delta_{\beta\mu} + x_\alpha x_\beta \delta_{\nu\mu} \big) + \delta_{\alpha\eta}\big(x_\gamma x_\nu \delta_{\beta\mu} + x_\beta x_\nu \delta_{\gamma\mu} + x_\beta x_\gamma \delta_{\nu\mu} \big) +$$

$$+ \delta_{\beta\eta}\big(x_\alpha x_\nu \delta_{\gamma\mu} + x_\gamma x_\nu \delta_{\alpha\mu} + x_\alpha x_\gamma \delta_{\nu\mu} \big) + \delta_{\beta\gamma}\big(x_\eta x_\nu \delta_{\alpha\mu} + x_\alpha x_\nu \delta_{\eta\mu} + x_\alpha x_\eta \delta_{\mu\nu} \big) +$$

$$+ \delta_{\alpha\gamma}\big(x_\eta x_\nu \delta_{\beta\mu} + x_\beta x_\nu \delta_{\eta\mu} + x_\beta x_\eta \delta_{\nu\mu} \big) + \delta_{\alpha\beta}\big(x_\eta x_\nu \delta_{\gamma\mu} + x_\gamma x_\nu \delta_{\eta\mu} + x_\eta x_\gamma \delta_{\nu\mu} \big) +$$

$$+ x_\mu \delta_{\gamma\eta}\big(x_\beta \delta_{\alpha\nu} + x_\alpha \delta_{\beta\nu} \big) + x_\mu \delta_{\alpha\eta}\big(x_\gamma \delta_{\beta\nu} + x_\beta \delta_{\gamma\nu} \big) + x_\mu \delta_{\beta\eta}\big(x_\alpha \delta_{\gamma\nu} + x_\gamma \delta_{\alpha\nu} \big) +$$

$$+ x_\mu \delta_{\beta\gamma}\big(x_\eta \delta_{\alpha\nu} + x_\alpha \delta_{\nu\eta} \big) + x_\mu \delta_{\alpha\gamma}\big(x_\eta \delta_{\beta\nu} + x_\beta \delta_{\eta\nu} \big) + x_\mu \delta_{\alpha\beta}\big(x_\eta \delta_{\gamma\nu} + x_\gamma \delta_{\eta\nu} \big) +$$

$$+ x_\mu x_\nu \big(\delta_{\alpha\beta}\delta_{\gamma\eta} + \delta_{\beta\gamma}\delta_{\eta\alpha} + \delta_{\alpha\gamma}\delta_{\beta\eta} \big) \Big] D(r) +$$

$$+ \frac{1}{r^3}\Big[\delta_{\gamma\eta}\big(\delta_{\alpha\nu}\delta_{\beta\mu} + \delta_{\alpha\mu}\delta_{\beta\nu} \big) + \delta_{\alpha\eta}\big(\delta_{\beta\nu}\delta_{\gamma\mu} + \delta_{\beta\mu}\delta_{\gamma\nu} \big) +$$

$$+ \delta_{\beta\eta}\big(\delta_{\alpha\mu}\delta_{\gamma\nu} + \delta_{\gamma\mu}\delta_{\alpha\nu} \big) + \delta_{\beta\gamma}\big(\delta_{\alpha\nu}\delta_{\eta\mu} + \delta_{\alpha\mu}\delta_{\eta\nu} \big) +$$

$$+ \delta_{\alpha\gamma}\big(\delta_{\beta\nu}\delta_{\eta\mu} + \delta_{\beta\mu}\delta_{\eta\nu} \big) + \delta_{\alpha\beta}\big(\delta_{\gamma\nu}\delta_{\eta\mu} + \delta_{\gamma\mu}\delta_{\eta\nu} \big) +$$

$$\left. + \delta_{\nu\mu}\big(\delta_{\alpha\beta}\delta_{\gamma\eta} + \delta_{\beta\gamma}\delta_{\alpha\eta} + \delta_{\alpha\gamma}\delta_{\beta\eta} \big) \Big] C(r) \right\} \Bigg|_{r = x(l_1 k_1; l_2 k_2)}$$

(2.55)

where

$$B(r) = \left(\phi''_{k_1 k_2}(r) - \frac{1}{r}\phi'_{k_1 k_2}(r) \right) \qquad (2.56)$$

$$C(r) = \left(\phi'''_{k_1k_2}(r) - \frac{3}{r}\phi''_{k_1k_2}(r) + \frac{3}{r^2}\phi'_{k_1k_2}(r) \right) \tag{2.57}$$

$$D(r) = \left(\phi^{iv}_{k_1k_2}(r) - \frac{6}{r}\phi'''_{k_1k_2}(r) + \frac{15}{r^2}\phi''_{k_1k_2}(r) - \frac{15}{r^3}\phi'_{k_1k_2}(r) \right) \tag{2.58}$$

$$E(r) = \left(\phi^{v}_{k_1k_2}(r) - \frac{10}{r}\phi^{iv}_{k_1k_2}(r) + \frac{45}{r^2}\phi'''_{k_1k_2}(r) - \frac{105}{r^3}\phi''_{k_1k_2}(r) + \frac{105}{r^4}\phi'_{k_1k_2}(r) \right) \tag{2.59}$$

$$F(r) = \left(\phi^{vi}_{k_1k_2}(r) - \frac{15}{r}\phi^{v}_{k_1k_2}(r) + \frac{105}{r^2}\phi^{iv}_{k_1k_2}(r) - \frac{420}{r^3}\phi'''_{k_1k_2}(r) + \frac{945}{r^4}\phi''_{k_1k_2}(r) - \frac{945}{r^5}\phi'_{k_1k_2}(r) \right) \tag{2.60}$$

and the primes denote differentiation with respect to the argument.

III MEAN SQUARE DISPLACEMENT

The thermal average of the atomic square displacement is defined as

$$\langle u^2 \rangle = \frac{\mathrm{Tr}\,(u^2 e^{-\beta H})}{\mathrm{Tr}\,(e^{-\beta H})} \tag{3.1}$$

where Tr stands for the algebraic operation of the trace of the operator in the square brackets, and the parameter β has the usual definition of $(k_B T)^{-1}$ with k_B representing Boltzmann's constant and T the temperature. Since H_0 and H_A (in the definition of H) are operators which do not commute, the exponentials in Eq.(3.1) can not be factorized into a product of two exponentials. However, $\exp[-\beta H]$ can be factorized into $\exp[-\beta H_0]$ and a function of H_A as follows

$$e^{-\beta H} = e^{-\beta H_0}\,\hat{S}(\beta) \tag{3.2}$$

where $\hat{S}(\beta)$ is an operator that satisfies the differential equation

$$\frac{\partial \hat{S}(\beta)}{\partial \beta} = -e^{+\beta H_0} H_A e^{-\beta H_0} \hat{S}(\beta) \tag{3.3}$$

Integrating Eq.(3.3) and noting that $\hat{S}(0) = 1$ gives

$$\hat{S}(\beta) = 1 - \int_0^{\beta} \tilde{H}_A(\beta')\,\hat{S}(\beta')\,d\beta' \tag{3.4}$$

where

$$\tilde{H}_A(\beta) = e^{+\beta H_0} H_A e^{-\beta H_0} \tag{3.5}$$

in the interaction representation of operators. Thus, by substituting the definition of H_A (Eq.(2.27)) and integrating Eq.(3.4), $\hat{S}(\beta)$ and consequently $\langle u^2 \rangle$ can be found to any order of anharmonic perturbation through the ordering parameter λ. In what follows, all contributions to $\langle u^2 \rangle$ will be found up to and including order λ^4 of anharmonic perturbation theory.

In the basis of H_0, the Tr in the numerator of Eq.(3.1) can be written as

$$\mathrm{Tr}\left[u^2 e^{-\beta H}\right] = \mathrm{Tr}\left[u^2 e^{-\beta H_0}\hat{S}(\beta)\right] = \sum_n \langle n | u^2 e^{-\beta H_0}\hat{S}(\beta) | n \rangle \tag{3.6}$$

(with a similar result for the denominator), where $|n\rangle$ is the eigenstates of H_0. A partial expansion of the numerator up to second order matrix elements is

$$\sum_n \langle n|u^2 e^{-\beta H_0}\hat{S}(\beta)|n\rangle = \sum_n e^{-\beta E_n^0}\langle n|u^2|n\rangle - \sum_n \sum_m{}' \langle n|u^2|m\rangle \left\{ \lambda^2 \langle m|H_4|n\rangle + \lambda^4 \langle m|H_6|n\rangle \right\} \times$$

$$\times \left[\frac{e^{-\beta E_n^0} - e^{-\beta E_m^0}}{E_m^0 - E_n^0} \right] + \sum_n \sum_m{}' \sum_l{}' \langle n|u^2|m\rangle \left\{ \lambda^2 \langle m|H_3|l\rangle\langle l|H_3|n\rangle + \lambda^4 \langle m|H_4|l\rangle\langle l|H_4|n\rangle + \right.$$

$$\left. + \lambda^4 \left(\langle m|H_3|l\rangle\langle l|H_5|n\rangle + \langle m|H_5|l\rangle\langle l|H_3|n\rangle \right) \right\} \left[\frac{e^{-\beta E_n^0} - e^{-\beta E_m^0}}{\left(E_m^0 - E_n^0\right)\left(E_l^0 - E_n^0\right)} + \frac{e^{-\beta E_m^0} - e^{-\beta E_l^0}}{\left(E_m^0 - E_l^0\right)\left(E_l^0 - E_n^0\right)} \right] - \cdots \tag{3.7}$$

and a partial expansion of the denominator is

$$\sum_n \langle n | e^{-\beta H_0}\hat{S}(\beta) | n \rangle = \sum_n e^{-\beta E_n^0} -$$

$$- \lambda^2 \beta \sum_n e^{-\beta E_n^0} \langle n|H_4|n\rangle - \lambda^4 \beta \sum_n e^{-\beta E_n^0} \langle n|H_6|n\rangle + \cdots \tag{3.8}$$

where H_3, H_4, H_5 and H_6 are simply H_A with n=3, n=4, n=5, and n=6, respectively. In order to generate a contribution the operators contained in Eq.(3.7) are paired. The operators acting on normalized wave functions obey the following relations

$$a(\lambda_i)|\, n(\lambda_1) \ldots n(\lambda_i) \ldots > \;=\; [n(\lambda_i)]^{1/2} \,|\, n(\lambda_1) \ldots n(\lambda_i)-1 \ldots > \qquad (3.9)$$

$$a^{+}(\lambda_i)|\, n(\lambda_1) \ldots n(\lambda_i) \ldots > \;=\; [n(\lambda_i)+1]^{1/2} \,|\, n(\lambda_1) \ldots n(\lambda_i)+1 \ldots > \qquad (3.10)$$

keeping in mind the orthonormality condition

$$< \ldots n(\lambda_i) \ldots | \ldots n(\lambda_i)\pm 1 \ldots > \;=\; \delta_{n(\lambda_i),n(\lambda_i)\pm 1} \;=\; 0 \qquad (3.11)$$

As a result, any term containing an odd number of operators gives zero contribution to MSD.

The first contribution to be derived is the finite temperature quasiharmonic contribution. The first term of Eq.(3.7) is

$$A \;=\; \sum_{n} e^{-\beta E_n^0} < n\,|u^2|\,n > \qquad (3.12)$$

and the first term in the denominator is

$$B \;=\; \sum_{n} e^{-\beta E_n^0} \qquad (3.13)$$

where the relation

$$< n\,|\, e^{-\beta H_0} \;=\; e^{-\beta E_n^0} < n\,| \qquad (3.14)$$

has been used, and

$$E^{0}_{n(\lambda_i)} = (n(\lambda_i) + 1/2)\hbar\omega(\lambda_i) \qquad (3.15)$$

Dividing each term in the denominator by B leaves it in a form that allows it to be expanded using the binomial theorem (the reason for this will be discussed later). Each term in the numerator is also divided by B and as a result the first term of Eq.(3.1) is

$$\langle u^2\rangle_{QH} = B^{-1}\frac{\hbar}{2MN}\sum_{\vec{q}_1 j_1 j_2}[\omega(\vec{q}_1 j_1)\omega(-\vec{q}_1 j_2)]^{-1/2}\sum_{\alpha} e_\alpha(\vec{q}_1 j_1)e_\alpha(-\vec{q}_1 j_2)\times$$

$$\times\sum_{n} e^{-\beta E^{0}_{n}} < n\,|A(\vec{q}_1 j_1)A(-\vec{q}_1 j_2)|\,n > \qquad (3.16)$$

after substituting for $u_\alpha(l)$ and pairing the operators by setting $\vec{q}_2 = -\vec{q}_1$. The summation over α is done according to the orthonormality condition (Eq.(2.15)) and after evaluating the matrix element using Eqs.(3.9) and (3.10), Eq.(3.16) reduces to

$$\langle u^2\rangle_{QH} = B^{-1}\frac{\hbar}{2MN}\sum_{\lambda_1}\sum_{n}[\omega(\lambda_1)]^{-1}[2n(\lambda_1)+1]e^{-\beta E^{0}_{n}} \qquad (3.17)$$

Since each state $n(\lambda_i)$ is independent, B becomes

$$B = \sum_{n(\lambda_1)} e^{-\beta E^{0}_{n(\lambda_1)}}\sum_{n(\lambda_2)} e^{-\beta E^{0}_{n(\lambda_2)}}\cdots \qquad (3.18)$$

and hence, $\langle u^2\rangle_{QH,FT}$ can be rewritten as

$$\langle u^2\rangle_{QH,FT} = \frac{\hbar}{2MN}\sum_{\lambda_1}[\omega(\lambda_1)]^{-1}[2\bar{n}(\lambda_1)+1] \qquad (3.19)$$

where

$$\bar{n}(\lambda_i) = [\exp(\beta\hbar\omega(\lambda_i)) - 1]^{-1} \tag{3.20}$$

After some rearranging, the finite temperature QH contribution is

$$\langle u^2 \rangle_{QH,FT} = \frac{\hbar}{2MN} \sum_{\lambda_1} \frac{\coth[\beta\hbar\omega(\lambda_1)/2]}{\omega(\lambda_1)} \tag{3.21}$$

which, in the high temperature limit ($\beta\hbar\omega(\lambda_i)<<1$) reduces to

$$\langle u^2 \rangle_{QH} = \frac{k_B T}{MN} \sum_{\lambda_1} \frac{1}{\omega^2(\lambda_1)} \tag{3.22}$$

where $\coth[\frac{1}{2}\beta\hbar\omega(\lambda_i)]$ has been approximated by $2/\beta\hbar\omega(\lambda_i)$ in the high temperature limit.

In order to facilitate the discussion of the individual anharmonic contributions, these contributions have been depicted by diagrams. Shukla and Cowley (1971) have derived the diagrams associated with the anharmonic contributions to the free energy to $O(\lambda^4)$ PT. The free energy diagrams of $O(\lambda^2)$ are shown in Fig. 1, and all of the free energy diagrams of $O(\lambda^4)$ are shown in Fig. 2. The diagrams corresponding to MSD can be generated by inserting, in all possible ways, the u^2-vertex (denoted by $\odot$) in the free energy diagrams. The resulting MSD diagrams of $O(\lambda^2)$ are shown in Fig. 1, and all of the MSD diagrams of $O(\lambda^4)$ are shown in Fig. 3. For example, diagram $\langle u^2 \rangle_{1(a)}$ is generated from diagram $F_{1(a)}$ using

Figure 1

Diagrams of $O(\lambda^2)$

(A) Free Energy

(B) Mean Square Displacement

(A)

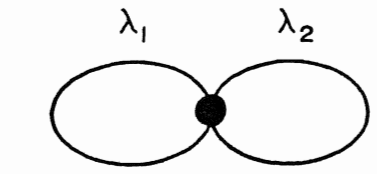
λ_1
λ_2

I(a)

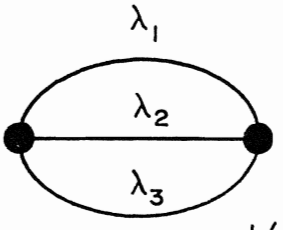
λ_1
λ_2
λ_3

I(b)

(B)

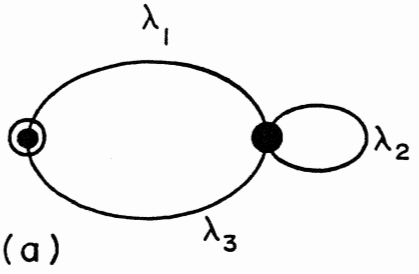
λ_1
λ_2
λ_3

I(a)

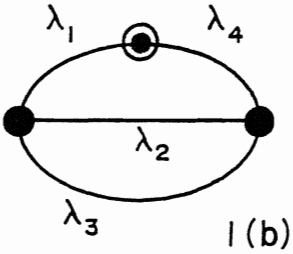
λ_1
λ_4
λ_2
λ_3

I(b)

Figure 2

Free Energy Diagrams of $O(\lambda^4)$

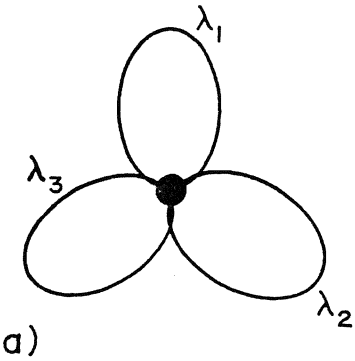

2(a)

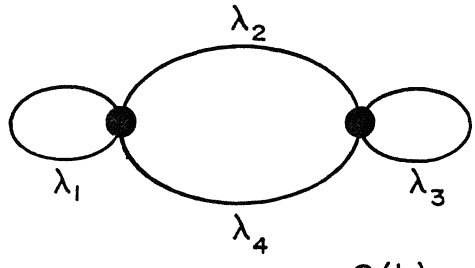

2(b)

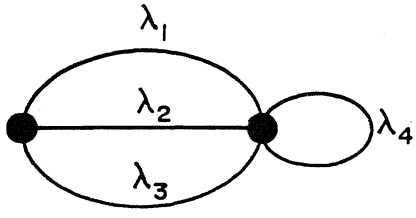

2(c)

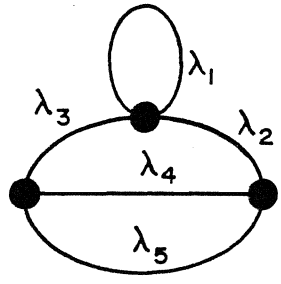

2(d)

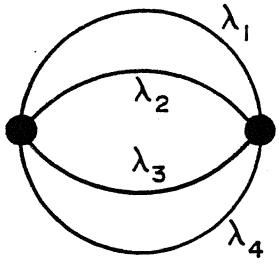

2(e)

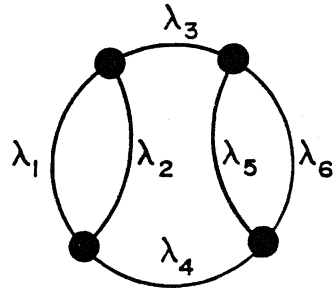

2(f)

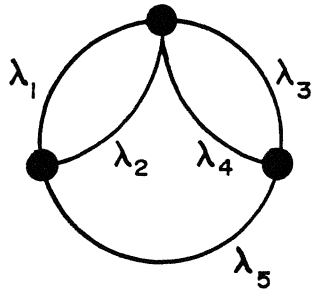

2(g)

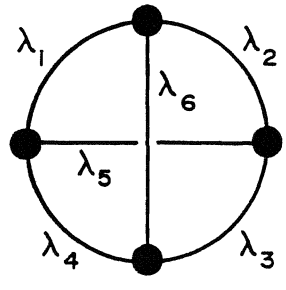

2(h)

Figure 3

Mean Square Displacement Diagrams of $O(\lambda^4)$

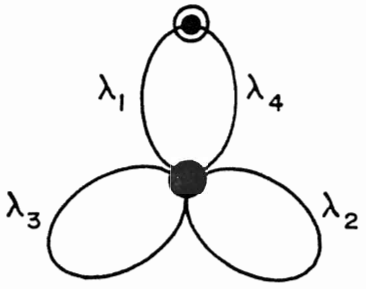

2(a)

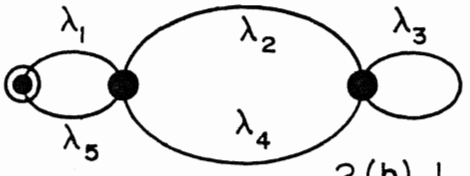

2(b), 1

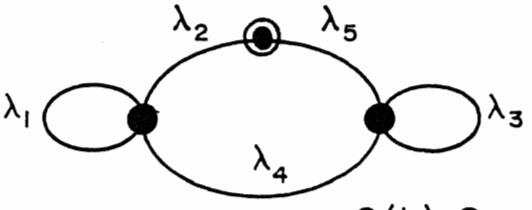

2(b), 2

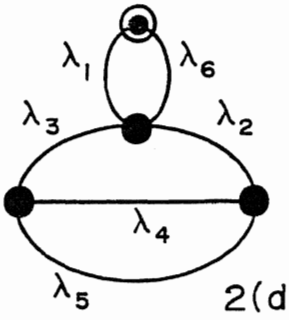

2(d), 1

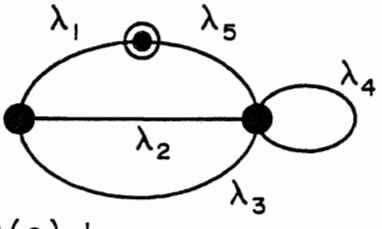

2(c), 1

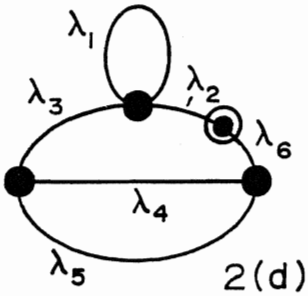

2(d), 2

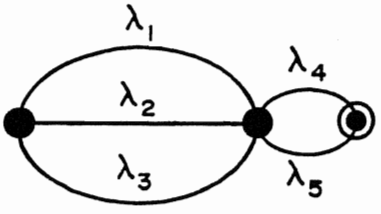

2(c), 2

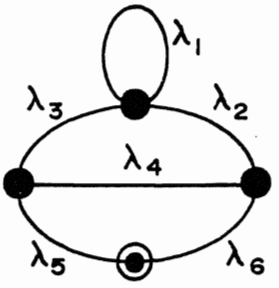

2(d), 3

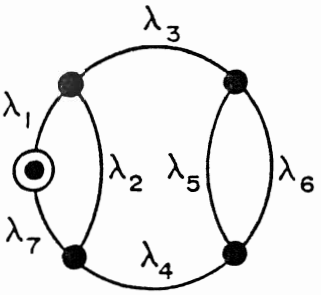

2(f),1

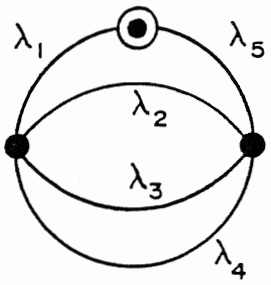

2(e)

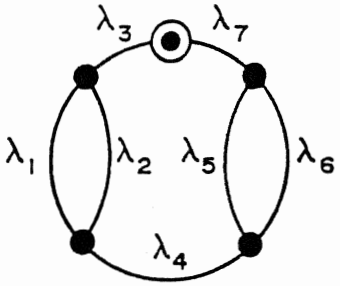

2(f),2

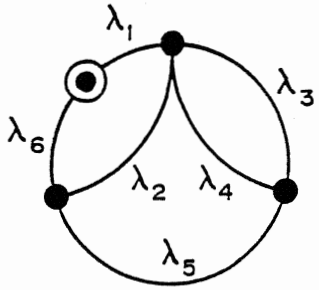

2(g),1

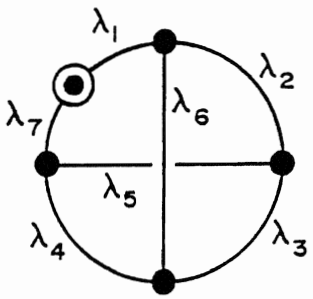

2(h)

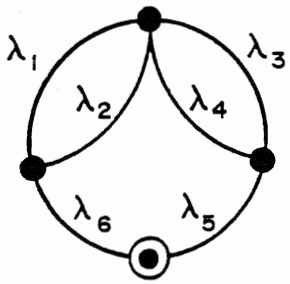

2(g),2

the above method, noting that the same diagram results regardless of which phonon line is selected for the insertion of the u^2-vertex.

Furthermore, the above mentioned mean square displacement diagrams serve another purpose. They are a pictorial representation of how the operators are paired for that particular diagram. For example, the contribution $\langle u^2 \rangle_{1(a)}$ is

$$\left\langle u^2 \right\rangle_{1(a)} = -B^{-1}\left(\frac{12\hbar}{2MN}\right)\sum_{\lambda_1\lambda_2\lambda_3}\frac{V(-\lambda_1;\lambda_2;-\lambda_2;\lambda_3)e^{i(\vec{q}_1-\vec{q}_3)\bullet\vec{x}(l)}}{\left[\omega(\lambda_1)\omega(-\lambda_3)\right]^{1/2}}\sum_{\alpha} e_\alpha(\lambda_1)e_\alpha(-\lambda_3)\times$$

$$\times\sum_n\sum_m{}' e^{-\beta E_n^0}\langle n\,|\,A(\lambda_1)A(-\lambda_3)\,|\,m\rangle\langle m\,|\,A(-\lambda_1)A(\lambda_2)A(-\lambda_2)A(\lambda_3)\,|\,n\rangle\left[\frac{e^{-\beta E_n^0}-e^{-\beta E_m^0}}{E_m^0-E_n^0}\right] \tag{3.23}$$

where the factor of 12 represents the number of ways in which the operators can be paired for this contribution. At this point, the reason for dividing each term in the numerator and denominator by B and expanding the denominator, as previously mentioned, is discussed. In Eq.(3.23), if the limit as m approaches n is taken, Eq.(3.23) reduces to

$$\left\langle u^2 \right\rangle_{1(a)\,m\to n} = -3\beta B^{-1}\left(\frac{\hbar}{2MN}\right)\sum_{\lambda_1\lambda_2\lambda_3}\frac{V(\lambda_2;-\lambda_2;\lambda_3;-\lambda_3)}{\omega(\lambda_1)}\times$$

$$\times\coth[\beta\hbar\omega(\lambda_1)/2]\coth[\beta\hbar\omega(\lambda_2)/2]\coth[\beta\hbar\omega(\lambda_3)/2] \tag{3.24}$$

This is simply the product of the finite temperature quasiharmonic term and the second term in the denominator (Eq.(3.8)). Therefore, when the denominator is expanded up to

its linear term, and multiplied with the numerator the terms like Eq.(3.24) algebraically cancel.

After evaluating the matrix elements, Eq.(3.23) reduces to

$$\left\langle u^2\right\rangle_{1(a),FT} = -\frac{12}{MN}\sum_{\lambda_1\lambda_2\lambda_3}\frac{V(-\lambda_1;\lambda_2;-\lambda_2;\lambda_3)e^{i(\vec{q}_1-\vec{q}_3)\bullet\vec{x}(l)}}{\left[\omega(\lambda_1)\omega(-\lambda_3)\right]^{1/2}}\sum_{\alpha}e_\alpha(\lambda_1)e_\alpha(-\lambda_3)\times$$

$$\times\coth[\beta\hbar\omega(\lambda_2)/2]\left[\frac{\bar{n}(\lambda_1)+\bar{n}(\lambda_3)+1}{\omega(\lambda_1)+\omega(\lambda_3)}+\frac{\bar{n}(\lambda_3)-\bar{n}(\lambda_1)}{\omega(\lambda_1)-\omega(\lambda_3)}\right] \qquad (3.25)$$

where the summation over n gives $\bar{n}$. All that remains now is for the momentum to be conserved at the $\langle u^2\rangle$-vertex, resulting in $\vec{q}_3 = \vec{q}_1$. The orthonormality condition (Eq.(2.15)) then gives $j_3 = j_1$. However, to consider this condition, the limit must be taken. As j_3 approaches j_1, $\langle u^2\rangle_{1(a)}$ becomes

$$\left\langle u^2\right\rangle_{1(a),FT} = -\frac{12}{MN}\sum_{\lambda_1\lambda_2}\frac{V(\lambda_1;-\lambda_1;\lambda_2;-\lambda_2)}{\omega(\lambda_1)}\coth[\beta\hbar\omega(\lambda_2)/2]\times$$

$$\times\left[\frac{\coth[\beta\hbar\omega(\lambda_1)/2]}{2\omega(\lambda_1)}+\beta\hbar\bar{n}(\lambda_1)\left[\bar{n}(\lambda_1)+1\right]\right] \qquad (3.26)$$

In a similar fashion, the remaining $O(\lambda^2)$ anharmonic contribution to MSD is

$$\left\langle u^2\right\rangle_{1(b),FT} = \frac{18}{\hbar MN}\sum_{\lambda_1\lambda_2\lambda_3}\frac{\left|V(\lambda_1;-\lambda_2;-\lambda_3)\right|^2}{\omega(\lambda_1)}\sum_{k_1k_2k_3}\left[\frac{-k_1k_2k_3}{\omega(\lambda_1)}\left\{\frac{N_1N_2N_3}{k_1\omega(\lambda_1)+k_2\omega(\lambda_2)+k_3\omega(\lambda_3)}\right\}-\right.$$

$$\left.-k_2k_3\left\{\frac{\beta\hbar N_1(N_1+1)N_2N_3}{k_1\omega(\lambda_1)+k_2\omega(\lambda_2)+k_3\omega(\lambda_3)}+\frac{N_1N_2N_3}{\left[k_1\omega(\lambda_1)+k_2\omega(\lambda_2)+k_3\omega(\lambda_3)\right]^2}\right\}\right] \qquad (3.27)$$

where $N_i = \bar{n}(\lambda_i)$ for $k_i = +1$ and $N_i = -[\bar{n}(\lambda_i)+1]$ for $k_i = -1$ and

i is an integer (i=1,2,3). The following are some of the $O(\lambda^4)$ contributions to MSD evaluated in the same manner

$$\langle u^2\rangle_{2(a),FT} = -\frac{90}{MN}\sum_{\lambda_1\lambda_2\lambda_3}\frac{V(\lambda_1;-\lambda_1;\lambda_2;-\lambda_2;\lambda_3;-\lambda_3)}{\omega(\lambda_1)}\coth[\beta\hbar\omega(\lambda_2)/2]\coth[\beta\hbar\omega(\lambda_3)/2]\times$$

$$\times\left[\frac{\coth[\beta\hbar\omega(\lambda_1)/2]}{2\omega(\lambda_1)} + \beta\hbar\bar{n}(\lambda_1)\left[\bar{n}(\lambda_1)+1\right]\right] \tag{3.28}$$

$$\langle u^2\rangle_{2(b),1,FT} = \frac{144}{\hbar MN}\sum_{\lambda_1\lambda_2\lambda_3\lambda_4}\frac{V(\lambda_1;-\lambda_1;\lambda_2;-\lambda_4)V(-\lambda_2;\lambda_3;-\lambda_3;\lambda_4)}{\omega(\lambda_1)}\coth[\beta\hbar\omega(\lambda_3)/2]\times$$

$$\times\left\{\frac{\coth[\beta\hbar\omega(\lambda_1)/2]}{\omega(\lambda_1)} + 2\beta\hbar\bar{n}(\lambda_1)\left(\bar{n}(\lambda_1)+1\right)\right\}\times$$

$$\times\left[\frac{\left(\bar{n}(\lambda_2)+1\right)\left(\bar{n}(\lambda_3)+1\right) - \bar{n}(\lambda_2)\,\bar{n}(\lambda_3)}{\omega(\lambda_2)+\omega(\lambda_3)} + \frac{\left(\bar{n}(\lambda_2)+1\right)\bar{n}(\lambda_3) - \bar{n}(\lambda_2)\left(\bar{n}(\lambda_3)+1\right)}{\omega(\lambda_2)-\omega(\lambda_3)}\right] \tag{3.29}$$

$$\langle u^2\rangle_{2(b),2,FT} = \frac{144}{\hbar MN}\sum_{\lambda_1\lambda_2\lambda_3\lambda_4}\frac{V(\lambda_1;-\lambda_1;\lambda_2;-\lambda_4)V(-\lambda_2;\lambda_3;-\lambda_3;\lambda_4)}{\omega(\lambda_2)}\coth[\beta\hbar\omega(\lambda_1)/2]\coth[\beta\hbar\omega(\lambda_3)/2]\times$$

$$\times\left\{\frac{1}{2\omega(\lambda_2)}\left[\frac{\coth[\beta\hbar\omega(\lambda_2)/2]+\coth[\beta\hbar\omega(\lambda_4)/2]}{\omega(\lambda_2)+\omega(\lambda_4)} + \frac{\coth[\beta\hbar\omega(\lambda_4)/2]-\coth[\beta\hbar\omega(\lambda_2)/2]}{\omega(\lambda_2)-\omega(\lambda_4)}\right] + \right.$$

$$+\beta\hbar\frac{\bar{n}(\lambda_2)\left(\bar{n}(\lambda_2)+1\right)}{\omega(\lambda_2)+\omega(\lambda_4)} + \frac{\left(\bar{n}(\lambda_2)+1\right)\left(\bar{n}(\lambda_4)+1\right) - \bar{n}(\lambda_2)\,\bar{n}(\lambda_4)}{\left(\omega(\lambda_2)+\omega(\lambda_4)\right)^2} -$$

$$\left.-\beta\hbar\frac{\bar{n}(\lambda_2)\left(\bar{n}(\lambda_2)+1\right)}{\omega(\lambda_2)-\omega(\lambda_4)} + \frac{\left(\bar{n}(\lambda_2)+1\right)\bar{n}(\lambda_4) - \bar{n}(\lambda_2)\left(\bar{n}(\lambda_4)+1\right)}{\left(\omega(\lambda_2)-\omega(\lambda_4)\right)^2}\right\} \tag{3.30}$$

$$\langle u^2\rangle_{2(c),1,FT} = \frac{360}{\hbar MN}\sum_{\lambda_1\lambda_2\lambda_3\lambda_4}\frac{V(\lambda_1;-\lambda_2;-\lambda_3)V(-\lambda_1;\lambda_2;\lambda_3;\lambda_4;-\lambda_4)}{\omega(\lambda_1)}\sum_{k_1k_2k_3}\Bigg[\frac{-k_1k_2k_3}{\omega(\lambda_1)}\Bigg\{\frac{N_1N_2N_3}{k_1\omega(\lambda_1)+k_2\omega(\lambda_2)+k_3\omega(\lambda_3)}\Bigg\} -$$

$$- k_2k_3\Bigg\{\frac{\beta\hbar N_1[N_1+1]N_2N_3}{k_1\omega(\lambda_1)+k_2\omega(\lambda_2)+k_3\omega(\lambda_3)} + \frac{N_1N_2N_3}{\left[k_1\omega(\lambda_1)+k_2\omega(\lambda_2)+k_3\omega(\lambda_3)\right]^2}\Bigg\}\Bigg]\coth[\beta\hbar\omega(\lambda_4)/2] \tag{3.31}$$

$$\langle u^2\rangle_{2(e),FT} = \frac{96}{\hbar MN}\sum_{\lambda_1\lambda_2\lambda_3\lambda_4}\frac{\left|V(\lambda_1;-\lambda_2;-\lambda_3;-\lambda_4)\right|^2}{\omega(\lambda_1)}\sum_{k_1k_2k_3k_4}\Bigg[\frac{-k_1k_2k_3k_4}{\omega(\lambda_1)}\Bigg\{\frac{N_1N_2N_3N_4}{k_1\omega(\lambda_1)+k_2\omega(\lambda_2)+k_3\omega(\lambda_3)+k_4\omega(\lambda_4)}\Bigg\} -$$

$$- k_2k_3k_4\Bigg\{\frac{\beta\hbar N_1[N_1+1]N_2N_3N_4}{k_1\omega(\lambda_1)+k_2\omega(\lambda_2)+k_3\omega(\lambda_3)+k_4\omega(\lambda_4)} + \frac{N_1N_2N_3N_4}{\left[k_1\omega(\lambda_1)+k_2\omega(\lambda_2)+k_3\omega(\lambda_3)+k_4\omega(\lambda_4)\right]^2}\Bigg\}\Bigg] \tag{3.32}$$

After taking the high temperature limit, the above $O(\lambda^2)$ and $O(\lambda^4)$ expressions are listed in Table 3.1. At this point, it was found that these high temperature MSD expressions could be generated from the high temperature free energy expressions of Shukla and Cowley (1971). These free energy expressions are listed in Table 3.2. To generate a high temperature MSD expression the corresponding free energy diagram in question must be modified as follows. First, multiply the expression by the numerical factor

-2×[the number of phonon lines in the F diagram into which the u^2-vertex can be inserted to yield an identical MSD diagram]/MN

where the 1/MN comes from the insertion of the u^2-vertex. Secondly, an extra $\omega^2(\lambda_i)$ must be included in the denominator of the expression corresponding to the λ_i phonon line which

TABLE 3.1 (a)

HIGH TEMPERATURE LIMITS FOR THE VARIOUS CONTRIBUTIONS TO THE MEAN SQUARE DISPLACEMENT

DIAGRAM	HIGH TEMPERATURE LIMIT
$\langle u^2 \rangle_{1(a)}$	$-\frac{12}{\beta^2 MN}\left(\frac{2}{\hbar}\right)^2 \sum_{\lambda_1 \lambda_2} \frac{V(\lambda_1;-\lambda_1;\lambda_2;-\lambda_2)}{\omega^3(\lambda_1)\omega(\lambda_2)}$
$\langle u^2 \rangle_{1(b)}$	$\frac{18}{\beta^2 MN}\left(\frac{2}{\hbar}\right)^3 \sum_{\lambda_1 \lambda_2 \lambda_3} \frac{\lvert V(\lambda_1;-\lambda_2;-\lambda_3)\rvert^2}{\omega^3(\lambda_1)\omega(\lambda_2)\omega(\lambda_3)}$
$\langle u^2 \rangle_{2(a)}$	$-\frac{90}{\beta^3 MN}\left(\frac{2}{\hbar}\right)^3 \sum_{\lambda_1 \lambda_2 \lambda_3} \frac{V(\lambda_1;-\lambda_1;\lambda_2;-\lambda_2;\lambda_3;-\lambda_3)}{\omega^3(\lambda_1)\omega(\lambda_2)\omega(\lambda_3)}$
$\langle u^2 \rangle_{2(b),1}$	$\frac{144}{\beta^3 MN}\left(\frac{2}{\hbar}\right)^4 \sum_{\lambda_1 \lambda_2 \lambda_3 \lambda_4} \frac{V(\lambda_1;-\lambda_1;\lambda_2;-\lambda_4)V(-\lambda_2;\lambda_3;-\lambda_3;\lambda_4)}{\omega^3(\lambda_1)\omega(\lambda_2)\omega(\lambda_3)\omega(\lambda_4)}$
$\langle u^2 \rangle_{2(b),2}$	$\frac{144}{\beta^3 MN}\left(\frac{2}{\hbar}\right)^4 \sum_{\lambda_1 \lambda_2 \lambda_3 \lambda_4} \frac{V(\lambda_1;-\lambda_1;\lambda_2;-\lambda_4)V(-\lambda_2;\lambda_3;-\lambda_3;\lambda_4)}{\omega(\lambda_1)\omega^3(\lambda_2)\omega(\lambda_3)\omega(\lambda_4)}$
$\langle u^2 \rangle_{2(c),1}$	$\frac{360}{\beta^3 MN}\left(\frac{2}{\hbar}\right)^4 \sum_{\lambda_1 \lambda_2 \lambda_3 \lambda_4} \frac{V(\lambda_1;-\lambda_2;-\lambda_3)V(-\lambda_1;\lambda_2;\lambda_3;\lambda_4;-\lambda_4)}{\omega^3(\lambda_1)\omega(\lambda_2)\omega(\lambda_3)\omega(\lambda_4)}$
$\langle u^2 \rangle_{2(c),2}$	$\frac{120}{\beta^3 MN}\left(\frac{2}{\hbar}\right)^4 \sum_{\lambda_1 \lambda_2 \lambda_3 \lambda_4} \frac{V(\lambda_1;-\lambda_2;-\lambda_3)V(-\lambda_1;\lambda_2;\lambda_3;\lambda_4;-\lambda_4)}{\omega(\lambda_1)\omega(\lambda_2)\omega(\lambda_3)\omega^3(\lambda_4)}$
$\langle u^2 \rangle_{2(d),1}$	$-\frac{216}{\beta^3 MN}\left(\frac{2}{\hbar}\right)^5 \sum_{\lambda_1 \lambda_2 \lambda_3 \lambda_4 \lambda_5} \frac{V(\lambda_1;-\lambda_1;\lambda_2;-\lambda_3)V(-\lambda_2;\lambda_4;\lambda_5)V(\lambda_3;-\lambda_4;-\lambda_5)}{\omega^3(\lambda_1)\omega(\lambda_2)\omega(\lambda_3)\omega(\lambda_4)\omega(\lambda_5)}$

TABLE 3.1 (b)

HIGH TEMPERATURE LIMITS FOR THE VARIOUS CONTRIBUTIONS TO THE MEAN SQUARE DISPLACEMENT

DIAGRAM	HIGH TEMPERATURE LIMIT
$\langle u^2 \rangle_{2(d),2}$	$-\frac{432}{\beta^3 MN}\left(\frac{2}{\hbar}\right)^5 \sum_{\lambda_1\lambda_2\lambda_3\lambda_4\lambda_5} \frac{V(\lambda_1;-\lambda_1;\lambda_2;-\lambda_3)V(-\lambda_2;\lambda_4;\lambda_5)V(\lambda_3;-\lambda_4;-\lambda_5)}{\omega(\lambda_1)\omega^3(\lambda_2)\omega(\lambda_3)\omega(\lambda_4)\omega(\lambda_5)}$
$\langle u^2 \rangle_{2(d),3}$	$-\frac{432}{\beta^3 MN}\left(\frac{2}{\hbar}\right)^5 \sum_{\lambda_1\lambda_2\lambda_3\lambda_4\lambda_5} \frac{V(\lambda_1;-\lambda_1;\lambda_2;-\lambda_3)V(-\lambda_2;\lambda_4;\lambda_5)V(\lambda_3;-\lambda_4;-\lambda_5)}{\omega(\lambda_1)\omega(\lambda_2)\omega(\lambda_3)\omega(\lambda_4)\omega^3(\lambda_5)}$
$\langle u^2 \rangle_{2(e)}$	$\frac{96}{\beta^3 MN}\left(\frac{2}{\hbar}\right)^4 \sum_{\lambda_1\lambda_2\lambda_3\lambda_4} \frac{\lvert V(\lambda_1;-\lambda_2;-\lambda_3;-\lambda_4)\rvert^2}{\omega^3(\lambda_1)\omega(\lambda_2)\omega(\lambda_3)\omega(\lambda_4)}$
$\langle u^2 \rangle_{2(f),1}$	$\frac{648}{\beta^3 MN}\left(\frac{2}{\hbar}\right)^6 \sum_{\lambda_1\lambda_2\lambda_3\lambda_4\lambda_5\lambda_6} \frac{V(\lambda_1;-\lambda_2;-\lambda_4)V(-\lambda_1;\lambda_2;\lambda_3)V(-\lambda_3;\lambda_5;\lambda_6)V(\lambda_4;-\lambda_5;-\lambda_6)}{\omega^3(\lambda_1)\omega(\lambda_2)\omega(\lambda_3)\omega(\lambda_4)\omega(\lambda_5)\omega(\lambda_6)}$
$\langle u^2 \rangle_{2(f),2}$	$\frac{324}{\beta^3 MN}\left(\frac{2}{\hbar}\right)^6 \sum_{\lambda_1\lambda_2\lambda_3\lambda_4\lambda_5\lambda_6} \frac{V(\lambda_1;-\lambda_2;-\lambda_4)V(-\lambda_1;\lambda_2;\lambda_3)V(-\lambda_3;\lambda_5;\lambda_6)V(\lambda_4;-\lambda_5;-\lambda_6)}{\omega(\lambda_1)\omega(\lambda_2)\omega^3(\lambda_3)\omega(\lambda_4)\omega(\lambda_5)\omega(\lambda_6)}$
$\langle u^2 \rangle_{2(g),1}$	$-\frac{864}{\beta^3 MN}\left(\frac{2}{\hbar}\right)^5 \sum_{\lambda_1\lambda_2\lambda_3\lambda_4\lambda_5} \frac{V(\lambda_1;-\lambda_2;-\lambda_5)V(-\lambda_1;\lambda_2;\lambda_3;\lambda_4)V(-\lambda_3;-\lambda_4;\lambda_5)}{\omega^3(\lambda_1)\omega(\lambda_2)\omega(\lambda_3)\omega(\lambda_4)\omega(\lambda_5)}$
$\langle u^2 \rangle_{2(g),2}$	$-\frac{216}{\beta^3 MN}\left(\frac{2}{\hbar}\right)^5 \sum_{\lambda_1\lambda_2\lambda_3\lambda_4\lambda_5} \frac{V(\lambda_1;-\lambda_2;-\lambda_5)V(-\lambda_1;\lambda_2;\lambda_3;\lambda_4)V(-\lambda_3;-\lambda_4;\lambda_5)}{\omega(\lambda_1)\omega(\lambda_2)\omega(\lambda_3)\omega(\lambda_4)\omega^3(\lambda_5)}$
$\langle u^2 \rangle_{2(h)}$	$\frac{648}{\beta^3 MN}\left(\frac{2}{\hbar}\right)^6 \sum_{\lambda_1\lambda_2\lambda_3\lambda_4\lambda_5\lambda_6} \frac{V(\lambda_1;-\lambda_4;-\lambda_5)V(-\lambda_1;\lambda_2;\lambda_6)V(-\lambda_2;\lambda_3;\lambda_5)V(-\lambda_3;\lambda_4;-\lambda_6)}{\omega^3(\lambda_1)\omega(\lambda_2)\omega(\lambda_3)\omega(\lambda_4)\omega(\lambda_5)\omega(\lambda_6)}$

TABLE 3.2

HIGH TEMPERATURE LIMITS FOR THE VARIOUS CONTRIBUTIONS TO THE FREE ENERGY

DIAGRAM	HIGH TEMPERATURE LIMIT
$F_{1(a)}$	$\frac{3}{\beta^2}\left(\frac{2}{\hbar}\right)^2 \sum_{\lambda_1\lambda_2} \frac{V(\lambda_1;-\lambda_1;\lambda_2;-\lambda_2)}{\omega(\lambda_1)\omega(\lambda_2)}$
$F_{1(b)}$	$-\frac{3}{\beta^2}\left(\frac{2}{\hbar}\right)^3 \sum_{\lambda_1\lambda_2\lambda_3} \frac{\left\|V(\lambda_1;-\lambda_2;-\lambda_3)\right\|^2}{\omega(\lambda_1)\omega(\lambda_2)\omega(\lambda_3)}$
$F_{2(a)}$	$\frac{15}{\beta^3}\left(\frac{2}{\hbar}\right)^3 \sum_{\lambda_1\lambda_2\lambda_3} \frac{V(\lambda_1;-\lambda_1;\lambda_2;-\lambda_2;\lambda_3;-\lambda_3)}{\omega(\lambda_1)\omega(\lambda_2)\omega(\lambda_3)}$
$F_{2(b)}$	$-\frac{36}{\beta^3}\left(\frac{2}{\hbar}\right)^4 \sum_{\lambda_1\lambda_2\lambda_3\lambda_4} \frac{V(\lambda_1;-\lambda_1;\lambda_2;-\lambda_4)V(-\lambda_2;\lambda_3;-\lambda_3;\lambda_4)}{\omega(\lambda_1)\omega(\lambda_2)\omega(\lambda_3)\omega(\lambda_4)}$
$F_{2(c)}$	$-\frac{60}{\beta^3}\left(\frac{2}{\hbar}\right)^4 \sum_{\lambda_1\lambda_2\lambda_3\lambda_4} \frac{V(\lambda_1;-\lambda_2;-\lambda_3)V(-\lambda_1;\lambda_2;\lambda_3;\lambda_4;-\lambda_4)}{\omega(\lambda_1)\omega(\lambda_2)\omega(\lambda_3)\omega(\lambda_4)}$
$F_{2(d)}$	$\frac{108}{\beta^3}\left(\frac{2}{\hbar}\right)^5 \sum_{\lambda_1\lambda_2\lambda_3\lambda_4\lambda_5} \frac{V(\lambda_1;-\lambda_1;\lambda_2;-\lambda_3)V(-\lambda_2;\lambda_4;\lambda_5)V(\lambda_3;-\lambda_4;-\lambda_5)}{\omega(\lambda_1)\omega(\lambda_2)\omega(\lambda_3)\omega(\lambda_4)\omega(\lambda_5)}$
$F_{2(e)}$	$-\frac{12}{\beta^3}\left(\frac{2}{\hbar}\right)^4 \sum_{\lambda_1\lambda_2\lambda_3\lambda_4} \frac{\left\|V(\lambda_1;-\lambda_2;-\lambda_3;-\lambda_4)\right\|^2}{\omega(\lambda_1)\omega(\lambda_2)\omega(\lambda_3)\omega(\lambda_4)}$
$F_{2(f)}$	$-\frac{81}{\beta^3}\left(\frac{2}{\hbar}\right)^6 \sum_{\lambda_1\lambda_2\lambda_3\lambda_4\lambda_5\lambda_6} \frac{V(\lambda_1;-\lambda_2;-\lambda_4)V(-\lambda_1;\lambda_2;\lambda_3)V(-\lambda_3;\lambda_5;\lambda_6)V(\lambda_4;-\lambda_5;-\lambda_6)}{\omega(\lambda_1)\omega(\lambda_2)\omega(\lambda_3)\omega(\lambda_4)\omega(\lambda_5)\omega(\lambda_6)}$
$F_{2(g)}$	$\frac{108}{\beta^3}\left(\frac{2}{\hbar}\right)^5 \sum_{\lambda_1\lambda_2\lambda_3\lambda_4\lambda_5} \frac{V(\lambda_1;-\lambda_2;-\lambda_5)V(-\lambda_1;\lambda_2;\lambda_3;\lambda_4)V(-\lambda_3;-\lambda_4;\lambda_5)}{\omega(\lambda_1)\omega(\lambda_2)\omega(\lambda_3)\omega(\lambda_4)\omega(\lambda_5)}$
$F_{2(h)}$	$-\frac{54}{\beta^3}\left(\frac{2}{\hbar}\right)^6 \sum_{\lambda_1\lambda_2\lambda_3\lambda_4\lambda_5\lambda_6} \frac{V(\lambda_1;-\lambda_4;-\lambda_5)V(-\lambda_1;\lambda_2;\lambda_6)V(-\lambda_2;\lambda_3;\lambda_5)V(-\lambda_3;\lambda_4;-\lambda_6)}{\omega(\lambda_1)\omega(\lambda_2)\omega(\lambda_3)\omega(\lambda_4)\omega(\lambda_5)\omega(\lambda_6)}$

was selected for the insertion of the u^2-vertex. The remaining high temperature MSD expressions were then derived in this manner. These high temperature limit expressions are listed in Table 3.1. As an example of this, consider the diagram 2(d) of F. Three MSD diagrams are generated from it. The first is generated by inserting the u^2-vertex in the loop λ_1. This results in MSD diagram 2(d),1 of Fig. 3. The MSD diagram 2(d),2 is generated by inserting the u^2-vertex in either phonon line λ_2 or λ_3 of 2(d) F. Finally, if the insertion is made in either phonon line λ_4 or λ_5 of 2(d) F then MSD diagram 2(d),3 is generated.

IV PEIERLS APPROXIMATION

In the previous section the high temperature expressions for the anharmonic contributions to MSD were derived. By implementing the Peierls approximation (Peierls (1955)), the anharmonic coefficients are cast in a form which allows the wave vector sums to be evaluated analytically; thereby greatly reducing the computer time involved in these calculations.

The definition of the monatomic anharmonic coefficient is

$$V(\vec{q}_1 j_1;\ldots;\vec{q}_n j_n) = \frac{1}{2}\left(\frac{\hbar}{2}\right)^{n/2}\frac{N^{1-n/2}}{M^{n/2}}\left(\frac{1}{n!}\right)\frac{\Delta(\vec{q}_1+\ldots+\vec{q}_n)}{[\omega(\vec{q}_1 j_1)\ldots\omega(\vec{q}_n j_n)]^{1/2}}\sum_1{}'\sum_{\alpha_1\ldots\alpha_n}\phi_{\alpha_1\ldots\alpha_n}(l)\times$$

$$\times e_{\alpha_1}(\vec{q}_1 j_1)\ldots e_{\alpha_n}(\vec{q}_n j_n)\left(1-e^{i\vec{q}_1\bullet\vec{x}(l)}\right)\ldots\left(1-e^{i\vec{q}_n\bullet\vec{x}(l)}\right) \qquad (4.1)$$

The crux of the Peierls approximation is to replace the Δ function, tensors and the phase factors by the following

$$\Delta(\vec{q}_1+\ldots+\vec{q}_n)\sum_1{}'\sum_{\alpha_1\ldots\alpha_n}\phi_{\alpha_1\ldots\alpha_n}(l)e_{\alpha_1}(\vec{q}_1 j_1)\ldots e_{\alpha_n}(\vec{q}_n j_n)\left(1-e^{i\vec{q}_1\bullet\vec{x}(l)}\right)\ldots\left(1-e^{i\vec{q}_n\bullet\vec{x}(l)}\right) =$$

$$= M^{n/2}\Delta(\vec{q}_1+\ldots+\vec{q}_n)\omega(\vec{q}_1 j_1)\ldots\omega(\vec{q}_n j_n)C(\vec{q}_1 j_1;\ldots;\vec{q}_n j_n) \qquad (4.2)$$

where the functions $C(\vec{q}_1 j_1;\ldots;\vec{q}_n j_n)$ are treated as a slowly varying functions of their arguments (in other words a constant). Because of this condition, $C(\vec{q}_1 j_1;\ldots;\vec{q}_n j_n)$ is found by summing both sides of Eq.(4.2) over the arguments

$\vec{q}_1 j_1, \ldots, \vec{q}_n j_n$. With this replacement, the coefficient becomes

$$V(\vec{q}_1 j_1;\ldots;\vec{q}_n j_n) = \frac{1}{2}\left(\frac{\hbar}{2}\right)^{n/2} \frac{N^{1-n/2}}{n!} \Delta(\vec{q}_1 + \ldots + \vec{q}_n)[\omega(\vec{q}_1 j_1)\ldots\omega(\vec{q}_n j_n)]^{1/2} C(\vec{q}_1 j_1;\ldots;\vec{q}_n j_n) \tag{4.3}$$

which is now substituted into the MSD and free energy expressions given in Sec.III in Tables 3.1 and 3.2.

As an example, the contribution from diagram $\langle u^2 \rangle_{1(b)}$ becomes (after substitution of Eq.(4.3))

$$\left\langle u^2 \right\rangle_{1(b)} = \frac{(k_B T)^2}{8N^2 M} \left| C(\vec{q}_1 j_1;\vec{q}_2 j_2;\vec{q}_3 j_3) \right|^2 \sum_{\vec{q}_1\vec{q}_2\vec{q}_3} \sum_{j_1 j_2 j_3} \frac{\Delta(\vec{q}_1 + \vec{q}_2 + \vec{q}_3)}{\omega^2(\vec{q}_1 j_1)}$$

$$= \frac{9(k_B T)^2}{8N^2 M} \left| C(\vec{q}_1 j_1;\vec{q}_2 j_2;\vec{q}_3 j_3) \right|^2 \frac{1}{N} \sum_{l} \left[\sum_{\vec{q}} e^{i\vec{q}\cdot\vec{x}(l)} \right]^2 \sum_{\vec{q}_1 j_1} \frac{e^{i\vec{q}_1\cdot\vec{x}(l)}}{\omega^2(\vec{q}_1 j_1)} \tag{4.4}$$

where the following plane wave representation of the Δ function has been used

$$\Delta(\vec{q}_1 + \ldots + \vec{q}_n) = \sum_{l} e^{i(\vec{q}_1 + \ldots + \vec{q}_n)\cdot\vec{x}(l)} \tag{4.5}$$

with the sum over l including all direct lattice vectors. The sum over $\vec{q}$ can be carried further by using the relation

$$\sum_{\vec{q}} e^{i\vec{q}\cdot\vec{x}(l)} = N\Delta(l) \tag{4.6}$$

where the Δ function is unity if its argument is the zero vector and zero otherwise. Using this gives

$$\left\langle u^2 \right\rangle_{1(b)} = \frac{9(k_B T)^2}{8NM} \left| C(\vec{q}_1 j_1;\vec{q}_2 j_2;\vec{q}_3 j_3) \right|^2 \sum_{\vec{q} j} \frac{1}{\omega^2(\vec{q} j)} \tag{4.7}$$

The sum appearing in Eq.(4.7) arises in all of the MSD contributions in the Peierls approximation. If a similar treatment is carried out for any of the contributions listed in Table 3.2, $\omega(\vec{q}j)$ always cancels and consequently no such sum arises in the calculation of F in this approximation. What remains is to evaluate the constant $|C(\vec{q}_1 j_1;\vec{q}_2 j_2;\vec{q}_3 j_3)|^2$, which is accomplished by multiplying each side of Eq.(4.2) by its complex conjugate and then summing both sides over the indices $\vec{q}_1$, $\vec{q}_2$, $\vec{q}_3$, j_1, j_2 and j_3. After replacing the Δ functions by their plane wave representations and using the orthonormality condition (Eq.(2.15)) the result is

$$\frac{M^3}{N}\left| C(\vec{q}_1 j_1;\vec{q}_2 j_2;\vec{q}_3 j_3)\right|^2 \sum_l \left[\sum_{\vec{q}j} e^{i\vec{q}\cdot\vec{x}(l)}\omega^2(\vec{q}j)\right]^3 =$$

$$= N^2 \sum_l \sum_{l_1 l_2}{}' \sum_{\alpha\beta\gamma} \phi_{\alpha\beta\gamma}(l_1)\phi_{\alpha\beta\gamma}(l_2)[\Delta(l) - \Delta(l-l_1) - \Delta(l+l_2) + \Delta(l-l_1+l_2)]^3 \tag{4.8}$$

where Eq.(4.6) has been used. The left-hand side of Eq.(4.8) is simplified by noting that Eq.(2.13) can be rewritten (with the help of the orthonormality condition Eq.(2.15)) as

$$\omega^2(\vec{q}j) = \sum_{\alpha\beta} e^*_\alpha(\vec{q}j) D_{\alpha\beta}(\vec{q}) e_\beta(\vec{q}j) \tag{4.9}$$

for a monatomic system and hence

$$\sum_l \left[\sum_{\vec{q}j} e^{i\vec{q}\cdot\vec{x}(l)}\omega^2(\vec{q}j)\right]^3 = \sum_l \left[\sum_{\vec{q}j} e^{i\vec{q}\cdot\vec{x}(l)} \sum_{\alpha\beta} e^*_\alpha(\vec{q}j) D_{\alpha\beta}(\vec{q}) e_\beta(\vec{q}j)\right]^3 \tag{4.10}$$

Summing over j and substituting for $D_{\alpha\beta}(\vec{q})$ from Eq.(2.14) gives

$$\sum_{l}\left[\sum_{\vec{q}\,j} e^{i\vec{q}\cdot\vec{x}(l)}\omega^{2}(\vec{q}\,j)\right]^{3} = \frac{N^{3}}{M^{3}}\sum_{l}\left[\sum_{l_1}{}'\sum_{\alpha}\phi_{\alpha\alpha}(l_1)[\Delta(l) - \Delta(l+l_1)]\right]^{3} \qquad (4.11)$$

where in evaluating the sum over $\vec{q}$, Eq.(4.6) has been used. By restricting the sum over l_1 to nearest-neighbours and summing l over all direct lattice vectors, the final result becomes

$$\sum_{l}\left[\sum_{\vec{q}\,j} e^{i\vec{q}\cdot\vec{x}(l)}\omega^{2}(\vec{q}\,j)\right]^{3} = \frac{1716N^{3}}{M^{3}}A^{3}(r) \qquad (4.12)$$

where

$$A(r) = \phi''(r) + \frac{2}{r}\phi'(r) \qquad (4.13)$$

The right-hand side of Eq.(4.8) is evaluated by substituting the full form of $\phi_{\alpha\beta\gamma}(l)$ (Eq.(2.52)) and restricting the sums over l_1 and l_2 to nearest-neighbours. Therefore,

$$\sum_{l}\sum_{l_1 l_2}{}'\sum_{\alpha\beta\gamma}\phi_{\alpha\beta\gamma}(l_1)\phi_{\alpha\beta\gamma}(l_2)[\Delta(l) - \Delta(l-l_1) - \Delta(l+l_2) + \Delta(l-l_1+l_2)]^{3} =$$

$$= \frac{C^{2}(r)}{8}\left[1152 + 3456R_{BC} + 4320(R_{BC})^{2}\right] \qquad (4.14)$$

where

$$R_{BC} = \frac{2B(r)}{r\,C(r)} \qquad (4.15)$$

and as a result

$$\left| C(\vec{q}_1 j_1;\vec{q}_2 j_2;\vec{q}_3 j_3) \right|^2 = \frac{C^2(r)}{(8)(1716)A^3(r)}\left[1152 + 3456R_{BC} + 4320(R_{BC})^2\right] \tag{4.16}$$

The same procedure is followed in evaluating the remaining contributions to MSD and all of the contributions to F. Within the expressions for these contributions, the following coefficients are used

$$R_{BD} = \frac{B(r)}{r^2 D(r)} \tag{4.17}$$

$$R_{CD} = \frac{C(r)}{r D(r)} \tag{4.18}$$

$$R_{CE} = \frac{4C(r)}{r^2 E(r)} \tag{4.19}$$

$$R_{DE} = \frac{2D(r)}{r E(r)} \tag{4.20}$$

The final expressions for the MSD contributions in the Peierls approximation are given as follows. The $\langle u^2 \rangle_{1(a)}$ contribution and its coefficients are:

$$\left\langle u^2 \right\rangle_{1(a)} = -\frac{(k_B T)^2}{192 A^2(r)}\left[S_1 D(r) + 2S_2\frac{C(r)}{r} + 4S_3\frac{B(r)}{r^2}\right]\left[\frac{1}{MN}\sum_{\vec{q}j}\frac{1}{2\omega^2(\vec{qj})}\right] \tag{4.21}$$

where $S_1=48$, $S_2=240$ and $S_3=180$.

The $\langle u^2\rangle_{1(b)}$ contribution and its coefficients are:

$$\langle u^2\rangle_{1(b)} = \frac{9(k_BT)^2 C^2(r)}{109824A^2(r)}\left[S_1 + S_2 R_{BC} + S_3 (R_{BC})^2\right]\left[\frac{1}{MN}\sum_{\vec{q}j}\frac{1}{\omega^2(\vec{qj})}\right] \qquad (4.22)$$

where S_1=1152, S_2=3456 and S_3=4320. The $\langle u^2\rangle_{2(a)}$ contribution and its coefficients are:

$$\langle u^2\rangle_{2(a)} = -\frac{(k_BT)^3}{3072\,A^3(r)}\left[S_1 F(r) + 2S_2\frac{E(r)}{r} + 4S_3\frac{D(r)}{r^2} + 8S_4\frac{C(r)}{r^3}\right]\left[\frac{1}{MN}\sum_{\vec{q}j}\frac{1}{\omega^2(\vec{qj})}\right] \qquad (4.23)$$

where S_1=96, S_2=1008, S_3=2520 and S_4=1260. The $\langle u^2\rangle_{2(b),1}$ and the $\langle u^2\rangle_{2(b),2}$ contributions and their coefficients are:

$$\langle u^2\rangle_{2(b),\alpha} = \frac{27(k_BT)^3 D^2(r)}{C_\alpha A^4(r)}\left[S_1 + 2S_2 R_{CD} + 4S_3 R_{BD} + 4S_4 (R_{CD})^2 + 8S_5 R_{CD} R_{BD} + 16S_6 (R_{BD})^2\right]\left[\frac{1}{MN}\sum_{\vec{q}j}\frac{1}{\omega^2(\vec{qj})}\right] \qquad (4.24)$$

where C_1=C_2=359424 and for both contributions S_1=960, S_2=9216, S_3=6240, S_4=22368, S_5=31200 and S_6=11700. The $\langle u^2\rangle_{2(c),1}$ and the $\langle u^2\rangle_{2(c),2}$ contributions and their coefficients are:

$$\langle u^2\rangle_{2(c),\alpha} = \frac{27(k_BT)^3 E(r) C(r)}{C_\alpha A^4(r)}\left[S_1 + S_2 R_{DE} + S_3 R_{CE} + S_4 R_{BC} + S_5 R_{DE} R_{BC} + S_6 R_{CE} R_{BC}\right]\left[\frac{1}{MN}\sum_{\vec{q}j}\frac{1}{\omega^2(\vec{qj})}\right] \qquad (4.25)$$

where C_1=1317888, C_2=3953664 and for both contributions S_1=2304, S_2=13824, S_3=12096, S_4=3456, S_5=24192 and S_6=30240. The $\langle u^2\rangle_{2(d),1}$, the $\langle u^2\rangle_{2(d),2}$ and the $\langle u^2\rangle_{2(d),3}$ contributions and their coefficients are:

$$\langle u^2\rangle_{2(d),\alpha} = -\frac{3(k_BT)^3 D(r) C^2(r)}{C_\alpha A^5(r)}\left[S_1 + S_2 R_{BC} + S_3 (R_{BC})^2 + 2S_4 R_{CD} + 2S_5 R_{CD} R_{BC} + 2S_6 R_{CD} (R_{BC})^2 + \right.$$

$$\left. + 4S_7 R_{BD} + 4S_8 R_{BD} R_{BC} + 4S_9 R_{BD} (R_{BC})^2\right]\left[\frac{1}{MN}\sum_{\vec{q}j}\frac{1}{\omega^2(\vec{qj})}\right] \qquad (4.26)$$

where C_1=5046272, C_2=C_3=2523136 and for all three contributions S_1=87552, S_2=258048, S_3=317952, S_4=421632, S_5=1234944, S_6=1527552, S_7=288000, S_8=829440 and S_9=1036800. The $\langle u^2\rangle_{2(e)}$ contribution and its coefficients are:

$$\langle u^2\rangle_{2(e)} = \frac{3(k_BT)^3 D^2(r)}{885248\, A^4(r)}\left[S_1 + 2S_2 R_{CD} + 4S_3 R_{BD} + 4S_4 (R_{CD})^2 + 8S_5 R_{CD} R_{BD} + 16S_6 (R_{BD})^2\right]\left[\frac{1}{MN}\sum_{qj}\frac{1}{\omega^2(\vec{qj})}\right] \tag{4.27}$$

where S_1=7296, S_2=50688, S_3=21888, S_4=110592, S_5=109440 and S_6=41040. The $\langle u^2\rangle_{2(f),1}$ and the $\langle u^2\rangle_{2(f),2}$ contributions and their coefficients are:

$$\langle u^2\rangle_{2(f),\alpha} = \frac{27(k_BT)^3 C^4(r)}{C_\alpha A^6(r)}\left[S_1 + S_2 R_{BC} + S_3 (R_{BC})^2 + S_4 (R_{BC})^3 + S_5 (R_{BC})^4\right]\left[\frac{1}{MN}\sum_{qj}\frac{1}{\omega^2(\vec{qj})}\right] \tag{4.28}$$

where C_1=2048, C_2=4096 and for both contributions S_1=491760, S_2=2977920, S_3=8382240, S_4=11664000 and S_5=7277040. The $\langle u^2\rangle_{2(g),1}$ and the $\langle u^2\rangle_{2(g),2}$ contributions and their coefficients are:

$$\langle u^2\rangle_{2(g),\alpha} = -\frac{27(k_BT)^3 D(r)\, C^2(r)}{C_\alpha A^5(r)}\left[S_1 + S_2 R_{BC} + S_3 (R_{BC})^2 + 2S_4 R_{CD} + 2S_5 R_{CD} R_{BC} + 2S_6 R_{CD} (R_{BC})^2 + \right.$$

$$\left. + 4S_7 R_{BD} + 4S_8 R_{BD} R_{BC} + 4S_9 R_{BD} (R_{BC})^2\right]\left[\frac{1}{MN}\sum_{qj}\frac{1}{\omega^2(\vec{qj})}\right] \tag{4.29}$$

where C_1=256, C_2=1024 and for both contributions S_1=32640, S_2=101376, S_3=84480, S_4=110592, S_5=384768, S_6=388608, S_7=48384, S_8=185856 and S_9=232320. Lastly, the $\langle u^2\rangle_{2(h)}$ contribution and its coefficients are:

$$\langle u^2\rangle_{2(h)} = \frac{81(k_BT)^3 C^4(r)}{2048\, A^6(r)}\left[S_1 + S_2 R_{BC} + S_3 (R_{BC})^2 + S_4 (R_{BC})^3 + S_5 (R_{BC})^4\right]\left[\frac{1}{MN}\sum_{qj}\frac{1}{\omega^2(\vec{qj})}\right] \tag{4.30}$$

where S_1=184320, S_2=1105920, S_3=2691072, S_4=1991808 and S_5=2216448.

The final expressions for the free energy contributions in the Peierls approximation are given as follows. The $F_{1(a)}$ contribution and its coefficients are:

$$F_{1(a)} = \frac{N(k_BT)^2}{256\,A^2(r)}\left[S_1 D(r) + 2S_2\frac{C(r)}{r} + 4S_3\frac{B(r)}{r^2}\right] \qquad (4.31)$$

where S_1=48, S_2=240 and S_3=180. The $F_{1(b)}$ contribution and its coefficients are:

$$F_{1(b)} = -\frac{9N(k_BT)^2 C^2(r)}{219648\,A^2(r)}\left[S_1 + S_2 R_{BC} + S_3 (R_{BC})^2\right] \qquad (4.32)$$

where S_1=1152, S_2=3456 and S_3=4320. The $F_{2(a)}$ contribution and its coefficients are:

$$F_{2(a)} = \frac{N(k_BT)^3}{6144\,A^3(r)}\left[S_1 F(r) + 2S_2\frac{E(r)}{r} + 4S_3\frac{D(r)}{r^2} + 8S_4\frac{C(r)}{r^3}\right] \qquad (4.33)$$

where S_1=96, S_2=1008, S_3=2520 and S_4=1260. The $F_{2(b)}$ contribution and its coefficients are:

$$F_{2(b)} = -\frac{81N(k_BT)^3 D^2(r)}{1437696\,A^4(r)}\left[S_1 + 2S_2 R_{CD} + 4S_3 R_{BD} + 4S_4 (R_{CD})^2 + 8S_5 R_{CD} R_{BD} + 16S_6 (R_{BD})^2\right] \qquad (4.34)$$

where S_1=960, S_2=9216, S_3=6240, S_4=22368, S_5=31200 and S_6=11700. The $F_{2(c)}$ contribution and its coefficients are:

$$F_{2(c)} = -\frac{27N(k_BT)^3 E(r) C(r)}{2635776\,A^4(r)}\left[S_1 + S_2 R_{DE} + S_3 R_{CE} + S_4 R_{BC} + S_5 R_{DE} R_{BC} + S_6 R_{CE} R_{BC}\right] \qquad (4.35)$$

where S_1=2304, S_2=13824, S_3=12096, S_4=3456, S_5=24192 and S_6=30240.

The $F_{2(d)}$ contribution and its coefficients are:

$$F_{2(d)} = \frac{N(k_BT)^3 D(r) C^2(r)}{100925 A^5(r)}\left[S_1 + S_2 R_{BC} + S_3(R_{BC})^2 + 2S_4 R_{CD} + 2S_5 R_{CD} R_{BC} + 2S_6 R_{CD}(R_{BC})^2 + \right.$$

$$\left. + 4S_7 R_{BD} + 4S_8 R_{BD} R_{BC} + 4S_9 R_{BD}(R_{BC})^2\right] \qquad (4.36)$$

where S_1=87552, S_2=258048, S_3=317952, S_4=421632, S_5=1234944, S_6=1527552, S_7=288000, S_8=829440 and S_9=1036800. The $F_{2(e)}$ contribution and its coefficients are:

$$F_{2(e)} = -\frac{9N(k_BT)^3 D^2(r)}{7081984 A^4(r)}\left[S_1 + 2S_2 R_{CD} + 4S_3 R_{BD} + 4S_4(R_{CD})^2 + 8S_5 R_{CD} R_{BD} + 16S_6(R_{BD})^2\right] \qquad (4.37)$$

where S_1=7296, S_2=50688, S_3=21888, S_4=110592, S_5=109440 and S_6=41040. The $F_{2(f)}$ contribution and its coefficients are:

$$F_{2(f)} = -\frac{81N(k_BT)^3 C^4(r)}{16384 A^6(r)}\left[S_1 + S_2 R_{BC} + S_3(R_{BC})^2 + S_4(R_{BC})^3 + S_5(R_{BC})^4\right] \qquad (4.38)$$

where S_1=491760, S_2=2977920, S_3=8382240, S_4=11664000 and S_5=7277040. The $F_{2(g)}$ contribution and its coefficients are:

$$F_{2(g)} = \frac{81N(k_BT)^3 D(r) C^2(r)}{100925 A^5(r)}\left[S_1 + S_2 R_{BC} + S_3(R_{BC})^2 + 2S_4 R_{CD} + 2S_5 R_{CD} R_{BC} + 2S_6 R_{CD}(R_{BC})^2 + \right.$$

$$\left. + 4S_7 R_{BD} + 4S_8 R_{BD} R_{BC} + 4S_9 R_{BD}(R_{BC})^2\right] \qquad (4.39)$$

where S_1=32640, S_2=101376, S_3=84480, S_4=110592, S_5=384768, S_6=388608, S_7=48384, S_8=185856 and S_9=232320. Lastly, the $F_{2(h)}$ contribution and its coefficients are:

$$F_{2(h)} = -\frac{81N(k_BT)^3 C^4(r)}{8192 A^6(r)}\left[S_1 + S_2 R_{BC} + S_3(R_{BC})^2 + S_4(R_{BC})^3 + S_5(R_{BC})^4\right] \qquad (4.40)$$

where S_1=184320, S_2=1105920, S_3=2691072, S_4=1991808 and

S_5=2216448.

V NUMERICAL EVALUATION

The calculation of the MSD contributions to $O(\lambda^2)$ and $O(\lambda^4)$ presented in Sec. III requires a method of performing the multiple Brillouin zone (BZ) sums, with constraints. When the constraints, in the form of Δ functions, are represented as plane waves it is possible to express the multiple BZ sums (including the constraints) as products of tensor functions involving single whole BZ sums (Shukla and Wilk (1974)). The calculation also requires the knowledge of a two-body potential function from which the elements of the tensors of various ranks are found including $D_{\alpha\beta}(\vec{q})$. The diagonalization of $D_{\alpha\beta}(\vec{q})$ using the Jacobi method yields the quantities $\omega(\vec{q}j)$ and $\vec{e}(\vec{q}j)$.

In the calculation of the high temperature quasiharmonic contribution to MSD and in the calculations of all of the MSD contributions using the Peierls approximation, the following sum arises

$$S = \sum_{\vec{q}j} \frac{1}{\omega^2(\vec{q}j)} \tag{5.1}$$

where the sum over $\vec{q}$ is over the whole BZ. The eigenvalues $\omega(\vec{q}j)$ are invariant under the 48 point group symmetry operations of the cubic crystal. As a result, the function $\omega^{-2}(\vec{q}j)$ of Eq.(5.1) can be carried out for $\vec{q}$ vectors in the $1/48^{-th}$ portion of the BZ by incorporating the weighting factor

associated with each $\vec{q}$.

The following two tensors are used in the calculation of the remaining MSD and F contributions. They are

$$S_{\alpha\beta}(l) = \sum_{\vec{q}j} \frac{e_\alpha(\vec{qj})e_\beta(\vec{qj})}{\lambda^2(\vec{qj})} \cos(\vec{q}\cdot\vec{x}(l)) \tag{5.2}$$

and

$$T_{\alpha\beta}(l) = \sum_{\vec{q}j} \frac{e_\alpha(\vec{qj})e_\beta(\vec{qj})}{\lambda^4(\vec{qj})} \cos(\vec{q}\cdot\vec{x}(l)) \tag{5.3}$$

where again the sums over $\vec{q}$ are over the whole zone. Since the eigenvectors $\vec{e}(\vec{q}j)$ transform as $\vec{q}$ and due to the presence of the $\cos(\vec{q}\cdot\vec{x}(l))$, the sums either have to be performed over the whole BZ or the summands must be transformed to an invariant form. Shukla and Wilk (1974) derived the $S_{\alpha\beta}$ tensor elements in the invariant form which needs to be evaluated over the $1/48^{-th}$ portion of the BZ with proper weighting factors. The invariant $T_{\alpha\beta}$ tensor elements, introduced in Shukla and Mountain (1982), can be obtained in a similar manner.

From Shukla and Wilk (1974), a simple cubic mesh of points in $\vec{q}$ space was used with

$$\vec{q} = \frac{\pi\vec{p}}{L\,a_0} \tag{5.4}$$

where L is the step size, a_0 is the lattice constant and the

boundaries of the $1/48^{-th}$ portion of the BZ are defined by

$$p_x + p_y + p_z < 1.5L \tag{5.5}$$

and

$$L \geq p_x \geq p_y \geq p_z \geq 0 \tag{5.6}$$

where p_x, p_y, p_z and L are integers. This results in $4L^3$ points in the whole zone including the origin. Consequently, the $S_{\alpha\beta}$ and $T_{\alpha\beta}$ tensor elements were calculated as accurately as possible for a large number of direct lattice vectors and stored. What is meant by as accurately as possible is that a large step length was used in the calculation and the origin was excluded in the normalization process.

The nearest-neighbour potential chosen for the calculations of the MSD and F contributions is the Lennard-Jones potential, given as

$$\phi(r) = \varepsilon\left[\left(\frac{r_0}{r}\right)^{12} - 2\left(\frac{r_0}{r}\right)^{6}\right] \tag{5.7}$$

where ϵ is the well depth and r_0 gives the location of the minimum of $\phi(r)$. For a monatomic cubic crystal the dynamical matrix elements are obtained from Shukla (1966).

For any of the anharmonic MSD and F calculations the anharmonic coefficients (Eq.(2.49)) are substituted and the plane wave representation is used for each of the independent Δ functions. This introduces different direct lattice sum

indices for each of the independent Δ functions. The other direct lattice vector sums coming from the $\phi_{\alpha\beta\gamma}(1)$ tensor and other tensors are restricted to nearest-neighbours only. As a result, many combinations of direct lattice vectors must be considered. In the calculation of the contributions $F_{1(b)}$ and $\langle u^2 \rangle_{1(b)}$ the sum from the plane wave representation was carried out to the fourteenth shell of neighbours. At the seventh shell, the numbers were well converged with the change in the results in going to the fourteenth shell being only .05%. From this, the decision was made to truncate all of the sums arising from the plane wave representations after the seventh shell.

To evaluate some of the diagrams it was convenient to initially evaluate and store pieces of diagrams. These pieces, referred to as loops and bubbles, are shown in Fig. 4. From the MSD and F diagrams of Figs. 1, 2 and 3, a number of these diagrams can be formed from combinations of loops and bubbles. The evaluation of a particular diagram becomes simply a matter of multiplying the appropriate stored pieces together under the rules of matrix multiplication. The MSD and F contributions associated with the diagram types 1(a), 1(b), 2(b), 2(d) and 2(f) were evaluated using this method. The only drawback to this procedure is that computer-time restrictions limits the maximum value of L that can be used. While this is not a problem with the F contributions (a larger step length causes only a small change in the actual

Figure 4

Loop and Bubble Diagrams

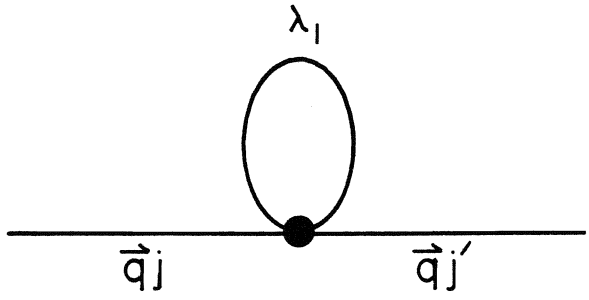

LOOP

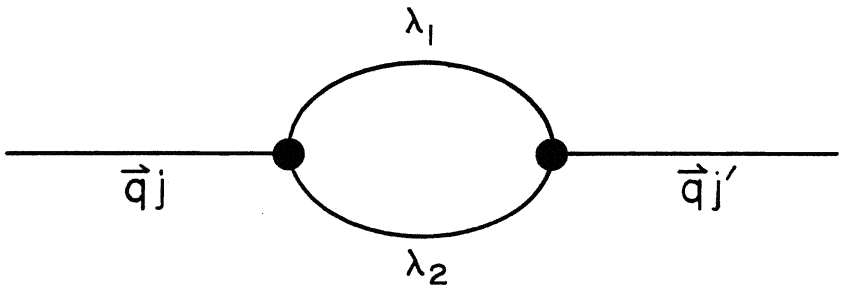

BUBBLE

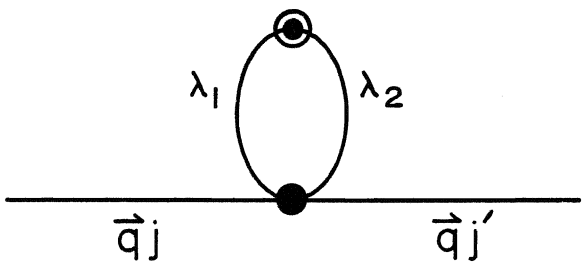

LOOP WITH INSERTION

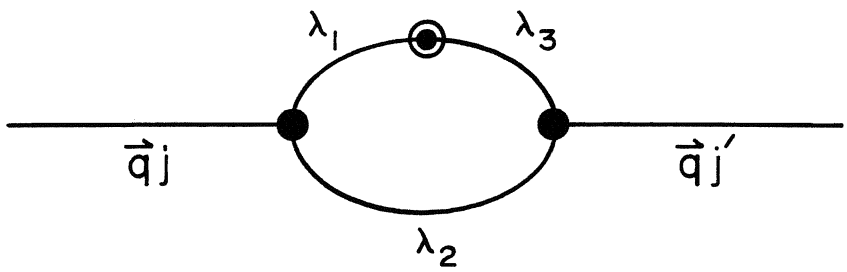

BUBBLE WITH INSERTION

contribution), the same is not true for an MSD contribution, where a larger step length results in an increased numerical value for the contribution. However, a plot of numerical contribution versus 1/L for an MSD diagram shows a linear relationship (Heiser, Shukla and Cowley (1986)). Therefore, the MSD contributions can be extrapolated for an infinite step length (in other words $\vec{q}\rightarrow 0$). For diagrams where a large step length could be used, the calculations were done for L=7 and L=30 and then the MSD contributions were extrapolated. For diagrams comprised of loops and bubbles (as well as diagram 2(g)) the calculations were done for L=4 and L=10 and then the corresponding MSD contributions were extrapolated. All of the diagrams, MSD and F, were also evaluated using the leading term approximation.

The evaluation of the diagram 2(h) is somewhat complicated. Unfortunately, the program to evaluate the MSD and F contributions in full (using the full representations of all the third rank tensors) and using the plane wave representations of the Δ functions was too time consuming due to the extremely nested nature of the sums. However, the MSD and F contributions could be evaluated in the leading term approximation in the plane wave representation because of the simplification of the third rank tensors. Initially all of the contributions to MSD and F were evaluated for the equilibrium case $r=r_0$. This was done to check the accuracy of the programs with the free energy results of Shukla and Wilk

(1974). The results agreed quite well with their published values in all those cases where the plane wave representation was used in their work. In other cases where a different procedure was used (Shukla and Wilk (1974) and Shukla unpublished) an excellent agreement was obtained.

In order to see if the sum of the QH, $O(\lambda^2)$ and $O(\lambda^4)$ contributions to MSD yield a better agreement with the MC results of HSC, all of the MSD contributions were evaluated for the six reduced temperatures (in other words lattice constants) used in HSC. These are the lattice constants at which the pressure is zero for the corresponding temperatures in the Monte Carlo calculation. The lattice constants and their corresponding temperatures are presented in Table 5.1. All that remained was to have full calculation contributions from diagram 2(h). In order to accomplish this, it was discovered that there were certain relations which were present between certain diagrams. For example, for free energy, the ratio of 2(h) to 2(g) in the leading term approximation remains fairly constant for each of the volumes. These ratios were then averaged and this average value was then multiplied with 2(g), from the full calculation, in order to estimate 2(h) for the full calculation. In the case of MSD, the ratio of 2(h) to 2(g),2 in the leading term approximation was averaged and used to estimate 2(h) for the full calculation. Using this procedure, it was estimated that the predicted value of $\langle u^2 \rangle_{2(h)}$ will be approximately larger by

TABLE 5.1

NEAREST-NEIGHBOUR DISTANCES AND CORRESPONDING REDUCED TEMPERATURES[a]

$T\ (\varepsilon/k_B)$	$R(r_0)$
0.125	1.0087
0.225	1.0164
0.300	1.0231
0.375	1.0307
0.450	1.0395
0.500	1.0464

(a) From Shukla unpublished.

2% and smaller by 2% for the lowest and highest volumes, respectively. In order to see this estimation procedure, the MSD contributions calculated using the leading term approximation are presented in Table 5.3 and the F contributions calculated using the leading term approximation are presented in Table 5.5. Table 5.2 presents the MSD contributions computed for the full calculation and the F contributions in the full calculation are presented in Table 5.4.

Table 5.6 shows the result of adding all the λ^4 contributions, MSD(λ^4), to the sum of the QH and MSD(λ^2) results from the full calculation: this total is compared with the MC results. The MSD(λ^4) results are also calculated in another manner. The λ^4 contributions, evaluated for $r=r_0$, are summed and then multiplied by the appropriate temperatures. When added to the $O(\lambda^2)$ PT values, the results, $\lambda^4 r_0$ PT, are compared with the MC results. Table 5.7 presents the results of adding the λ^4 contributions to the sum of the QH and λ^2 contributions with all of the contributions being obtained in the leading term approximation. The MSD contributions using Peierls approximation and the full calculation are presented in Table 5.8 and the MSD contributions using both Peierls and the leading term approximation are presented in Table 5.9. For the free energy using Peierls approximation, Table 5.10 presents the contributions computed in the full calculation and the results using the leading term approximation are

presented in Table 5.11. The accuracy of the Peierls approximation is examined in Table 5.12 by adding all the $O(\lambda^4)$ contributions to the sum of the QH and $O(\lambda^2)$ contributions, all computed in the full calculation, and comparing with the MC results. Table 5.13 examines the accuracy of the Peierls approximation in the same manner but using the leading term approximation.

The convergence of the perturbation expansion is examined by taking the ratio of $O(\lambda^4)$ PT to $O(\lambda^2)$ PT. Figure 5 plots these ratios as a function of temperature for the full exact calculation, the leading term approximation and the Peierls approximation.

The specific heat at constant volume C_v is defined as

$$C_v = -T\left[\frac{\partial^2 F}{\partial T^2}\right]_v \qquad (5.8)$$

The accuracy of the Peierls approximation in the calculation of F is examined by calculating C_v from the $O(\lambda^2)$ and $O(\lambda^4)$ theories using the full exact calculation and the Peierls approximation. These results are plotted as a function of temperature in Figure 6 with the Monte Carlo points of Shukla and Cowley (1985).

TABLE 5.2

EXTRAPOLATED QUASIHARMONIC[a], $O(\lambda^2)$[b] and $O(\lambda^4)$[c] CONTRIBUTIONS TO MEAN SQUARE DISPLACEMENT USING THE FULL CALCULATION

CONT	r_0	r_1	r_2	r_3	r_4	r_5	r_6
QH	0.0175	0.0204	0.0234	0.0264	0.0304	0.0358	0.0409
1(a)	-0.0152	-0.0210	-0.0283	-0.0368	-0.0502	-0.0728	-0.0988
1(b)	0.0130	0.0180	0.0241	0.0312	0.0424	0.0615	0.0836
2(a)	-0.0068	-0.0109	-0.0168	-0.0247	-0.0388	-0.0666	-0.1035
2(b),1	0.0141	0.0234	0.0372	0.0564	0.0918	0.1658	0.2702
2(b),2	0.0133	0.0220	0.0349	0.0526	0.0854	0.1536	0.2497
2(c),1	0.0288	0.0367	0.0566	0.0833	0.1310	0.2265	0.3556
2(c),2	0.0065	0.0105	0.0162	0.0238	0.0375	0.0651	0.1024
2(d),1	-0.0104	-0.0171	-0.0271	-0.0408	-0.0663	-0.1196	-0.1951
2(d),2	-0.0226	-0.0371	-0.0584	-0.0877	-0.1417	-0.2544	-0.4137
2(d),3	-0.0239	-0.0394	-0.0623	-0.0940	-0.1525	-0.2750	-0.4485
2(e)	0.0104	0.0169	0.0262	0.0389	0.0617	0.1077	0.1703
2(f),1	0.0180	0.0295	0.0463	0.0696	0.1124	0.2022	0.3297
2(f),2	0.0099	0.0161	0.0252	0.0378	0.0608	0.1091	0.1779
2(g),1	-0.0298	-0.0488	-0.0764	-0.1143	-0.1834	-0.3257	-0.5237
2(g),2	-0.0085	-0.0139	-0.0218	-0.0326	-0.0525	-0.0934	-0.1507
2(h)	0.0083	0.0136	0.0214	0.0320	0.0515	0.0916	0.1477

a) QH in units of $(k_BT/\epsilon)r_0^2$.

b) $O(\lambda^2)$ in units of $(k_BT/\epsilon)^2r_0^2$.

c) $O(\lambda^4)$ in units of $(k_BT/\epsilon)^3r_0^2$.

TABLE 5.3

EXTRAPOLATED QUASIHARMONIC[a], $O(\lambda^2)$[b] and $O(\lambda^4)$[c] CONTRIBUTIONS TO MEAN SQUARE DISPLACEMENT USING THE LEADING TERM APPROXIMATION

CONT	r_0	r_1	r_2	r_3	r_4	r_5	r_6
QH	0.0175	0.0202	0.0230	0.0257	0.0293	0.0340	0.0384
1(a)	-0.0225	-0.0301	-0.0391	-0.0492	-0.0642	-0.0882	-0.1139
1(b)	0.0133	0.0177	0.0229	0.0287	0.0374	0.0511	0.0659
2(a)	-0.0121	-0.0186	-0.0275	-0.0388	-0.0577	-0.0926	-0.1355
2(b),1	0.0290	0.0451	0.0675	0.0964	0.1456	0.2385	0.3561
2(b),2	0.0290	0.0449	0.0665	0.0944	0.1417	0.2302	0.3416
2(c),1	0.0284	0.0439	0.0651	0.0923	0.1383	0.2239	0.3308
2(c),2	0.0085	0.0132	0.0196	0.0277	0.0415	0.0671	0.0990
2(d),1	-0.0155	-0.0241	-0.0357	-0.0507	-0.0763	-0.1244	-0.1851
2(d),2	-0.0343	-0.0528	-0.0780	-0.1102	-0.1649	-0.2672	-0.3962
2(d),3	-0.0343	-0.0532	-0.0791	-0.1125	-0.1694	-0.2766	-0.4124
2(e)	0.0097	0.0151	0.0226	0.0323	0.0488	0.0798	0.1189
2(f),1	0.0185	0.0285	0.0422	0.0598	0.0896	0.1457	0.2166
2(f),2	0.0104	0.0160	0.0235	0.0332	0.0496	0.0804	0.1193
2(g),1	-0.0312	-0.0483	-0.0717	-0.1019	-0.1532	-0.2494	-0.3708
2(g),2	-0.0089	-0.0138	-0.0206	-0.0293	-0.0442	-0.0722	-0.1077
2(h)	0.0088	0.0137	0.0202	0.0287	0.0431	0.0703	0.1048

a) QH in units of $(k_BT/\epsilon)r_0^2$.

b) $O(\lambda^2)$ in units of $(k_BT/\epsilon)^2r_0^2$.

c) $O(\lambda^4)$ in units of $(k_BT/\epsilon)^3r_0^2$.

TABLE 5.4

ALL $O(\lambda^2)^a$ and $O(\lambda^4)^b$
CONTRIBUTIONS TO FREE ENERGY
USING THE FULL CALCULATION

CONT	r_0	r_1	r_2	r_3	r_4	r_5	r_6
1(a)	0.6909	0.8262	0.9735	1.1286	1.3438	1.6626	1.9841
1(b)	-0.3426	-0.4077	-0.4787	-0.5536	-0.6580	-0.8140	-0.9732
2(a)	0.2048	0.2847	0.3843	0.5028	0.6891	1.0091	1.3814
2(b)	-0.6424	-0.9209	-1.2819	-1.7280	-2.4598	-3.7884	-5.4283
2(c)	-0.6015	-0.8355	-1.1291	-1.4811	-2.0398	-3.0142	-4.1688
2(d)	0.9423	1.3426	1.8600	2.4984	3.5458	5.4526	7.8198
2(e)	-0.2231	-0.3137	-0.4286	-0.5677	-0.7908	-1.1844	-1.6559
2(f)	-0.3567	-0.5049	-0.6958	-0.9310	-1.3169	-2.0213	-2.9010
2(g)	0.5967	0.8436	1.1596	1.5457	2.1724	3.2966	4.6705
2(h)	-0.1012	-0.1431	-0.1967	-0.2621	-0.3684	-0.5591	-0.7921

a) $O(\lambda^2)$ in units of $N(k_BT)^2/\epsilon$.

b) $O(\lambda^4)$ in units of $N(k_BT)^3/\epsilon^2$.

TABLE 5.5

ALL $O(\lambda^2)^a$ and $O(\lambda^4)^b$
CONTRIBUTIONS TO FREE ENERGY
USING THE LEADING TERM APPROXIMATION

CONT	r_0	r_1	r_2	r_3	r_4	r_5	r_6
1(a)	0.9661	1.1267	1.2953	1.4668	1.6956	2.0181	2.3262
1(b)	-0.3439	-0.3987	-0.4560	-0.5141	-0.5916	-0.7007	-0.8052
2(a)	0.3452	0.4643	0.6069	0.7698	1.0145	1.4103	1.8423
2(b)	-1.2446	-1.6929	-2.2385	-2.8727	-3.8442	-5.4587	-7.2730
2(c)	-0.7327	-0.9888	-1.2971	-1.6516	-2.1885	-3.0670	-4.0382
2(d)	1.3292	1.7967	2.3627	3.0181	4.0190	5.6785	7.5425
2(e)	-0.2158	-0.2938	-0.3888	-0.4991	-0.6683	-0.9481	-1.2620
2(f)	-0.3614	-0.4857	-0.6355	-0.8085	-1.0721	-1.5088	-1.9996
2(g)	0.6174	0.8347	1.0975	1.4015	1.8651	2.6314	3.4891
2(h)	-0.1058	-0.1423	-0.1864	-0.2374	-0.3151	-0.4437	-0.5884

a) $O(\lambda^2)$ in units of $N(k_BT)^2/\epsilon$.

b) $O(\lambda^4)$ in units of $N(k_BT)^3/\epsilon^2$.

TABLE 5.6

COMPARISON WITH MONTE CARLO RESULTS FOR THE MEAN SQUARE DISPLACEMENT USING THE FULL CALCULATION[a]

TEMP[b]	QH	MSD(λ^2)	O(λ^2)PT	MSD(λ^4)	O(λ^4)PT	$\lambda^4 r_o$ PT	MC[c]
0.125	3.21	-0.059	3.15	0.004	3.15	3.17	3.15
0.225	6.63	-0.268	6.36	0.017	6.38	6.46	6.38
0.300	9.98	-0.635	9.34	0.010	9.35	9.59	9.69
0.375	14.4	-1.38	13.0	-0.412	12.6	13.5	13.7
0.450	20.3	-2.88	17.4	-1.50	15.9	18.2	19.2
0.500	25.8	-4.79	21.0	-4.99	16.0	22.1	23.2

a) Columns 2-8 in units of $\sigma^2/1000$.

b) In units of ε/k_B.

c) From Heiser, Shukla and Cowley (1986)

TABLE 5.7

COMPARISON WITH MONTE CARLO RESULTS FOR THE MEAN SQUARE DISPLACEMENT USING THE LEADING TERM APPROXIMATION[a]

TEMP[b]	QH	MSD(λ^2)	O(λ^2)PT	MSD(λ^4)	O(λ^4)PT	$\lambda^4 r_o$ PT	MC[c]
0.125	3.18	-0.244	2.94	0.024	2.96	2.95	3.15
0.225	6.52	-1.03	5.49	0.210	5.70	5.58	6.38
0.300	9.71	-2.32	7.39	0.728	8.12	7.59	9.69
0.375	13.8	-4.75	9.05	2.16	11.2	9.45	13.7
0.450	19.3	-9.47	9.83	6.14	16.0	10.5	19.2
0.500	24.2	-15.1	9.10	12.5	21.6	10.0	23.2

a) Columns 2-8 in units of $\sigma^2/1000$.

b) In units of ε/k_B.

c) From Heiser, Shukla and Cowley (1986)

TABLE 5.8

EXTRAPOLATED QUASIHARMONIC[a], $O(\lambda^2)$[b] and $O(\lambda^4)$[c]
CONTRIBUTIONS TO MEAN SQUARE DISPLACEMENT USING PEIERLS APPROXIMATION
AND THE FULL CALCULATION

CONT	r_0	r_1	r_2	r_3	r_4	r_5	r_6
QH	0.0175	0.0204	0.0234	0.0264	0.0304	0.0358	0.0409
1(a)	-0.0174	-0.0245	-0.0333	-0.0439	-0.0605	-0.0890	-0.1220
1(b)	0.0103	0.0145	0.0198	0.0262	0.0364	0.0542	0.0752
2(a)	-0.0080	-0.0131	-0.0205	-0.0307	-0.0489	-0.0856	-0.1351
2(b),1	0.0212	0.0359	0.0579	0.0888	0.1468	0.2691	0.4424
2(b),2	0.0212	0.0359	0.0579	0.0888	0.1468	0.2691	0.4424
2(c),1	0.0189	0.0316	0.0504	0.0765	0.1246	0.2245	0.3638
2(c),2	0.0063	0.0105	0.0168	0.0255	0.0415	0.0748	0.1212
2(d),1	-0.0116	-0.0197	-0.0319	-0.0493	-0.0822	-0.1525	-0.2536
2(d),2	-0.0232	-0.0394	-0.0639	-0.0987	-0.1643	-0.3049	-0.5073
2(d),3	-0.0232	-0.0394	-0.0639	-0.0987	-0.1643	-0.3049	-0.5073
2(e)	0.0108	0.0182	0.0292	0.0445	0.0730	0.1328	0.2168
2(f),1	0.0124	0.0212	0.0346	0.0537	0.0902	0.1695	0.2854
2(f),2	0.0062	0.0106	0.0173	0.0268	0.0451	0.0847	0.1427
2(g),1	-0.0221	-0.0374	-0.0606	-0.0935	-0.1555	-0.2878	-0.4778
2(g),2	-0.0055	-0.0094	-0.0152	-0.0234	-0.0389	-0.0719	-0.1194
2(h)	0.0050	0.0085	0.0139	0.0217	0.0365	0.0687	0.1160

a) QH in units of $(k_BT/\varepsilon)r_0^2$.

b) $O(\lambda^2)$ in units of $(k_BT/\varepsilon)^2r_0^2$.

c) $O(\lambda^4)$ in units of $(k_BT/\varepsilon)^3r_0^2$.

TABLE 5.9

EXTRAPOLATED QUASIHARMONIC[a], $O(\lambda^2)$[b] and $O(\lambda^4)$[c] CONTRIBUTIONS TO MEAN SQUARE DISPLACEMENT USING PEIERLS APPROXIMATION AND THE LEADING TERM APPROXIMATION

CONT	r_0	r_1	r_2	r_3	r_4	r_5	r_6
QH	0.0175	0.0202	0.0230	0.0257	0.0293	0.0340	0.0384
1(a)	-0.0225	-0.0324	-0.0453	-0.0614	-0.0877	-0.1361	-0.1964
1(b)	0.0101	0.0150	0.0215	0.0300	0.0446	0.0729	0.1106
2(a)	-0.0121	-0.0207	-0.0341	-0.0533	-0.0907	-0.1739	-0.2996
2(b),1	0.0335	0.0601	0.1033	0.1689	0.3036	0.6276	1.1586
2(b),2	0.0335	0.0601	0.1033	0.1689	0.3036	0.6276	1.1586
2(c),1	0.0215	0.0384	0.0655	0.1065	0.1900	0.3891	0.7125
2(c),2	0.0072	0.0128	0.0218	0.0355	0.0633	0.1297	0.2375
2(d),1	-0.0144	-0.0265	-0.0469	-0.0789	-0.1473	-0.3214	-0.6238
2(d),2	-0.0287	-0.0530	-0.0937	-0.1579	-0.2947	-0.6429	-1.2476
2(d),3	-0.0287	-0.0530	-0.0937	-0.1579	-0.2947	-0.6429	-1.2476
2(e)	0.0115	0.0206	0.0354	0.0579	0.1041	0.2152	0.3972
2(f),1	0.0121	0.0229	0.0417	0.0724	0.1403	0.3230	0.6589
2(f),2	0.0060	0.0115	0.0209	0.0362	0.0701	0.1615	0.3294
2(g),1	-0.0229	-0.0423	-0.0748	-0.1259	-0.2351	-0.5127	-0.9951
2(g),2	-0.0057	-0.0106	-0.0187	-0.0315	-0.0588	-0.1282	-0.2488
2(h)	0.0049	0.0094	0.0171	0.0296	0.0573	0.1320	0.2692

a) QH in units of $(k_BT/\varepsilon)r_0^2$.

b) $O(\lambda^2)$ in units of $(k_BT/\varepsilon)^2r_0^2$.

c) $O(\lambda^4)$ in units of $(k_BT/\varepsilon)^3r_0^2$.

TABLE 5.10

ALL $O(\lambda^2)^a$ and $O(\lambda^4)^b$ CONTRIBUTIONS TO FREE ENERGY USING PEIERLS APPROXIMATION AND THE FULL CALCULATION

CONT	r_0	r_1	r_2	r_3	r_4	r_5	r_6
1(a)	0.7474	0.9003	1.0681	1.2458	1.4938	1.8630	2.2363
1(b)	-0.2931	-0.3548	-0.4232	-0.4965	-0.6001	-0.7573	-0.9195
2(a)	0.2287	0.3217	0.4393	0.5806	0.8050	1.1946	1.6515
2(b)	-0.9094	-1.3189	-1.8550	-2.5226	-3.6244	-5.6332	-8.1120
2(c)	-0.5410	-0.7747	-1.0765	-1.4474	-2.0513	-3.1334	-4.4462
2(d)	0.9930	1.4476	2.0476	2.8012	4.0582	6.3836	9.3007
2(e)	-0.2319	-0.3342	-0.4672	-0.6318	-0.9017	-1.3899	-1.9880
2(f)	-0.2656	-0.3893	-0.5539	-0.7624	-1.1140	-1.7741	-2.6160
2(g)	0.4730	0.6883	0.9719	1.3275	1.9196	3.0123	4.3799
2(h)	-0.0712	-0.1045	-0.1490	-0.2054	-0.3006	-0.4796	-0.7083

a) $O(\lambda^2)$ in units of $N(k_BT)^2/\varepsilon$.

b) $O(\lambda^4)$ in units of $N(k_BT)^3/\varepsilon^2$.

TABLE 5.11

ALL $O(\lambda^2)^a$ and $O(\lambda^4)^b$ CONTRIBUTIONS TO FREE ENERGY USING PEIERLS APPROXIMATION AND THE LEADING TERM APPROXIMATION

CONT	r_0	r_1	r_2	r_3	r_4	r_5	r_6
1(a)	0.9661	1.2042	1.4799	1.7889	2.2489	2.9977	3.8352
1(b)	-0.2891	-0.3706	-0.4686	-0.5834	-0.7614	-1.0711	-1.4404
2(a)	0.3452	0.5131	0.7412	1.0369	1.5497	2.5535	3.9006
2(b)	-1.4361	-2.2310	-3.3697	-4.9235	-7.7811	-13.8248	-22.6291
2(c)	-0.6157	-0.9501	-1.4252	-2.0702	-3.2458	-5.7147	-9.2777
2(d)	1.2320	1.9684	3.0590	4.6035	7.5524	14.1617	24.3668
2(e)	-0.2462	-0.3824	-0.5777	-0.8440	-1.3339	-2.3699	-3.8793
2(f)	-0.2592	-0.4259	-0.6810	-1.0555	-1.7976	-3.5575	-6.4343
2(g)	0.4913	0.7850	1.2199	1.8358	3.0118	5.6476	9.7173
2(h)	-0.0706	-0.1160	-0.1855	-0.2875	-0.4897	-0.9691	-1.7528

a) $O(\lambda^2)$ in units of $N(k_BT)^2/\epsilon$.

b) $O(\lambda^4)$ in units of $N(k_BT)^3/\epsilon^2$.

TABLE 5.12

COMPARISON WITH MONTE CARLO RESULTS FOR THE MEAN SQUARE DISPLACEMENT USING PEIERLS APPROXIMATION AND THE FULL CALCULATION[a]

TEMP[b]	QH	MSD(λ^2)	O(λ^2)PT	MSD(λ^4)	O(λ^4)PT	$\lambda^4 r_o$ PT	MC[c]
0.125	3.21	-0.197	3.01	0.035	3.05	3.03	3.15
0.225	6.63	-0.861	5.77	0.316	6.09	5.89	6.38
0.300	9.98	-2.01	7.97	1.09	9.06	8.26	9.69
0.375	14.4	-4.27	10.1	3.35	13.5	10.7	13.7
0.450	20.3	-8.88	11.4	9.83	21.2	12.4	19.2
0.500	25.8	-14.7	11.1	20.5	31.6	12.4	23.2

a) Columns 2-8 in units of $\sigma^2/1000$.

b) In units of ε/k_B.

c) From Heiser, Shukla and Cowley (1986)

TABLE 5.13

COMPARISON WITH MONTE CARLO RESULTS FOR THE MEAN SQUARE DISPLACEMENT USING PEIERLS APPROXIMATION AND THE LEADING TERM APPROXIMATION[a]

TEMP[b]	QH	MSD(λ^2)	O(λ^2)PT	MSD(λ^4)	O(λ^4)PT	$\lambda^4 r_o$ PT	MC[c]
0.125	3.18	-0.343	2.84	0.073	2.91	2.88	3.15
0.225	6.52	-1.52	5.00	0.676	5.68	5.25	6.38
0.300	9.71	-3.56	6.15	2.40	8.55	6.75	9.69
0.375	13.8	-7.64	6.16	7.38	13.5	7.34	13.7
0.450	19.3	-16.1	3.20	21.1	24.3	5.23	19.2
0.500	24.2	-27.0	-2.80	40.9	38.1	-0.012	23.2

a) Columns 2-8 in units of $\sigma^2/1000$.

b) In units of ε/k_B.

c) From Heiser, Shukla and Cowley (1986)

Figure 5

Convergence of the Perturbation Expansion

The solid lines are calculations using the full calculation, leading term approximation and Peierls approximation.

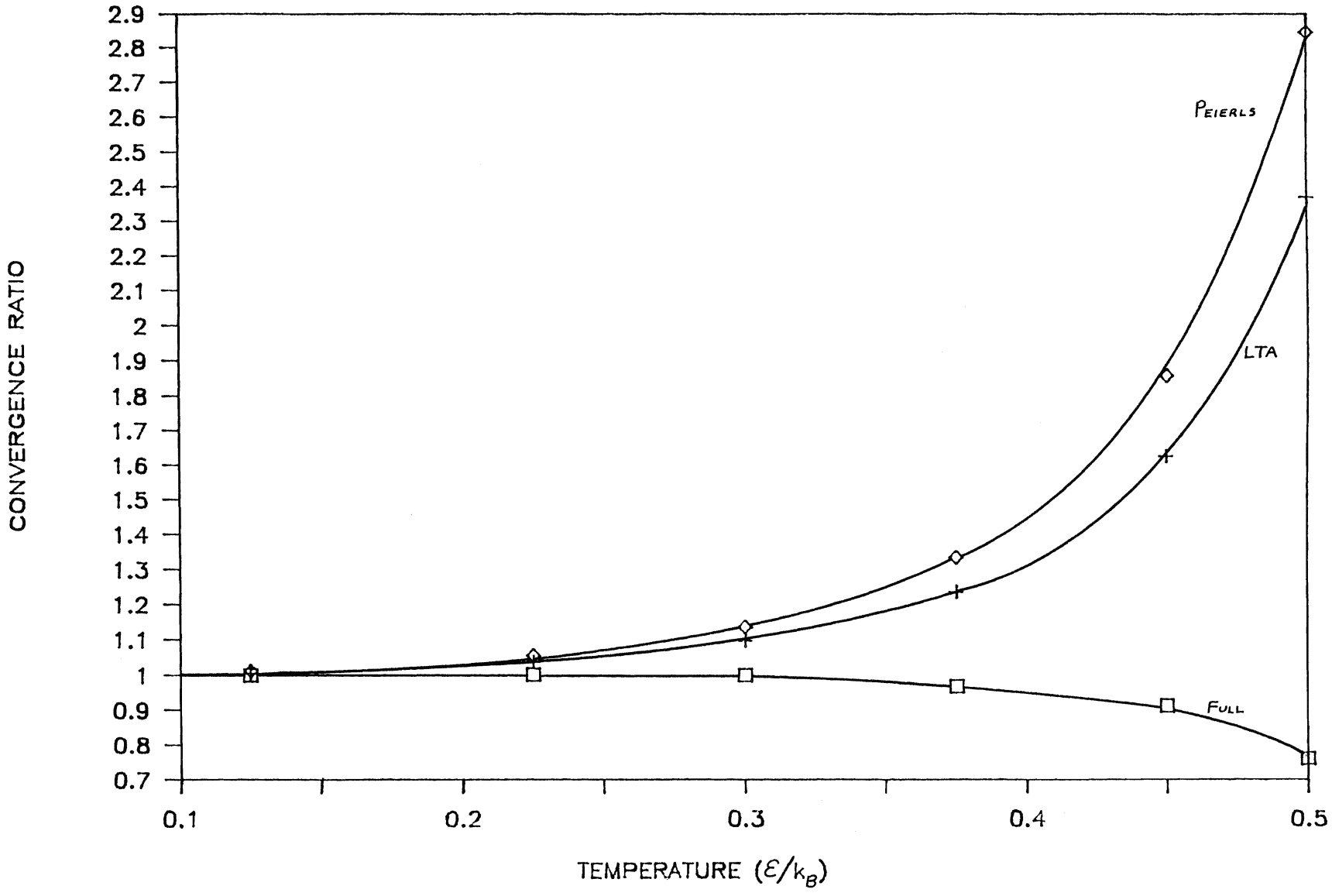
CONVERGENCE RATIO
2.9
2.8
2.7
2.6
2.5
2.4
2.3
2.2
2.1
2
1.9
1.8
1.7
1.6
1.5
1.4
1.3
1.2
1.1
1
0.9
0.8
0.7
0.1
0.2
0.3
0.4
0.5
TEMPERATURE (ε/k_B)
PEIERLS
LTA
FULL

Figure 6

Specific Heat at Constant Volume (C_v)
for the Classical Nearest-Neighbour
Lennard-Jones Solid

The solid lines are the $O(\lambda^2)$ and $O(\lambda^4)$ perturbation theory results for the full exact calculation and the Peierls approximation. The boxes are the Monte Carlo points of Shukla and Cowley (1985).

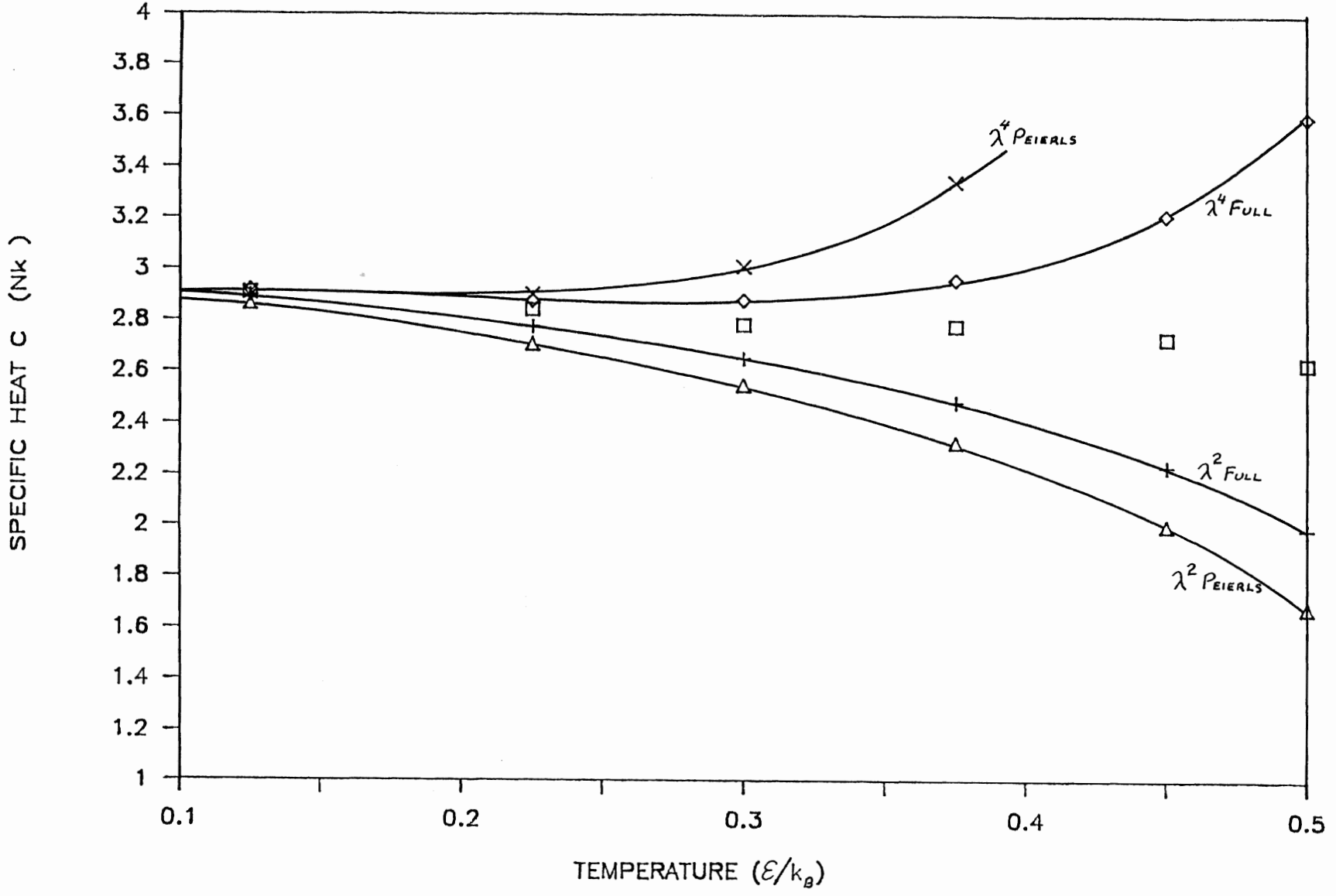
SPECIFIC HEAT C (Nk)
4
3.8
3.6
3.4
3.2
3
2.8
2.6
2.4
2.2
2
1.8
1.6
1.4
1.2
1
0.1
0.2
0.3
0.4
0.5
TEMPERATURE (ε/k_B)
λ⁴ P_EIERLS
λ⁴ FULL
λ² FULL
λ² P_EIERLS

VI SELECTED HIGHER ORDER CONTRIBUTIONS

In the Green's function work of Shukla and Hübschle (1989), the MSD in the high temperature limit is evaluated from Eq.(16) of their paper; namely,

$$\langle u^2 \rangle = \frac{k_B T}{MN} \sum_{\lambda} \frac{1}{\Omega^2(\lambda)} \tag{6.1}$$

where

$$\Omega^2(\lambda) = \omega^2(\lambda) + \Delta_4(\lambda) + \Delta_3(\lambda) \tag{6.2}$$

and $\Delta_3(\lambda)$ and $\Delta_4(\lambda)$ are the cubic and quartic frequency shifts from the corresponding terms in the Hamiltonian. The general anharmonic coefficient (Eq.(2.49)) can be rewritten as

$$V(\lambda_1;\ldots;\lambda_n) = \frac{1}{n!}\left(\frac{\hbar}{2}\right)^{n/2} \frac{N^{1-n/2}\Delta(\vec{q_1}+\ldots+\vec{q_n})}{\left[\omega(\lambda_1)\ldots\omega(\lambda_n)\right]^{1/2}} \Phi(\lambda_1;\ldots;\lambda_n) \tag{6.3}$$

where

$$\Phi(\lambda_1;\ldots;\lambda_n) = \frac{1}{2M^{n/2}} \sum_{1}^{/} \sum_{\alpha_1\ldots\alpha_v} \phi_{\alpha_1\ldots\alpha_n}(l) e_{\alpha_1}(\lambda_1)\ldots e_{\alpha_n}(\lambda_n)\left(1-e^{i\vec{q_1}\bullet\vec{x}(l)}\right)\ldots\left(1-e^{i\vec{q_n}\bullet\vec{x}(l)}\right) \tag{6.4}$$

From the high temperature limit of Eq.(2) of Shukla and Hübschle (1989) and this definition of the V functions, simplified expressions for $\Delta_3(\lambda)$ and $\Delta_4(\lambda)$ can be written. These are

$$\Delta_4(\lambda) = \frac{k_B T}{2N} \sum_{\lambda_1} \frac{\Phi(\lambda_1;-\lambda_1;\lambda;-\lambda)}{\omega^2(\lambda)} \tag{6.5}$$

and

$$\Delta_3(\lambda) = -\frac{k_B T}{2N}\sum_{\lambda_1}\sum_{\lambda_2}\frac{\left|\Phi(\lambda;\lambda_1;\lambda_2)\right|^2 \Delta(\vec{q}+\vec{q_1}+\vec{q_2})}{\omega^2(\lambda_1)\omega^2(\lambda_2)} \qquad (6.6)$$

By rewriting Eq.(6.2) in the following form

$$\Omega^2(\lambda) = \omega^2(\lambda)\left[1 + \frac{k_B T}{2N\omega^2(\lambda)} A\right] \qquad (6.7)$$

where

$$A = \sum_{\lambda_1}\frac{\Phi(\lambda_1;-\lambda_1;\lambda;-\lambda)}{\omega^2(\lambda_1)} - \sum_{\lambda_1}\sum_{\lambda_2}\frac{\left|\Phi(\lambda;\lambda_1;\lambda_2)\right|^2 \Delta(\vec{q}+\vec{q_1}+\vec{q_2})}{\omega^2(\lambda_1)\omega^2(\lambda_2)} \qquad (6.8)$$

$\Omega^{-2}(\vec{q}j)$ can be expanded in a binomial expansion. As a result Eq.(6.1) becomes

$$\langle u^2 \rangle = \frac{k_B T}{MN}\sum_{\lambda}\frac{1}{\omega^2(\lambda)}\left[1 - \frac{k_B T}{2N\omega^2(\lambda)} A + \frac{(k_B T)^2}{4N^2\omega^4(\lambda)} A^2 - \ldots\right] \qquad (6.9)$$

and the expansion can be carried to any even order in λ since A is already of $O(\lambda^2)$. As detailed in Shukla and Hübschle (1989), the first term in Eq.(6.9) is simply the quasiharmonic contribution to MSD, while the second term correctly represents the quartic and cubic contributions (to be enumerated here as $GF2_1$ and $GF2_2$, respectively). However, what Eq.(6.9) reveals is that when A^2 is expanded, the terms $\langle u^2\rangle_{2(b),2}$, $\langle u^2\rangle_{2(d),3}$ and $\langle u^2\rangle_{2(f),2}$ are correctly represented. The following is the demonstration of the identification of these

terms with those derived in Sec. III. From the expansion of A^2, the following terms arise

$$GF4_1 = \frac{144}{\beta^3 MN}\left(\frac{2}{\hbar}\right)^4 \sum_{\lambda\lambda_1\lambda_2} \frac{V(\lambda_1;-\lambda_1;\lambda;-\lambda)\, V(\lambda_2;-\lambda_2;\lambda;-\lambda)}{\omega(\lambda_1)\omega(\lambda_2)\omega^4(\lambda)} \tag{6.10}$$

$$GF4_2 = -\frac{432}{\beta^3 MN}\left(\frac{2}{\hbar}\right)^5 \sum_{\lambda\lambda_1\lambda_2\lambda_3} \frac{V(\lambda_1;-\lambda_1;\lambda;-\lambda)\left|V(\lambda;\lambda_2;\lambda_3)\right|^2}{\omega(\lambda_1)\omega(\lambda_2)\omega(\lambda_3)\omega^4(\lambda)} \tag{6.11}$$

$$GF4_3 = \frac{324}{\beta^3 MN}\left(\frac{2}{\hbar}\right)^6 \sum_{\lambda\lambda_1\lambda_2\lambda_3\lambda_4} \frac{\left|V(\lambda;\lambda_1;\lambda_2)\right|^2\left|V(\lambda;\lambda_3;\lambda_4)\right|^2}{\omega(\lambda_1)\omega(\lambda_2)\omega(\lambda_3)\omega(\lambda_4)\omega^4(\lambda)} \tag{6.12}$$

where the V notation has been used in order to facilitate the comparison. The above expressions are seen to be the $\langle u^2\rangle_{2(b),2}$, $\langle u^2\rangle_{2(d),3}$ and $\langle u^2\rangle_{2(f),2}$ expressions of Table 3.1, but in the diagonal approximation (in other words, only the diagonal elements are needed when the loops and bubbles are multiplied together). Based on the equivalence of terms of $O(\lambda^2)$ and $O(\lambda^4)$, as given by the detailed derivation presented in Sec. III and the expansion of Eq.(6.1), terms of $O(\lambda^6)$ and $O(\lambda^8)$ are enumerated. The diagrams representing these contributions are shown in Fig.7 and their respective high temperature expressions are listed in Table 6.1. These are also in the diagonal approximation.

All these contributions are evaluated using the method of loops and bubbles described in Sec.III for L=4 and L=10 and then extrapolated to an infinite crystal limit. In order to compare with the MC results of HSC the same six volumes are

Figure 7

Selected Higher-Order Mean Square

Displacement Diagrams

(A) Selected diagrams of $O(\lambda^6)$

(B) Selected diagrams of $O(\lambda^8)$

(A)

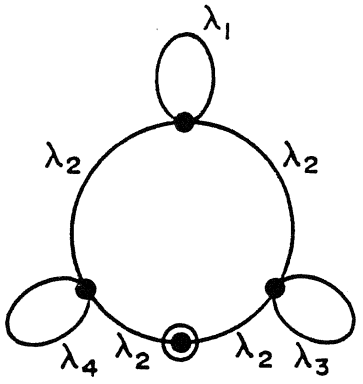

GF6$_1$

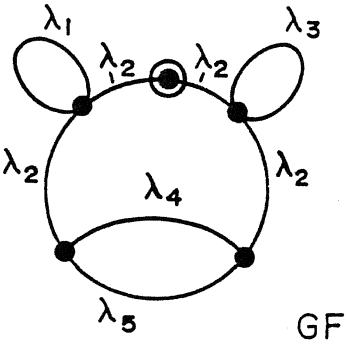

GF6$_2$

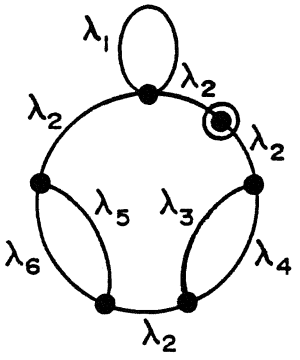

GF6$_3$

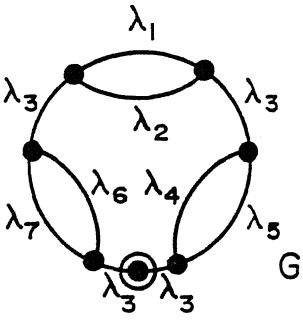

GF6$_4$

(B)

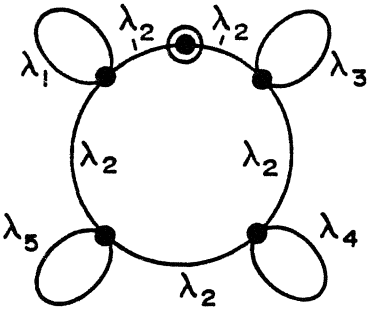

GF8$_1$

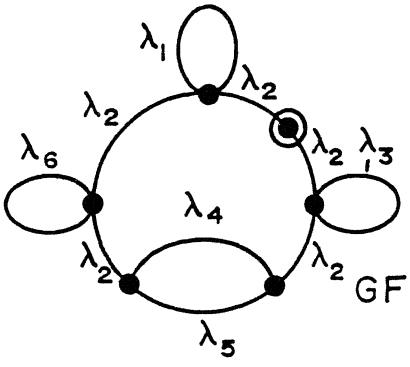

GF8$_2$

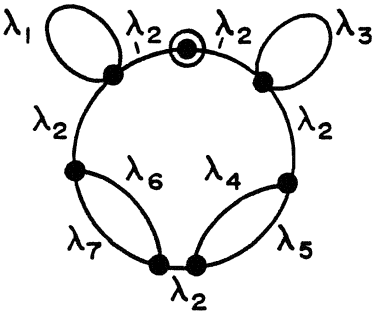

GF8$_3$

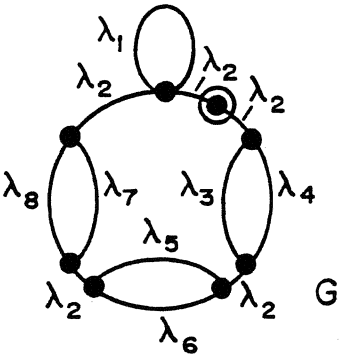

GF8$_4$

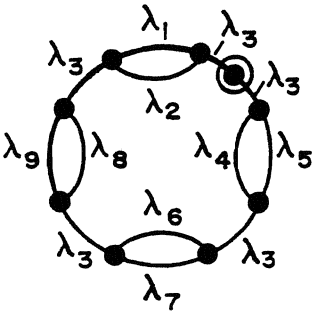

GF8$_5$

TABLE 6.1

HIGH TEMPERATURE LIMITS FOR THE SELECTED $O(\lambda^6)$ AND $O(\lambda^8)$ CONTRIBUTIONS TO THE MEAN SQUARE DISPLACEMENT

DIAGRAM	HIGH TEMPERATURE LIMIT
$GF6_1$	$-\frac{(k_BT)^4}{8MN^4}\sum_{\lambda\lambda_1\lambda_2}\sum_{\lambda_3}\frac{\Phi(\lambda_1;-\lambda_1;\lambda;-\lambda)\Phi(\lambda_2;-\lambda_2;\lambda;-\lambda)\Phi(\lambda_3;-\lambda_3;\lambda;-\lambda)}{\omega^2(\lambda_1)\omega^2(\lambda_2)\omega^2(\lambda_3)\omega^8(\lambda)}$
$GF6_2$	$\frac{3(k_BT)^4}{8MN^4}\sum_{\lambda\lambda_1\lambda_2}\sum_{\lambda_3\lambda_4}\frac{\Phi(\lambda_1;-\lambda_1;\lambda;-\lambda)\Phi(\lambda_2;-\lambda_2;\lambda;-\lambda)\left\|\Phi(\lambda;\lambda_3;\lambda_4)\right\|^2}{\omega^2(\lambda_1)\omega^2(\lambda_2)\omega^2(\lambda_3)\omega^2(\lambda_4)\omega^8(\lambda)}$
$GF6_3$	$-\frac{3(k_BT)^4}{8MN^4}\sum_{\lambda\lambda_1\lambda_2}\sum_{\lambda_3\lambda_4\lambda_5}\frac{\Phi(\lambda_1;-\lambda_1;\lambda;-\lambda)\left\|\Phi(\lambda;\lambda_2;\lambda_3)\right\|^2\left\|\Phi(\lambda;\lambda_4;\lambda_5)\right\|^2}{\omega^2(\lambda_1)\omega^2(\lambda_2)\omega^2(\lambda_3)\omega^2(\lambda_4)\omega^2(\lambda_5)\omega^8(\lambda)}$
$GF6_4$	$\frac{(k_BT)^4}{8MN^4}\sum_{\lambda\lambda_1\lambda_2}\sum_{\lambda_3\lambda_4\lambda_5}\sum_{\lambda_6}\frac{\left\|\Phi(\lambda;\lambda_1;\lambda_2)\right\|^2\left\|\Phi(\lambda;\lambda_3;\lambda_4)\right\|^2\left\|\Phi(\lambda;\lambda_5;\lambda_6)\right\|^2}{\omega^2(\lambda_1)\omega^2(\lambda_2)\omega^2(\lambda_3)\omega^2(\lambda_4)\omega^2(\lambda_5)\omega^2(\lambda_6)\omega^8(\lambda)}$
$GF8_1$	$\frac{(k_BT)^5}{16MN^5}\sum_{\lambda\lambda_1\lambda_2}\sum_{\lambda_3\lambda_4}\frac{\Phi(\lambda_1;-\lambda_1;\lambda;-\lambda)\Phi(\lambda_2;-\lambda_2;\lambda;-\lambda)\Phi(\lambda_3;-\lambda_3;\lambda;-\lambda)\Phi(\lambda_4;-\lambda_4;\lambda;-\lambda)}{\omega^2(\lambda_1)\omega^2(\lambda_2)\omega^2(\lambda_3)\omega^2(\lambda_4)\omega^{10}(\lambda)}$
$GF8_2$	$-\frac{(k_BT)^5}{4MN^5}\sum_{\lambda\lambda_1\lambda_2}\sum_{\lambda_3\lambda_4\lambda_5}\frac{\Phi(\lambda_1;-\lambda_1;\lambda;-\lambda)\Phi(\lambda_2;-\lambda_2;\lambda;-\lambda)\Phi(\lambda_3;-\lambda_3;\lambda;-\lambda)\left\|\Phi(\lambda;\lambda_4;\lambda_5)\right\|^2}{\omega^2(\lambda_1)\omega^2(\lambda_2)\omega^2(\lambda_3)\omega^2(\lambda_4)\omega^2(\lambda_5)\omega^{10}(\lambda)}$
$GF8_3$	$\frac{3(k_BT)^5}{8MN^5}\sum_{\lambda\lambda_1\lambda_2}\sum_{\lambda_3\lambda_4\lambda_5}\sum_{\lambda_6}\frac{\Phi(\lambda_1;-\lambda_1;\lambda;-\lambda)\Phi(\lambda_2;-\lambda_2;\lambda;-\lambda)\left\|\Phi(\lambda;\lambda_3;\lambda_4)\right\|^2\left\|\Phi(\lambda;\lambda_5;\lambda_6)\right\|^2}{\omega^2(\lambda_1)\omega^2(\lambda_2)\omega^2(\lambda_3)\omega^2(\lambda_4)\omega^2(\lambda_5)\omega^2(\lambda_6)\omega^{10}(\lambda)}$
$GF8_4$	$-\frac{(k_BT)^5}{4MN^5}\sum_{\lambda\lambda_1\lambda_2}\sum_{\lambda_3\lambda_4\lambda_5}\sum_{\lambda_6\lambda_7}\frac{\Phi(\lambda_1;-\lambda_1;\lambda;-\lambda)\left\|\Phi(\lambda;\lambda_2;\lambda_3)\right\|^2\left\|\Phi(\lambda;\lambda_4;\lambda_5)\right\|^2\left\|\Phi(\lambda;\lambda_6;\lambda_7)\right\|^2}{\omega^2(\lambda_1)\omega^2(\lambda_2)\omega^2(\lambda_3)\omega^2(\lambda_4)\omega^2(\lambda_5)\omega^2(\lambda_6)\omega^2(\lambda_7)\omega^{10}(\lambda)}$
$GF8_5$	$\frac{(k_BT)^5}{16MN^5}\sum_{\lambda\lambda_1\lambda_2}\sum_{\lambda_3\lambda_4\lambda_5}\sum_{\lambda_6\lambda_7\lambda_8}\frac{\left\|\Phi(\lambda;\lambda_1;\lambda_2)\right\|^2\left\|\Phi(\lambda;\lambda_3;\lambda_4)\right\|^2\left\|\Phi(\lambda;\lambda_5;\lambda_6)\right\|^2\left\|\Phi(\lambda;\lambda_7;\lambda_8)\right\|^2}{\omega^2(\lambda_1)\omega^2(\lambda_2)\omega^2(\lambda_3)\omega^2(\lambda_4)\omega^2(\lambda_5)\omega^2(\lambda_6)\omega^2(\lambda_7)\omega^2(\lambda_8)\omega^{10}(\lambda)}$

used in these computations with the results being shown in Table 6.2. The contributions of a particular order are summed and then added to the QH result. Table 6.3 presents these results with a comparison of the MC results and the renormalized frequency results of Shukla and Hübschle (1989).

TABLE 6.2

CONTRIBUTION ARISING IN THE GREEN'S FUNCTION METHOD
UP TO AND INCLUDING $O(\lambda^8)$
USING THE FULL CALCULATION

CONT	r_0	r_1	r_2	r_3	r_4	r_5	r_6
QH[a]	0.0175	0.0204	0.0234	0.0264	0.0304	0.0358	0.0409
$GF2_1$[b]	-0.0152	-0.0210	-0.0283	-0.0368	-0.0502	-0.0728	-0.0988
$GF2_2$	0.0130	0.0180	0.0241	0.0312	0.0424	0.0615	0.0836
$GF4_1$[c]	0.0133	0.0220	0.0349	0.0526	0.0854	0.1536	0.2497
$GF4_2$	-0.0239	-0.0394	-0.0623	-0.0940	-0.1525	-0.2750	-0.4485
$GF4_3$	0.0099	0.0161	0.0252	0.0378	0.0608	0.1091	0.1779
$GF6_1$[d]	-0.0118	-0.0234	-0.0438	-0.0768	-0.1492	-0.3354	-0.6578
$GF6_2$	0.0297	0.0583	0.1082	0.1889	0.3650	0.8176	1.6038
$GF6_3$	-0.0257	-0.0500	-0.0922	-0.1603	-0.3086	-0.6903	-1.3570
$GF6_4$	0.0076	0.0147	0.0270	0.0467	0.0898	0.2011	0.3971
$GF8_1$[e]	0.0106	0.0253	0.0560	0.1146	0.2677	0.7564	1.8017
$GF8_2$	-0.0351	-0.0827	-0.1816	-0.3697	-0.8584	-2.4167	-5.7588
$GF8_3$	0.0450	0.1050	0.2290	0.4638	1.0725	3.0155	7.2049
$GF8_4$	-0.0264	-0.0611	-0.1324	-0.2672	-0.6165	-1.7354	-4.1682
$GF8_5$	0.0059	0.0137	0.0295	0.0594	0.1369	0.3869	0.9364

a) QH in units of $(k_BT/\varepsilon)r_0^2$.
b) O(GF2) in units of $(k_BT/\varepsilon)^2r_0^2$.
c) O(GF4) in units of $(k_BT/\varepsilon)^3r_0^2$.
d) O(GF6) in units of $(k_BT/\varepsilon)^4r_0^2$.
e) O(GF8) in units of $(k_BT/\varepsilon)^5r_0^2$.

TABLE 6.3

COMPARISON WITH MONTE CARLO RESULTS FOR THE SELECTED CONTRIBUTIONS TO THE MEAN SQUARE DISPLACEMENT USING THE FULL CALCULATION[a]

TEMP[b]	QH	O(GF2)	O(GF4)	O(GF6)	O(GF8)	MC[c]	RE[d]
0.125	3.21	3.15	3.15	3.15	3.15	3.15	3.15
0.225	6.63	6.36	6.38	6.38	6.38	6.38	6.38
0.300	9.98	9.34	9.43	9.41	9.41	9.69	9.41
0.375	14.4	13.0	13.3	13.2	13.2	13.7	13.2
0.450	20.3	17.4	18.4	18.0	18.2	19.2	18.1
0.500	25.8	21.0	23.2	22.1	22.7	23.2	22.5

a) Columns 2-8 in units of $\sigma^2/1000$.

b) In units of ε/k_B.

c) From Heiser, Shukla and Cowley (1986).

d) From Shukla and Hübschle (1989).

VII DEBYE-WALLER FACTOR

The Debye-Waller factor (DWF), exp[-2W(T)], at a temperature T in Kelvin is related to the Mössbauer recoilless fraction (f) from Callaway (1974) and Gupta (1983) by

$$f = e^{-2W(T)} \tag{7.1}$$

where

$$2W(T) = \frac{1}{3}\left(\frac{E_\gamma}{c\hbar}\right)^2 \langle u^2 \rangle \tag{7.2}$$

and E_γ is the energy of the γ-radiation scattered by the crystal and c is the speed of light in a vacuum. The theoretical values for f can be calculated, up to and including $O(\lambda^4)$ PT, using the MSD expressions derived in Sec. III. These results are then plotted with the experimental recoilless fractions presented in Gilbert and Violet (1968) (as corrected by Kolk (1971)) for Kr.

The MSD results, as evaluated and presented in Sec. V, were calculated for the Lennard-Jones potential. The potential parameters for Kr are derived in Shukla and Shanes (1985) including the harmonic and anharmonic contributions to the zero point energy and the self-consistent solution of the total energy. The values for these parameters are listed in Table 7.1. Substituting these parameters into the results of Sec. V, the MSD contributions up to and including $O(\lambda^4)$ were

TABLE 7.1

PARAMETERS FOR THE LENNARD-JONES AND AZIZ POTENTIALS FOR KRYPTON

PARAMETER	Lennard-Jones[a]	Aziz[b]
A	-	12153120
α	-	16.496763
C_6	-	1.1561739
C_8	-	0.5414923
C_{10}	-	0.2839735
γ	-	2.4
D	-	1.28
ϵ/k_B (K)	235.3	199.9
r_m (Å)	3.965	4.012

(a) From Shukla and Shanes (1985).

(b) From Aziz (1979).

obtained for Kr for the six volumes listed. For Kr, the value of E_γ is 9.3 keV and with this, the MSD results are converted to values of f. In Fig. 8 the theoretical recoilless fractions are plotted with the experimental results of Kolk (1971).

As previously mentioned, the MSD results are also calculated using the Aziz (1979) potential for Kr. This potential has the form

$$V(r) = \varepsilon V^*(x) \tag{7.3}$$

where

$$V^*(x) = Ax^\gamma e^{-\alpha x} - \left(\frac{C_6}{x^6} + \frac{C_8}{x^8} + \frac{C_{10}}{x^{10}}\right)F(x) \tag{7.4}$$

and

$$F(x) = \exp\left[-\left(\frac{D}{x} - 1\right)^2\right] \qquad \text{for } x<D$$

$$= 1 \qquad \text{for } x\geq D \tag{7.5}$$

where

$$x = \frac{r}{r_m} \tag{7.6}$$

The parameters used in this potential are also listed in Table 7.1. The high temperature QH contribution was calculated

Figure 8

Comparison of Experimental Recoilless Fractions to Theoretical Values for the Lennard-Jones Potential

The solid lines correspond to the QH, $O(\lambda^2)$, and $O(\lambda^4)$ results. The boxes are the experimental values of Kolk (1971).

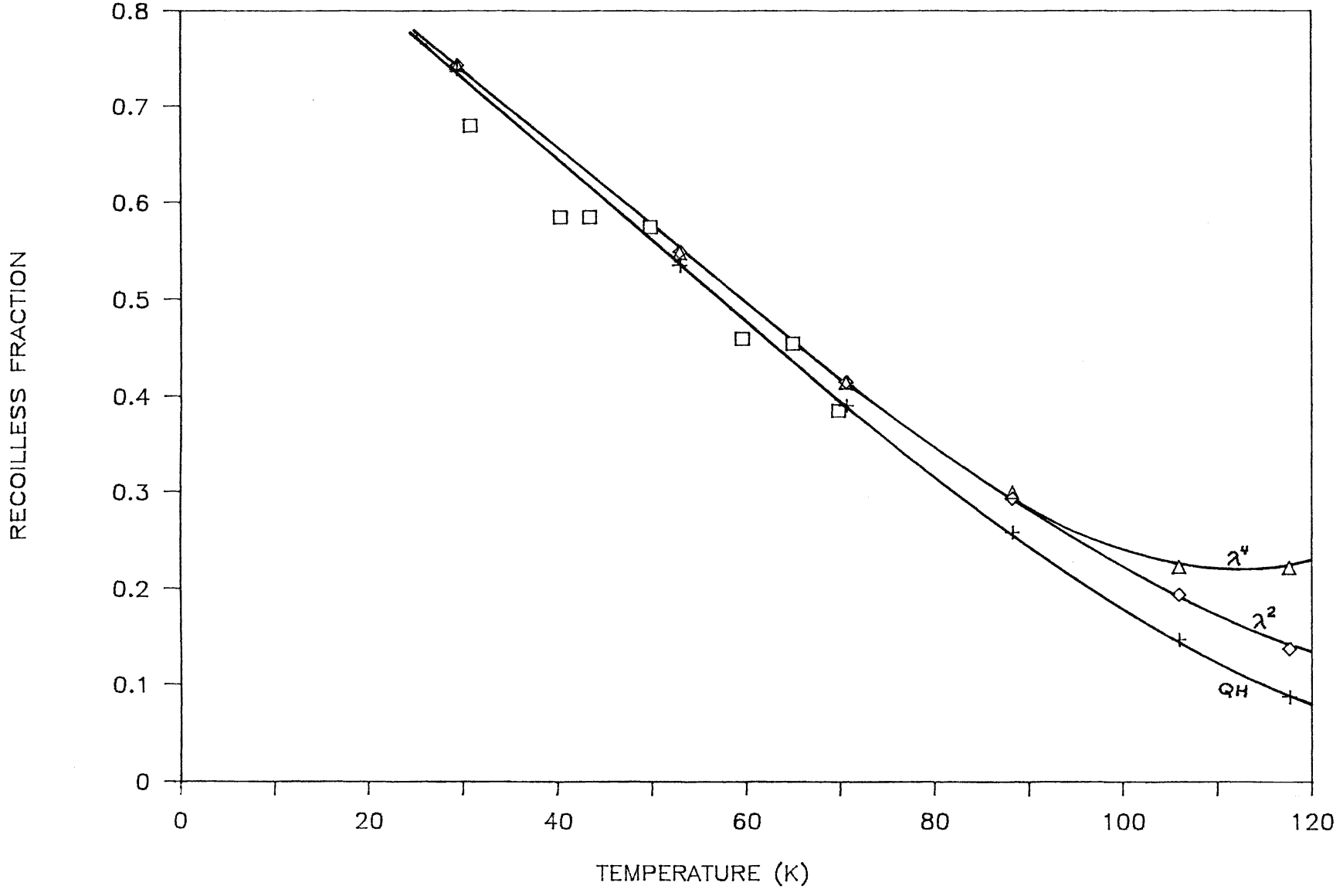
RECOILLESS FRACTION
0.8
0.7
0.6
0.5
0.4
0.3
0.2
0.1
0
0
20
40
60
80
100
120
TEMPERATURE (K)
λ⁴
λ²
QH

using the lattice parameters given in Korpiun and Lüscher (1976) for a number of temperatures. The $O(\lambda^2)$ and $O(\lambda^4)$ MSD contributions were calculated using the equilibrium volume, and added to the QH results at the appropriate temperatures. After converting the MSD results to recoilless fractions they are plotted in Fig. 9 with the experimental results.

Figure 9

Comparison of Experimental Recoilless Fractions to Theoretical Values for the Aziz Potential

The solid lines correspond to the QH, $O(\lambda^2)$, and $O(\lambda^4)$ results. The experimental results of Kolk (1971) are depicted as boxes.

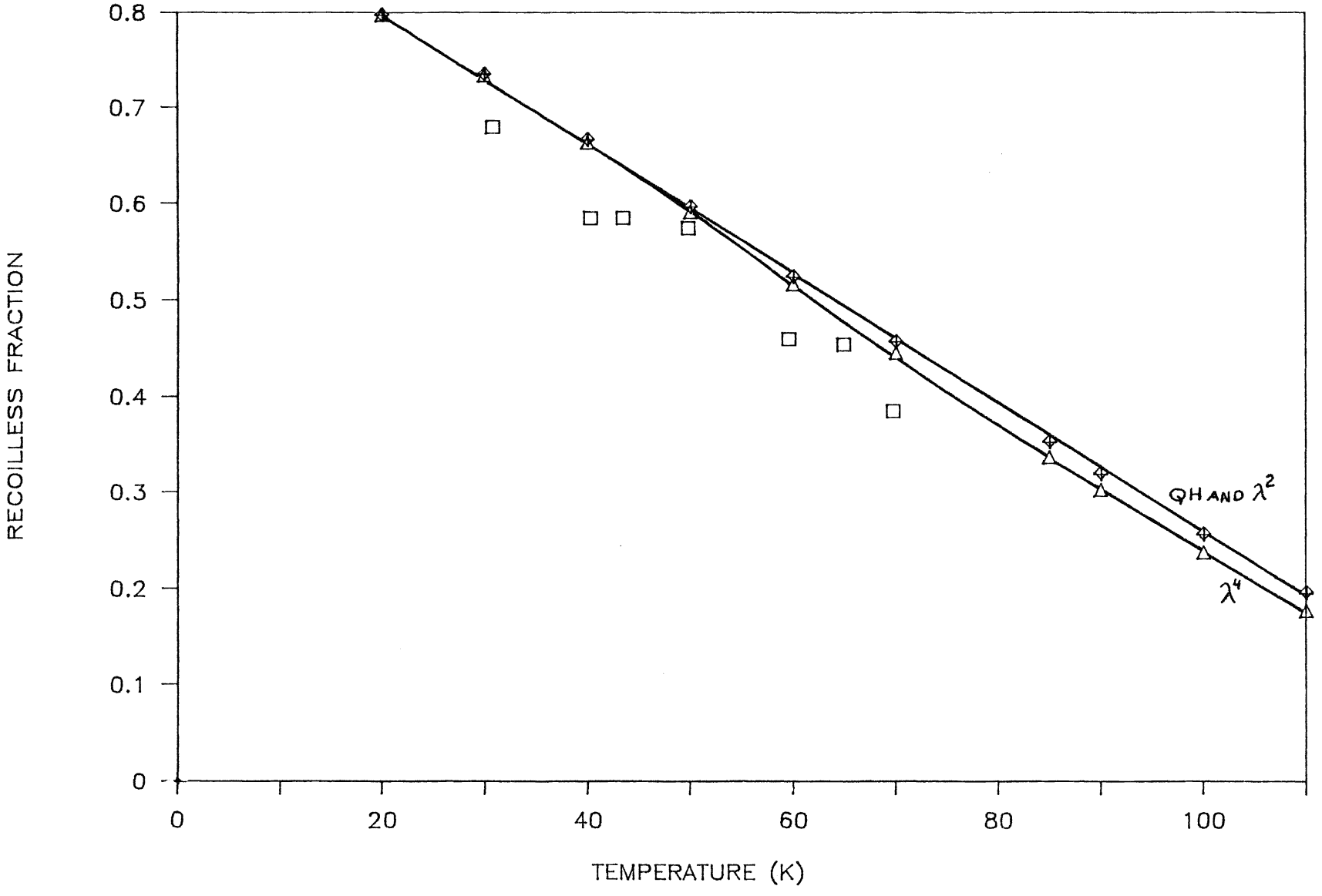
RECOILLESS FRACTION
0.8
0.7
0.6
0.5
0.4
0.3
0.2
0.1
0
0
20
40
60
80
100
TEMPERATURE (K)
QH AND λ^2
λ^4

VIII DISCUSSION

The aim of this research was to present, in a progressive manner, an examination of all the anharmonic contributions to the mean square displacement up to and including $O(\lambda^4)$ PT. This was accomplished by first deriving all of the $O(\lambda^4)$ contributions. A number of these contributions ($\langle u^2\rangle_{1(a)}$, $\langle u^2\rangle_{1(b)}$, $\langle u^2\rangle_{2(a)}$, $\langle u^2\rangle_{2(b),1}$, $\langle u^2\rangle_{2(b),2}$, $\langle u^2\rangle_{2(c),1}$ and $\langle u^2\rangle_{2(e)}$) were derived algebraically (as outlined in Sec. III), and then taken to the high temperature limit. At this point, it was found that these high temperature expressions could be derived from the corresponding high temperature free energy expressions of Shukla and Cowley (1971). This procedure was then used to derive the remaining $O(\lambda^4)$ contributions to MSD. The numerical evaluation of the perturbation expansion contributions to MSD was evaluated in the plane wave representation of the delta function.

First, all of the MSD contributions were evaluated without making any approximations for the six temperatures of Heiser, Shukla and Cowley (1986). An examination of Table 5.2 reveals that for $O(\lambda^4)$ there are contributions which are of the same order of magnitude but of opposite sign. For example, $\langle u^2\rangle_{2(a)}$ with $\langle u^2\rangle_{2(c),1}$, $\langle u^2\rangle_{2(g),2}$ with $\langle u^2\rangle_{2(h)}$ and $\langle u^2\rangle_{2(d),1}$ with $\langle u^2\rangle_{2(e)}$. These hold for all of the nearest-neighbour distances. When the remaining contributions are included there is extreme cancellation for all volumes.

Consequently, no λ^4 contribution is small enough to be ignored or large enough to dominate. The effect of this cancellation can be seen from Table 5.6 where the total of all the λ^4 contributions, MSD(λ^4), are presented for the six nearest-neighbour distances. Also presented in this Table is the result of adding MSD(λ^2) to QH. The resulting O(λ^2) PT results agree with the corresponding results of Shukla and Hübschle (1989) which incorporated the extrapolation of the cubic contribution. For all but the first reduced temperature, the O(λ^2) PT result is lower than the MC result. Consequently, when the λ^4 contributions are added, a better agreement with the MC results will be achieved only if the sign of MSD(λ^4) is positive. For the first temperature, the magnitude of MSD(λ^4) is too small to make a noticeable change in the O(λ^4) PT result. The total MSD result is brought into agreement with the MC result for the second temperature and at the third temperature, the agreement between the perturbation theory and the MC result is marginally better. Starting with the fourth temperature; however, the sign of MSD(λ^4) changes to negative and the agreement with the MC results gets worse for the last three temperatures. This change of sign is unaffected even when the error associated with the estimation of $\langle u^2 \rangle_{2(h)}$ is taken into consideration. When the λ^4 contributions were calculated for $r=r_0$ and then multiplied by the appropriate temperatures, the agreement with the MC results improves. This is seen in Table 5.6 by comparing the $\lambda^4 r_0$ PT results with

the MC results. The explanation of this lies in the manner in which the six nearest-neighbour distances were derived. Since they were obtained for a Monte Carlo calculation, where all orders of anharmonicity are present, it is reasonable to say that the effects of higher order contributions are entering into the calculations where the nearest-neighbour distances are explicitly used. For this reason, the λ^4 contributions calculated at equilibrium, and multiplied by the appropriate temperatures, can be considered as a correction to the $O(\lambda^2)$ PT. In Figure 8 the ratio of $O(\lambda^4)$ PT to $O(\lambda^2)$ PT is plotted in order to assess the convergence of the perturbation expansion. From this plot the expansion appears to be converging well up to approximately 75% of the melting temperature T_M. After this temperature the perturbation theory breaks down.

Using the leading term approximation (LTA), the QH, λ^2 and λ^4 MSD results are presented in Table 5.3. To assess the accuracy of the LTA, these results must be compared with those of the full calculation presented in Table 5.2. This comparison shows that some of the contributions are approximated very well for certain volumes and worse for other volumes. For example, $\langle u^2 \rangle_{1(b)}$ is approximately 2% larger for the lowest volume but is then 21% lower for the highest volume. The same trend occurs for diagrams $\langle u^2 \rangle_{2(c),2}$, $\langle u^2 \rangle_{2(f),1}$, $\langle u^2 \rangle_{2(f),2}$, $\langle u^2 \rangle_{2(g),1}$, $\langle u^2 \rangle_{2(g),2}$ and $\langle u^2 \rangle_{2(h)}$. On the other hand, diagrams $\langle u^2 \rangle_{2(b),1}$ and $\langle u^2 \rangle_{2(b),2}$ are greater by more than a

factor of 2 for the lowest value of r (in other words r_0), but as the volume increases, these results get better. At the largest volume, the LTA over estimates these contributions by 32% and 37%, respectively. Consequently, this approximation can be used as an order of magnitude calculation for individual anharmonic contributions. A comparison of the totals of all the diagrams for $O(\lambda^2)$ yields totals of the same sign; however, the magnitudes vary from as little as a factor of 2 for volume four to as large as a factor of 4 for volume one. For $O(\lambda^4)$, the MSD changes sign in the full calculation; whereas, in LTA it remains positive for all the volumes, and the magnitudes are roughly 10 times larger. Consequently, this approximation does not accurately predict the total contribution to MSD for a particular order in λ. However, when MSD(λ^2) and MSD (λ^4) are added to the QH result these inaccuracies tend to counterbalance each other and except for the largest volume give a good approximation of the full results. A reasonable approximation of the MC results is obtained for all but the second largest volume. It must be noted that $\lambda^4 r_0$ PT does not give a better agreement in this approximation. To assess the convergence of the perturbation expansion for the LTA, the ratio of $O(\lambda^4)$ PT and $O(\lambda^2)$ PT, calculated in LTA, is also plotted in Fig. 8. From this plot, the perturbation theory is seen to break down for temperatures above 45% of T_M.

In order to simplify the calculation of the MSD and F contributions, the Peierls approximation was introduced in Sec. IV. For MSD, this approximation allows all but one of the zone sums to be evaluated analytically and hence all that needs to be calculated are the potential derivatives. A comparison of Table 5.2 with Table 5.8 reveals that the Peierls approximation gives an accurate order of magnitude calculation for each of the terms in MSD. Once again there are contributions which are approximated very well at certain volumes but not well at others. For example, diagrams $\langle u^2\rangle_{1(a)}$, $\langle u^2\rangle_{2(c),2}$, $\langle u^2\rangle_{2(d),2}$, $\langle u^2\rangle_{2(d),3}$ and $\langle u^2\rangle_{2(e)}$ are approximated very well for $r=r_0$ but the approximation gets worse for the largest volume. The worst case, once again, occurs for diagrams $\langle u^2\rangle_{2(b),1}$ and $\langle u^2\rangle_{2(b),2}$ where the Peierls approximation is out by as much as a factor of 2. The remarkable thing is the ease with which the calculation was carried out. As stated previously, only one BZ sum had to be evaluated numerically, since the remaining zone sums were evaluated analytically. This results in an extremely time-efficient method of evaluating these perturbation expansion contributions. The Peierls approximation inaccurately predicts the sum for diagrams of a particular order, MSD(λ^2) and MSD(λ^4) as seen in Tables 5.12 and 5.13; however, the change in sign of MSD(λ^4) is not present in this approximation. Once again, the inaccuracies cancel out and good agreement is achieved with the exact results for the first four volumes and a good

agreement with the MC results for the first five volumes. Again, it must be noted that $\lambda^4 r_0$ PT does not yield a better agreement with the MC results. From Fig. 8, using the Peierls approximation in the calculation of $O(\lambda^2)$ PT and $O(\lambda^4)$ PT, the perturbation expansion is seen to break down for temperatures above 45% of T_M.

Combining the leading term approximation with the Peierls approximation causes a complete break down of the theory as can be seen in Table 5.13, where for the largest volume, the $MSD(\lambda^2)$ result is larger than the QH result and consequently the $O(\lambda^2)$ PT value is negative. This makes any of these results (calculated using LTA in the Peierls approximation) very speculative and since the λ^2 and λ^4 contributions can be evaluated very fast using the full representations of the potential derivatives, it seems unnecessary to make any further approximations.

The free energy was initially computed as a check of the programs; however, it can be used to also check the accuracy of the Peierls approximation. From the calculation of the free energy using Peierls approximation, a comparison of Tables 5.4 and 5.10 reveals that certain diagrams are approximated more accurately than others. The same conditions outlined for the MSD contributions exist for the same diagram types in the free energy. From Figure 9 it can be seen that the values of $C_v(\lambda^2)$, calculated using Peierls approximation, are in good agreement with the values of $C_v(\lambda^2)$ computed for

the full calculation. However, this plot also reveals that the λ^4 theory, using Peierls approximation, yields a curve that exceeds the full calculation λ^4 curve at all temperatures. At the higher temperatures the $O(\lambda^2)$ and $O(\lambda^4)$ C_v results using Peierls approximation are not in any kind of agreement with the Monte Carlo points. From this it is evident that the Peierls approximation does not accurately predict the total free energy in a given order of λ.

The anharmonic contributions to MSD, arising in the Green's function method of Shukla and Hübschle (1989), have been derived up to and including $O(\lambda^8)$ in Sec. VI. The $O(\lambda^2)$ contributions are correctly predicted and three of the $O(\lambda^4)$ contributions ($\langle u^2\rangle_{2(b),2}$, $\langle u^2\rangle_{2(d),3}$ and $\langle u^2\rangle_{2(f),2}$) are also correctly predicted. In Table 6.2 all of the MSD contributions arising in the Green's function method, up to and including $O(\lambda^8)$, are listed. Once again, there is cancellation among the contributions of a given order in λ. From Table 6.3, the O(GF4) results are in excellent agreement with the MC results, for all temperatures. For the first four temperatures, the O(GF6) and O(GF8) results are small and yeild little or no change. However, for the last two temperatures, these contributions are appreciable. It is seen that most of the renormalized frequency results of Shukla and Hübschle (1989) come from considering these contributions up to $O(\lambda^8)$.

As shown in Sec. VII, the MSD is related to the

recoilless fraction. In the calculation of this fraction, the Lennard-Jones and Aziz potentials were employed for the case of krypton. The Lennard-Jones QH results agree excellently with the experimental results. The $O(\lambda^2)$ PT and $O(\lambda^4)$ PT results are also in excellent agreement with the experimental results over the range of temperatures used in the experiment. At higher temperatures the $O(\lambda^2)$ PT and $O(\lambda^4)$ PT results become larger than the QH results, but because the experimental results are not presented for these temperatures it cannot be ascertained which theory will give the best agreement in this temperature range. Using the Aziz potential yields results in good agreement with the experimental values for all temperatures, with the $O(\lambda^4)$ PT results falling a little closer to the experimental results. However, it must be noted that the $O(\lambda^2)$ PT and $O(\lambda^4)$ PT results were not calculated for individual lattice constants as was done with the QH results. If individual lattice constants were employed the agreement using the $O(\lambda^2)$ PT and $O(\lambda^4)$ PT theories may change.

The derivation of the general anharmonic coefficient (Eq.(2.48)) was carried out for the special case of the central force interaction with r atoms in the unit cell. As a final observation, it is noted that for systems with more than one atom in the unit cell, the contributions to the mean square displacement will have terms dependent on the types of atoms present in the unit cell. The eigenvalues and eigenvectors will be found from the diagonalization of a 3r×3r

dynamical matrix and the BZ sums will be carried out for the Brillouin zone associated with the system being considered.

IX CONCLUSIONS

A general derivation of the anharmonic coefficients of the anharmonic Hamiltonian have been presented. These coefficients were then specialized for the central force interaction potential. This Hamiltonian then was used for the enumeration of the mean square displacement (MSD) contributions to order λ^4 perturbation theory where λ is the expansion parameter. A correspondance of MSD contributions (diagrams) to free energy diagrams in the same order of λ is established.

Numerical results are obtained for all the MSD contributions to $O(\lambda^4)$ for the six volumes and temperatures for which the Monte Carlo results are available. A comparison of the Monte Carlo results (which include all anharmonic contributions) was made with the total $O(\lambda^4)$ MSD results. This comparison indicates the convergence of the perturbation expansion up to 75% of the melting temperature of the solid (T_M). However, a better agreement with the Monte Carlo results was not obtained when the total of all the λ^4 contributions was added to the $O(\lambda^2)$ perturbation theory results. This was because of a change in sign of the total of the λ^4 contributions.

The Peierls approximation is used to simplify the evaluation of the MSD contributions. Its usefullness as an order of magnitude calculation is shown, but the total $O(\lambda^4)$

MSD results show a break down of the perturbation expansion beyond 45% of T_M. This approximation does not accurately predict the total of the contributions of a given order in λ as can be seen by its poor agreement with the Monte Carlo results for the specific heat. As a check of its accuracy, the leading term approximation (LTA) is also used in the numerical evaluation of the MSD contributions. Like the Peierls approximation, the LTA is useful as an order of magnitude calculation but also shows a break down of the perturbation expansion beyond 45% of T_M.

The contributions arising in the Green's function Method of Shukla and Hübschle (1989), up to and including $O(\lambda^8)$, are derived and enumerated. When numerically evaluated, these selected contributions are seen to be enough to reproduce their results to within a percent.

All of the MSD contributions to $O(\lambda^4)$ are evaluated for krypton using the Lennard-Jones and Aziz potentials. These results are converted to recoilless fractions and compared to the experimental results of Kolk (1971). It is found that the theoretical values are in excellent agreement with the experimental values at all temperatures.

REFERENCES

Aziz, R.A. (1979), Molec. Phys. 38, 177.

Born, M. and K. Huang (1954), Dynamical Theory of Crystal Lattices (Oxford University Press, Oxford).

Callawy, J. (1974), Quantum Theory of the Solid State Part A (Academic Press, New York).

Cowley, E. R. and H. J. Nur (1975), Can. J. Phys. 53, 1449.

Gilbert, K. and C. E. Violet (1968), Phys. Letters 28A, 285.

Goldman, V. V. (1968), Phys. Rev. 174, 1041.

Gupta, N. P. (1983), Solid State Commun. 48, 919.

Hardy, R. J. and M. A. Day (1988), Phys. Rev. B 37, 7597.

Heiser, G. A., R. C. Shukla, and E. R. Cowley (1986), Phys. Rev. B 33, 2518.

Klein, M. L., G. K. Horton, and J. L. Feldman (1969), Phys. Rev. 184, 968.

Kolk, B. (1971), Phys. Letters 35A, 83.

Korpiun, P. and E. Lüscher (1976), Rare Gas Solids Vol. II, Edited by M. L. Klein and J. A. Venables (Academic Press, New York), pgs 778-9.

Landau, L. D. and E. M. Lifshitz (1965), Quantum Mechanics (Pergamon Press, Second Edition), pg 132.

Maradudin, A. A. and P. A. Flinn (1963), Phys. Rev. 129, 2529.

Maradudin, A. A., E. W. Montroll, G. H. Weiss and I. P. Ipatova (1971), Theory of Lattice Dynamics in the Harmonic Approximation (Academic Press, Second Edition, New York).

Peierls, R. E. (1955), Quantum Theory of Solids (Oxford University Press, Oxford).

Shukla, R. C. (1966), J. Chem. Phys. 45, 4178.

Shukla, R. C. and E. R. Cowley (1971), Phys. Rev. B 3, 4055.

Shukla, R. C. and E. R. Cowley (1985), Phys. Rev. B 31, 372.

Shukla, R. C. and G. A. Heiser (1986), Phys. Rev. B 33, 2152.

Shukla, R. C. and H. Hübschle (1989), Phys. Rev. B 40, 1555.

Shukla, R. C. and R. D. Mountain (1982), Phys. Rev. B 25, 3649.

Shukla, R. C. and F. Shanes (1985), Phys. Rev. B 32, 2513.

Shukla, R. C. and L. Wilk (1974), Phys. Rev. B 10, 3660.

Van Hove, L. (1961), Quantum Theory of Many Particle Systems (Benjamin, New York).